VOLUME 33 | SUPPLEMENT 2 | MARCH 2020

MODERN PATHOLOGY

ABSTRACTS

HEAD AND NECK PATHOLOGY (1235-1315)

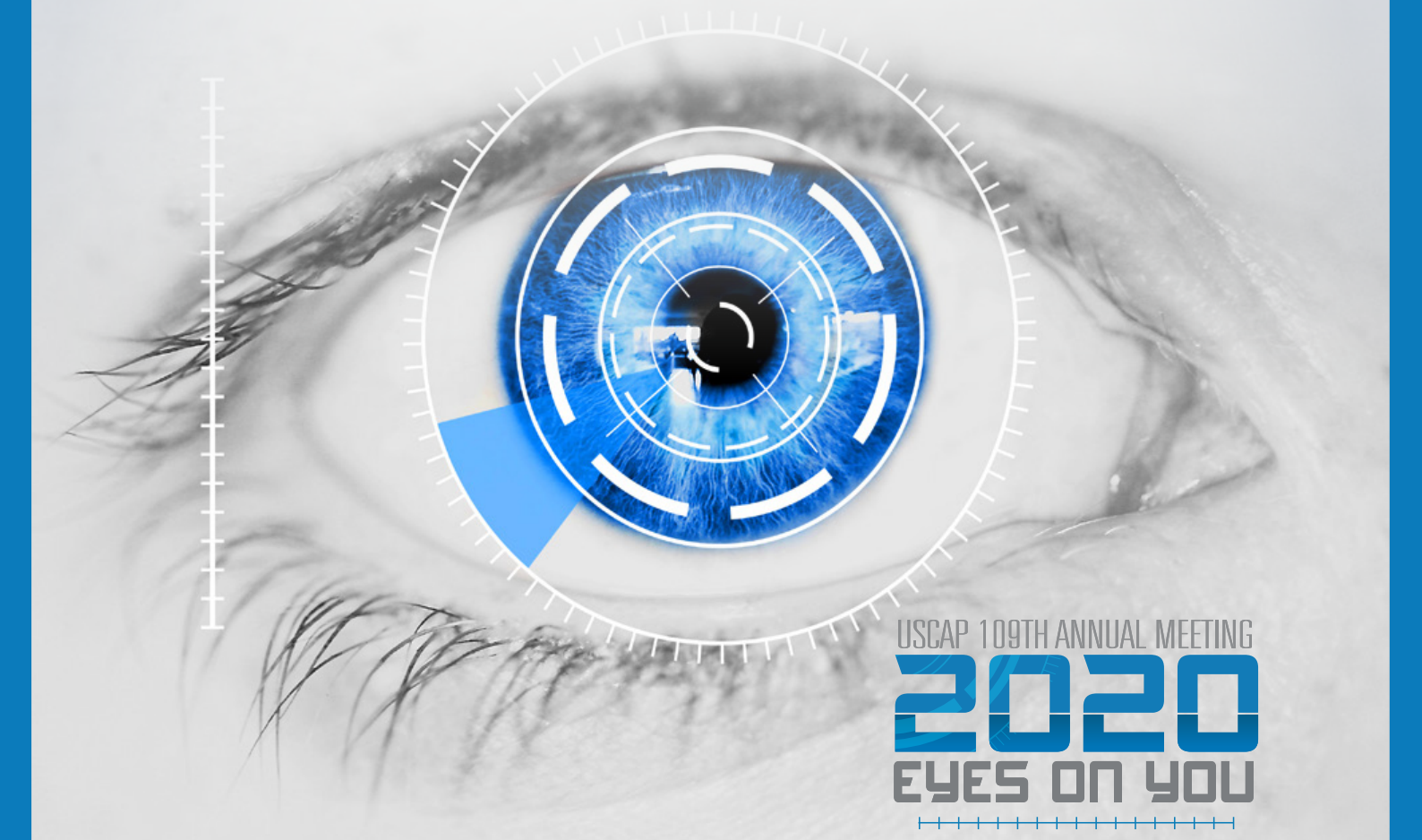

FEBRUARY 29-MARCH 5, 2020

LOS ANGELES CONVENTION CENTER
LOS ANGELES, CALIFORNIA

Published by
SPRINGER NATURE
www.ModernPathology.org

USCAP Creating a Better Pathologist
AN OFFICIAL JOURNAL OF THE UNITED STATES AND CANADIAN ACADEMY OF PATHOLOGY

EDUCATION COMMITTEE

Jason L. Hornick, Chair

Rhonda K. Yantiss, Chair, Abstract Review Board and Assignment Committee

Laura W. Lamps, Chair, CME Subcommittee

Steven D. Billings, Interactive Microscopy Subcommittee

Raja R. Seethala, Short Course Coordinator

Ilan Weinreb, Subcommittee for Unique Live Course Offerings

David B. Kaminsky (Ex-Officio)

Zubair Baloch
Daniel Brat
Ashley M. Cimino-Mathews
James R. Cook
Sarah Dry
William C. Faquin
Yuri Fedoriw
Karen Fritchie
Lakshmi Priya Kunju
Anna Marie Mulligan
Rish K. Pai
David Papke, Pathologist-in-Training
Vinita Parkash
Carlos Parra-Herran
Anil V. Parwani
Rajiv M. Patel
Deepa T. Patil
Lynette M. Sholl
Nicholas A. Zoumberos, Pathologist-in-Training

ABSTRACT REVIEW BOARD

Benjamin Adam
Narasimhan Agaram
Rouba Ali-Fehmi
Ghassan Allo
Isabel Alvarado-Cabrero
Catalina Amador
Roberto Barrios
Rohit Bhargava
Jennifer Boland
Alain Borczuk
Elena Brachtel
Marilyn Bui
Eric Burks
Shelley Caltharp
Barbara Centeno
Joanna Chan
Jennifer Chapman
Hui Chen
Beth Clark
James Conner
Alejandro Contreras
Claudiu Cotta
Jennifer Cotter
Sonika Dahiya
Farbod Darvishian
Jessica Davis
Heather Dawson
Elizabeth Demicco
Katie Dennis
Anand Dighe
Suzanne Dintzis
Michelle Downes
Andrew Evans
Michael Feely
Dennis Firchau
Gregory Fishbein
Andrew Folpe
Larissa Furtado
Billie Fyfe-Kirschner
Giovanna Giannico
Anthony Gill
Paula Ginter
Tamara Giorgadze
Purva Gopal
Anuradha Gopalan
Abha Goyal
Rondell Graham
Alejandro Gru
Nilesh Gupta
Mamta Gupta
Gillian Hale
Suntrea Hammer
Malini Harigopal
Douglas Hartman
John Higgins
Mai Hoang
Mojgan Hosseini
Aaron Huber
Peter Illei
Doina Ivan
Wei Jiang
Vickie Jo
Kirk Jones
Neerja Kambham
Chiah Sui Kao
Dipti Karamchandani
Darcy Kerr
Ashraf Khan
Francesca Khani
Rebecca King
Veronica Klepeis
Gregor Krings
Asangi Kumarapeli
Alvaro Laga
Steven Lagana
Keith Lai
Michael Lee
Cheng-Han Lee
Madelyn Lew
Zaibo Li
Faqian Li
Ying Li
Haiyan Liu
Xiuli Liu
Yen-Chun Liu
Lesley Lomo
Tamara Lotan
Anthony Magliocco
Kruti Maniar
Emily Mason
David McClintock
Bruce McManus
David Meredith
Anne Mills
Neda Moatamed
Sara Monaco
Atis Muehlenbachs
Bita Naini
Dianna Ng
Tony Ng
Michiya Nishino
Scott Owens
Jacqueline Parai
Yan Peng
Manju Prasad
Peter Pytel
Stephen Raab
Joseph Rabban
Stanley Radio
Emad Rakha
Preetha Ramalingam
Priya Rao
Robyn Reed
Michelle Reid
Natasha Rekhtman
Jordan Reynolds
Michael Rivera
Andres Roma
Avi Rosenberg
Esther Rossi
Peter Sadow
Steven Salvatore
Souzan Sanati
Anjali Saqi
Jeanne Shen
Jiaqi Shi
Gabriel Sica
Alexa Siddon
Deepika Sirohi
Kalliopi Siziopikou
Sara Szabo
Julie Teruya-Feldstein
Khin Thway
Rashmi Tondon
Jose Torrealba
Andrew Turk
Evi Vakiani
Christopher VandenBussche
Paul VanderLaan
Olga Weinberg
Sara Wobker
Shaofeng Yan
Anjana Yeldandi
Akihiko Yoshida
Gloria Young
Minghao Zhong
Yaolin Zhou
Hongfa Zhu
Debra Zynger

To cite abstracts in this publication, please use the following format: **Author A, Author B, Author C, et al. Abstract title (abs#). In "File Title."** ***Modern Pathology*** **2020; 33 (suppl 2): page#**

1235 Prevalence of Immunopositivity for BRAF VE1 in Papillary Thyroid Carcinoma as Validated by Next-Generation Sequencing

Meghana Agni[1], Vincent Cracolici[2], Lauren Ritterhouse[3], Jeremy Segal[4], Tatjana Antic[1], Girish Venkataraman[5], Nicole Cipriani[1]
[1]The University of Chicago, Chicago, IL, [2]University of Pittsburgh Medical Center, Pittsburgh, PA, [3]Massachusetts General Hospital, Harvard Medical School, Boston, MA, [4]The University of Chicago, Riverside, IL, [5]University of Chicago Medical Center, Chicago, IL

Disclosures: Meghana Agni: None; Vincent Cracolici: None; Lauren Ritterhouse: None; Tatjana Antic: None; Girish Venkataraman: *Employee*, Sylvant; Nicole Cipriani: None

Background: Papillary thyroid carcinoma (PTC) accounts for 80% of all thyroid carcinomas. PTC is associated with a *BRAF* gene mutation that results in a valine to glutamate substitution at position 600 (V600E), constitutively activating the MAP-kinase pathway. The incidence of the *BRAF* V600E mutation in PTCs is reportedly variable (43-90%) and has been associated with aggressive tumor behavior. Treatment with targeted *BRAF*-inhibitors may be considered in some patients. Thus, the presence of this mutation may have implications for prognosis and treatment. Initially, polymerase chain reaction (PCR) and/or direct Sanger sequencing were the ubiquitous molecular techniques used for *BRAF* V600E detection, albeit expensive and time-consuming. However, multiple authors have recently shown the high specificity and sensitivity of immunohistochemistry (IHC) staining via mouse monoclonal antibody (Clone VE1) for BRAF V600E detection in PTC. While most research efforts on the latter have originated from the fields of surgery, oncology and endocrinology, the feasibility of using IHC to test for BRAF V600E in PTC specimens deserves scrutiny in the pathology literature.

Design: *BRAF* V600E IHC (VE1 clone) was performed on all non-incidental papillary carcinomas, all incidental papillary microcarcinomas 0.6 cm or larger, and any incidental papillary microcarcinomas with adverse features. We retrospectively analyzed 66 consecutive PTCs that underwent BRAF VE1 IHC at our institution from October 2018 to September 2019. Ancillary validation was performed using next-generation genomic sequencing (NGS) on 6 historic cases, 3 with diffuse weak and 3 with diffuse moderate cytoplasmic BRAF expression.

Results: Of 66 consecutive PTC cases stained by *BRAF* V600E-specific antibody IHC, 56 (85%) were positive. All 6 validation cases (weak or moderate by IHC) were positive for the *BRAF* V600E mutation by NGS.

Conclusions: The 85% incidence in this study is high, and is in agreement with recent studies evaluating classic PTCs. Lower reported incidences may have reflected potential dilution with other follicular neoplasms including NIFTP and the follicular variant of PTC. Molecular techniques, especially NGS, are not universally accessible. Using IHC to detect *BRAF* mutation is more cost and time-efficient. Due to the potential treatment and prognostic implications of *BRAF* V600E, accurate and efficient detection is critical.

1236 Variability in Depth of Invasion Measurements of Oral Tongue Carcinoma and the Effect on Pathologic T Staging

Kathy Allen-Proctor[1], Mobeen Rahman[1], Deborah Chute[2], Aaron Hoschar[2], Christopher Griffith[3]
[1]Cleveland Clinic Pathology and Laboratory Medicine, Cleveland, OH, [2]Cleveland Clinic, Cleveland, OH, [3]Cleveland Clinic Foundation, Cleveland, OH

Disclosures: Kathy Allen-Proctor: None; Mobeen Rahman: None; Deborah Chute: None; Aaron Hoschar: None; Christopher Griffith: None

Background: Depth of invasion (DOI) is a key staging criteria for carcinoma of lip and oral cavity in the 8th ed. of the American Joint Committee on Cancer (AJCC) Manual. However, there are challenges to accurately determining DOI and studies examining variability in DOI have not been reported. The aim of this study is to investigate interobserver variability in DOI measurement and its effect on stage.

Design: Our laboratory information system (CoPath) was searched for excisions of squamous cell carcinoma of oral tongue from 1/1/2014 to 12/20/2016. Slides with significant tumor were selected for independent review by 4 head and neck pathologists. DOI was determined per AJCC guidelines and pathologic stage assigned in conjunction greatest dimension. Slide used for measurement and factors potentially impeding DOI assessment were noted. Variability in DOI and assignment of tumor stage were examined. Intraclass correlation coefficient was calculated (Mangold International) to determine reproducibility in DOI.

Results: 76 cases were identified, of which 65 had slides available. Intraclass correlation coefficient adjusted single score for DOI between observers was 0.929. The same slide was used by all observers for DOI assessment in only 37% of cases. 80% (n= 52) of tumors had uniform staging amongst all observers but 20% (n=13) had differences in T stage due to individual DOI differences. Of these, 10 had average measurements < 2 mm from a staging breakpoint (5 mm or 10 mm). 2 of 3 remaining cases were noted to have ulceration and irregular mucosal surfaces, and one had distant isolated tumor nests.

Conclusions: Despite excellent interobserver agreement of DOI, a considerable number of cases had differences in tumor stage as a result of variability. Most cases with discrepant staging had DOI near the 5 mm or 10 mm breakpoints. Irregular or ulcerated surfaces and ambiguous tissue orientation were also challenges in DOI assessment. Group consensus for DOI in cases near the breakpoints or with features hindering accurate measurement may be useful to ensure more uniform staging of oral tongue carcinomas within an institution.

1237 Exploring the Genetic Differences in Oral Squamous Cell Carcinoma in Patients with Different Demographic and Risk Factor Profiles

Mekhala Anjaria[1], Dario Strbenac[2], Mark McCabe[3], Laveniya Satgunaseelan[4], John Grady[5], Kitty Lo[6], Chia-Ling Chan[5], Carsten Palme[7], Jean Yang[2], Mark Cowley[8], Jonathan Clark[9], Ruta Gupta[10]

[1]Concord Clinical School, The University of Sydney, Sydney, NSW, Australia, [2]School of Mathematics and Statistics, The University of Sydney, Sydney, NSW, Australia, [3]Garvan Institute of Medical Research, Sydney, NSW, Australia, [4]Royal Prince Alfred Hospital, Camperdown, NSW, Australia, [5]Garvan Institute of Medical Research, Darlinghurst, NSW, Australia, [6]University of Sydney, Sydney, NSW, Australia, [7]Missenden Road, NSW, Australia, [8]Children's Cancer Institute, Randwick, NSW, Australia, [9]Chris O'Brien Lifehouse, Camperdown, NSW, Australia, [10]Royal Prince Alfred Hospital, Sydney, NSW, Australia

Disclosures: Mekhala Anjaria: None; Dario Strbenac: None; Mark McCabe: None; Laveniya Satgunaseelan: None; John Grady: None; Kitty Lo: None; Chia-Ling Chan: None; Carsten Palme: None; Jean Yang: None; Mark Cowley: None; Jonathan Clark: None; Ruta Gupta: None

Background: Oral squamous cell carcinoma (OSCC) is the sixth common malignancy globally with smoking and alcohol consumption as established risk factors. A recent trend of a rising incidence has been observed in young non-smoking women. The genetic landscape of OSCC in young patients as well as non-alcoholic and non-smoking patients is not well explored. Herein, we investigate the differences in the genetic alteration amongst OSCC patients of different ages, gender, smoking and alcohol habits.

Design: Clinicopathologic data for 37 anterior oral cavity SCC treated with curative intent and with fresh frozen tissues available was obtained from the Sydney Head and Neck Cancer Institute and included demographic, smoking and alcohol data. Capture panel sequencing was performed on extracted DNA for 412 cancer- associated genes. Tumour cellularity and variant allele frequency (VAF) were used to classify germline and somatic variants. The genome aggregation database and the Exome Aggregation Consortium were used to filter common genetic alterations. SNV with a VAF of ≥5% and CADD scores of >15 classified as pathogenic or likely pathogenic in ClinVar or with affected hotspots in COSMIC were identified for further manual review using Integrated Genome Viewer. Copy number variations (CNV) were considered at a ploidy of ≤3.3 and deletions at a ploidy of ≥1.5.

Results: The cohort includes 22 males and 15 females with five patients <45 years and 32 patients >45 years. Smoking data was available in 33 with 15 smokers and 18 never smokers. Alcohol consumption information was available in 28 with 18 consumers and 10 never consumers. During a follow up period ranging 72-24 months, there were five recurrences and one death due to OSCC.

A total of 168 somatic genetic alterations were detected. The most common mutations were in *TP53* (70%), *CDK4* (27%), *NOTCH1* (22%), *CDKN2A* (19%) and *EGFR* (19%). 19 patients exhibited loss of function mutations in p53 DNA binding domain. *EGFR* amplification was significantly more frequent in patients <45 years and in non-smokers. *NOTCH1* alterations were exclusively observed in those >45 years.

Table 1 Clinicopathologic characteristics of 37 patients with oral squamous cell carcinoma

Age	<45 (%)	≥45 (%)
	5 (14)	32 (86)
Sex		
Male	2 (40)	20 (62)
Female	3 (60)	12 (38)
Smoking history		
No	4 (80)	14 (44)
Yes	1 (20)	14 (44)
Alcohol consumption		
No	3 (60)	7 (22)
Low	1 (20)	8 (25)
High	1 (20)	8 (25)
Location		
Tongue		
Right side	1 (20)	7 (22)
Left side	1 (20)	6 (19)
Right lateral border	2 (40)	5 (16)
Left lateral border	1 (20)	5 (16)
Buccal mucosa		1 (3)
Right base		2 (6)
Left base		4 (13)
Mandible		2 (6)
Differentiation		
Well		3 (9)

Moderate	3 (60)	17 (53)
Poor	2 (40)	4 (13)
Lymph node involvement		
0	3 (60)	19 (59)
1-5	2 (40)	11 (34)
>5		1 (3)
Depth of invasion		
<5 mm	2 (40)	6 (19)
5 - 10 mm	2 (40)	11 (34)
>10 mm	1 (20)	15 (47)
Pattern of invasion		
Pushing		2 (6)
Infiltrative	5 (100)	30 (94)
Margins		
Clear	4 (80)	25 (78)
Close	1 (20)	5 (16)
Involved		2 (6)
Perineural invasion		
Yes	4 (80)	13 (41)
Lymphvascular invasion		
Yes	4 (80)	16 (50)
Pathological T category		
T1		9 (28)
T2	4 (80)	16 (50)
T3	1(20)	5 (16)
T4		2 (6)
Pathological N category		
N0	2 (40)	16 (50)
N1	1 (20)	2 (6)
N2a		1 (3)
N2b	2 (40)	8 (25)
Treatment		
Surgery	3 (60)	12(38)
Surgery + radiotherapy		13 (41)
Surgery + chemotherapy	1 (20)	3 (9)
Surgery + radiotherapy + chemotherapy	1 (20)	4 (13)
Immunosuppression		
Yes	1 (20)	3 (9)
Status at follow up		
Disease free survival	4 (80)	25 (78)
Disease recurrence	1 (20)	4 (13)
Death due to disease		1 (3)

Figure 1 - 1237

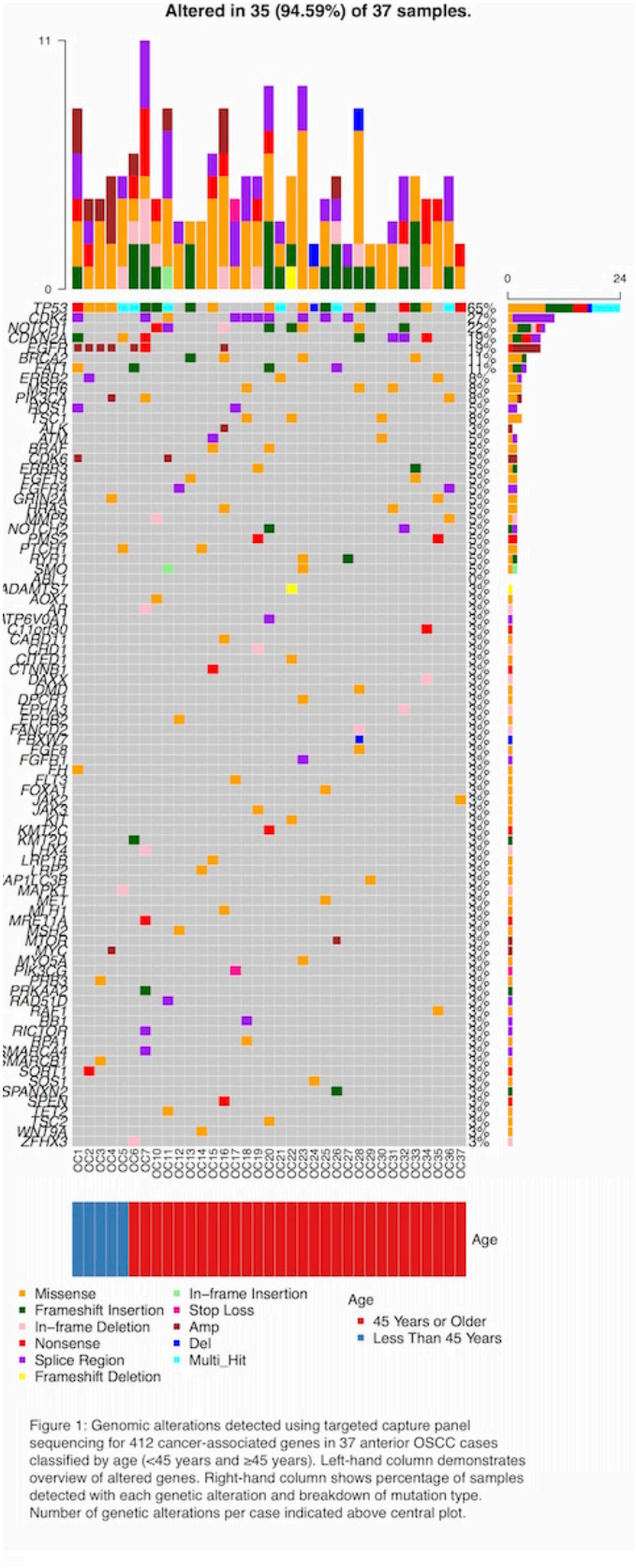

Figure 1: Genomic alterations detected using targeted capture panel sequencing for 412 cancer-associated genes in 37 anterior OSCC cases classified by age (<45 years and ≥45 years). Left-hand column demonstrates overview of altered genes. Right-hand column shows percentage of samples detected with each genetic alteration and breakdown of mutation type. Number of genetic alterations per case indicated above central plot.

Figure 2 - 1237

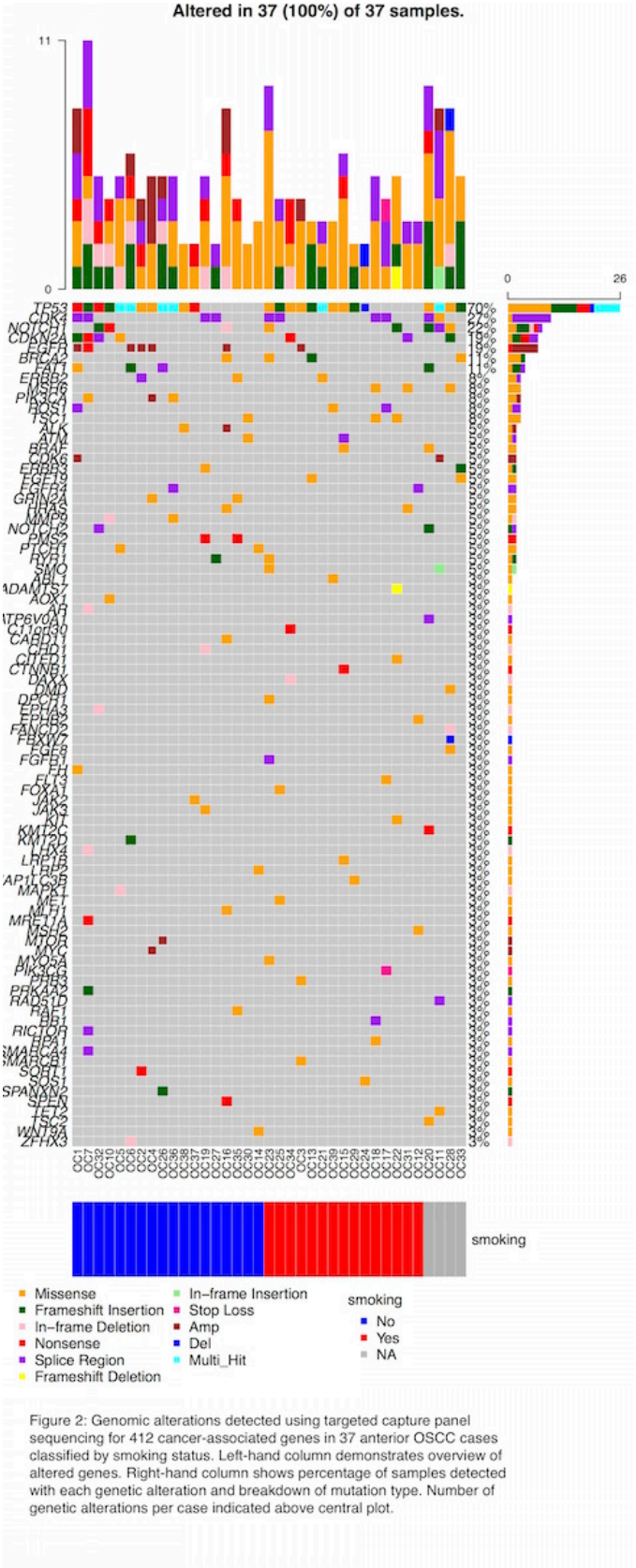

Figure 2: Genomic alterations detected using targeted capture panel sequencing for 412 cancer-associated genes in 37 anterior OSCC cases classified by smoking status. Left-hand column demonstrates overview of altered genes. Right-hand column shows percentage of samples detected with each genetic alteration and breakdown of mutation type. Number of genetic alterations per case indicated above central plot.

Conclusions: EGFR amplification and NOTCH1 dysregulation are well described in OSCC. Our preliminary analyses demonstrate that EGFR and NOTCH1 may play a role in carcinogenesis and progression in different demographic subsets of OSCC. While OSCC is rare in patients <45 years and non-smokers, this cohort may most likely to benefit from EGFR monoclonal antibody therapy.

1238 Papillary Cystic Adenocarcinoma of Minor Salivary Glands with Intestinal-Like Features. Clinicopathologic and Immunohistochemical Characteristics of 7 Cases

Prokopios Argyris[1], Lisa Rooper[2], Ioannis Koutlas[3], Justin Bishop[4]
[1]University of Minnesota, Minneapolis, MN, [2]The Johns Hopkins University School of Medicine, Baltimore, MD, [3]Malcolm Moos Health Science Tower, Minneapolis, MN, [4]University of Texas Southwestern Medical Center, Dallas, TX

Disclosures: Prokopios Argyris: None; Lisa Rooper: None; Ioannis Koutlas: None; Justin Bishop: None

Background: Intestinal-type adenocarcinomas (ITAC) of the sinonasal tract and base of the tongue are rare and reveal strong positivity for CK20 and CDX-2. However, a subset of papillary cystic adenocarcinomas with intestinal-like morphology (PCAIL) that are negative for CDX-2 and CK20 also can arise in minor salivary glands (SGs). Only two tumors with this unique morphology and immunophenotype have previously been described in the literature. Herein, we present 7 additional cases to raise awareness and understanding of PCAIL.

Design: All cases with features suggestive of PCAIL were retrieved from the archives of 3 diagnostic laboratories. The demographic, histopathologic and immunohistochemical features of the lesions, treatment and follow-up information were recorded.

Results: Seven PCAIL of minor SGs were identified with mean age 76.6 years (range= 60-94 years) and F:M ratio= 2:5. Three cases affected the tongue, 2 the buccal mucosa and 1 each the palate and the upper lip. Complete surgical excision was the treatment of choice. The patients did not have history of colonic adenocarcinoma. Microscopically, all PCAIL lacked encapsulation and exhibited pronounced cystic morphology with intraluminal papillary features, while focal cribriform architecture was seen in 3/7 lesions. The cyst-like spaces were lined by columnar or cuboidal epithelium with occasionally intestinal features and mucinous differentiation. The neoplastic epithelial cells featured cellular pleomorphism with enlarged, often hyperchromatic, round nuclei and prominent nucleoli. Rare mitotic figures were observed in 6/7 cases. By immunohistochemistry, PCAIL were consistently and diffusely positive for CK7 and cytoplasmic/membranous β-catenin, and negative for CK20, S100, calponin, α-SMA, p40, mammaglobin, TTF-1, and CDX-2. One case showed rare CDX-2 nuclear staining. Two tumors were probed and stained positively for e-cadherin, CK5/6 and CK8/18, while Ki67 ranged between 15-30%. Four patients showed no evidence of recurrence and one died of other causes during a mean follow-up period of 19.2 months (range= 4-60 months).

Conclusions: Herein, we propose PCAIL as a distinct clinicopathologic entity. The pathologist should be aware of similarities with ITAC and the presence of intestinal cytologic features in papillary adenocarcinomas. CK7, CK20 and CDX-2 immunostains aid in the differential diagnosis. Complete surgical removal appears to suffice for treatment.

1239 IgG4-Related Disease in Head and Neck – Clinicopathologic Study of 23 Cases in One Institution

Donghwa Baek[1], Paul Christensen[2], Mary Schwartz[1], Alberto Ayala[3], Jae Ro[1]
[1]Houston Methodist Hospital, Houston, TX, [2]Houston, TX, [3]The Methodist Hospital, Houston, TX

Disclosures: Donghwa Baek: None; Paul Christensen: None; Mary Schwartz: None; Jae Ro: None

Background: Immunoglobulin G4 (IgG4)-related disease (IgG4-RD) has been described in almost all organs in the body. IgG4-RD arising in the head and neck comprises a major proportion of this entity, although much of the emphasis have been placed on the salivary and lacrimal glands.

Design: Pathology reports at hour institution from January 2015 to July 2019 were carefully reviewed, and IgG4-RD cases were selected based on the morphologic features and the IgG4-RD consensus, including 1) an increased number of IgG4-positive plasma cells (more than 50/HPF) with an increase in the ratio of IgG4:IgG plasma cells of greater than 0.4, 2) sclerotic inflammation, and 3) obliterative phlebitis.

Results: The retrospective review yielded 370 cases in which IgG4-RD was suspected based on either morphologic or clinical features. Immunohistochemical staining for IgG4 with or without IgG was available in all of these cases, and 90 cases met the criteria described above. Among these, 23 cases arose in the head and neck excluding thyroid, orbit, lacrimal gland, skin, and soft tissue. Twelve patients were male, and 11 were female. The mean age of the patients was 52 years. Twelve cases arose in the mandible, and 5 cases arose in the maxilla. Accompanying pathologic findings included odontogenic cysts (8 cases), adamantinoma, fibrous dysplasia, osteonecrosis, chronic sinusitis, squamous papilloma, pseudoepitheliomatous hyperplasia, and granulomatosis with polyangiitis.

Figure 1 - 1239

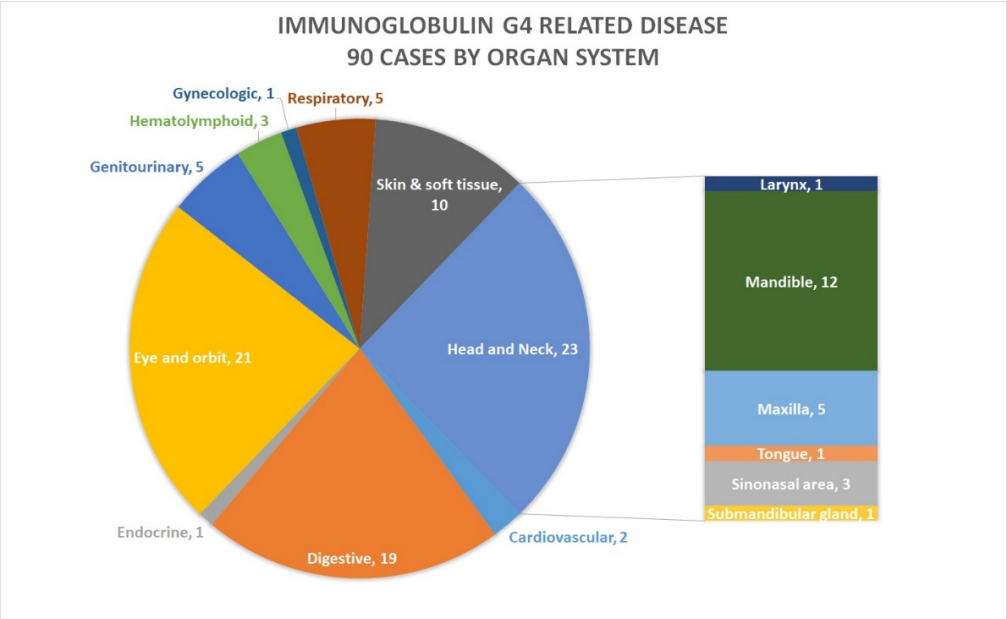

Conclusions: We report 23 cases of IgG4-RD in the head and neck, most of which arose in the mandible and maxilla rather than the salivary glands which predominate in the literature. Clinical presentation may be variable. When morphologic features of IgG4-RD including sclerotic inflammation and numerous plasma cells are present, IgG4 immunochemical stain and measurement of serum IgG4 level are recommended for accurate diagnosis and guiding clinical management.

1240 Tumor Infiltrating Lymphocytes in Head and Neck Squamous Cell Carcinoma: Characterization by Digital Image Analysis and Association with Clinicopathological Features and Survival

Javier Baena-Del Valle[1], Manuelita Ramos Calderón[1], Mauricio Palau[2], Ana Margarita Baldión-Elorza[1], Alberto Escallón-Cubillos[1], José Hakim-Tawil[1], Sandra Perdomo-Velásquez[1], Paula Andrea Rodriguez - Urrego[3]
[1]Fundacion Santa Fe de Bogota University Hospital, Bogotá, D.C., Colombia, [2]Bogotá, D.C., Colombia, [3]University Hospital Fundacion Santa Fe de Bogota, Bogotà, D.C., Colombia

Disclosures: Javier Baena-Del Valle: None; Manuelita Ramos Calderón: None; Mauricio Palau: None; Ana Margarita Baldión-Elorza: None; Alberto Escallón-Cubillos: None; José Hakim-Tawil: None; Sandra Perdomo-Velásquez: None; Paula Andrea Rodriguez - Urrego: None

Background: Head and neck squamous cell carcinoma (HNSCC) is the sixth most frequent neoplasm worldwide, with a 5-year survival of 60% approximately. Characterizing the tumor microenvironment has emerged as a new line of study in solid tumors, since quantification of tumor infiltrating lymphocytes (TILs) reflects the immune response in the tumors and helps determine patient outcome and sometimes response to therapy. In HNSCC, the role of TILs in prognosis is still controversial. It has been seen that high CD3+ and CD8+ infiltrates are often correlated with a superior overall survival, while there is no clear prognostic association with CD4+ T cells.

Design: 40 samples (20 oral cavity, 14 oropharynx and 6 larynx) from HNSCC patients from the Colombian cohort of the InterCHANGE study (IARC, Lyon, France) were included. Mean follow up time was 36 and 35 months from diagnosis and treatment initiation respectively. Low-density TMAs were constructed using a core size of 5 mm. Immunohistochemistry for CD3 (clone 2GV6, Roche), CD4 (clone 4B12, Dako), CD8 (clone SP57, Roche) and PD-L1 (clone SP263 Ventana and clone 22C3 Dako) was performed. Using QuPath v0.2.0-m4 software, the intratumor stromal areas were isolated with the "Pixel Classifier" tool and TILs within these areas were detected by using the "Positive cell detection" tool.

Results: The average age of the patients was 65±2.04. High CD8+ infiltrates were predominantly observed in the oropharynx tumors (37% and 64% higher than oral cavity and larynx tumors, respectively). Higher CD4+ and CD3+ infiltrates were associated with frequent alcohol consumption. Tumors rich in CD8+ T cells were associated with p16 positivity (p=0.0460) and positive lymph nodes at diagnosis (p=0.0369). In this study, CD3+, CD4+ and CD8+ TILs had no significant association with smoking status, PD-L1 expression, pathological stage and recurrence. There was a trend towards improved overall survival in patients with higher CD3+, CD4+ and CD8+ infiltrates. However, only high CD4+ expression was statistically significant.

Conclusions: Understanding the role tumor microenvironment in HNSCC could lead to the use of TILs as prognostic markers and help develop more precise and effective therapies. However, further studies with more samples and longer follow up time are needed in order to identify its prognostic value and to help standardize a reproducible and practical measurement of TILs in tumor samples.

1241 Neuroendocrine Carcinomas of the Larynx: Case-Series at a Single Tertiary-Care Oncology Centre

Munita Bal[1], Asawari Patil[2], Neha Mittal[3], Swapnil Rane[1]
[1]Tata Memorial Centre, Mumbai, India, [2]Tata Memorial Centre, Thane (west), Maharashtra, India, [3]Tata Memorial Hospital, Mumbai, Maharashtra, India

Disclosures: Munita Bal: None; Asawari Patil: None; Neha Mittal: None; Swapnil Rane: None

Background: Primary neuroendocrine carcinomas (NECs) of the larynx are rare and heterogeneous group of neoplasms. Laryngeal NEC encompass well-differentiated (WDNECs, G1), moderately-differentiated (MD-NEC, G2) and poorly-differentiated neuroendocrine carcinomas (PDNEC, G3). We aimed to study the clinicopathologic spectrum of these rare neoplasms.

Design: A retrospective review of clinicopathologic features of all primary laryngeal NEC diagnosed from 2005-2019 as per the WHO 2017 classification was undertaken

Results: A total of 27 patients were included. The median age was 60 years with a male preponderance (M:F ratio of 8:1). Supraglottis (n=19) was the commonest location followed by glottis (n=5) and subglottis (n=3). 11 (41%) patients had distant metastasis at presentation. Majority (67%) tumors were poorly-differentiated and included 16 small cell carcinoma and 2 large cell NEC cases. One-third cases were moderately-differentiated NEC. There were no well-differentiated NECs in our cohort. Among G2, tumor cells were epithelioid (2), plasmacytoid (3), clear (2), oncocytic (1) and rhabdoid (1). G2 tumors displayed organoid, solid and trabecular patterns; calcification (n=3) and intranuclear inclusions (n=2) were identified. Four G3 tumors had a mitotic rate <10/10 HPF with Ki-67 >55%. On immunohistochemistry, tumor cells expressed AE1/E3 (80%), synaptophysin (100%), chromogranin (100%), CD56 (100%), calcitonin (32%). INI1 (n=5) and ATRX (n=3) loss was not seen. p53 overexpression (8/9) and diffuse p16 immunoreactivity (4/4) was observed in small cell carcinoma. Among G2 cases, lymph node (52%) and distant metastasis (35%) was observed while G3 cases showed nodal (55%) and distant metastasis (80%).

Tumor type	Grade	N	Distant metastasis at presentation	Necrosis	Mitotic rate/10 HPF (range)	Ki67 (range)
Well-differentiated NEC (WD-NEC)	1	0		-	-	-
Moderately-differentiated NEC (MD-NEC)	2	9 (33%)	3	2 (22%)	2-5	5-18
Poorly-differentiated NEC (PD-NEC)						
Small cell carcinoma	3	16 (60%)	7	10 (63%)	5-25	55-80%
Large cell neuroendocrine carcinoma	3	2 (7%)	1	2 (100%)	10-22	75-80%

Conclusions: Laryngeal NEC are rare and aggressive neoplasms with a high rate of nodal and distant metastasis. WD-NEC are uncommon among laryngeal NEC. Ki-67 should be included in the grading of these tumors.

1242 What Hides Behind S100 protein/SOX10 Positive Oncocytomas of the Salivary Glands?

Martina Baneckova[1], Petr Martinek[2], Nikola Ptakova[3], Olga Stanowska[4], Adela Sukenikova[5], Marketa Horakova[6], Michal Michal[2], Ilmo Leivo[7], Alena Skalova[8]
[1]Charles University, Faculty of Medicine in Plzen, Pilsen, Czech Republic, [2]Biopticka laborator s.r.o., Plzen, Czech Republic, [3]Molecular and Genetic Laboratory, Biopticka Lab, Ltd, Plzen, Czech Republic, [4]Department of Pathology, Maria Sklodowska-Curie Cancer Center - Institute of Oncology, Warsaw, Poland, [5]Department of Pathology, Charles University, Faculty of Medicine in Plzen, Plzen, Czech Republic, Pilsen, Czech Republic, [6]Charles University, Plzen, Czech Republic, [7]University of Turku, Turku, Varsinais-Suomi, Finland, [8]Charles University, Faculty of Medicine in Plzen, Plzen, Czech Republic

Disclosures: Martina Baneckova: None; Petr Martinek: None; Nikola Ptakova: None; Olga Stanowska: None; Adela Sukenikova: None; Marketa Horakova: None; Michal Michal: None; Ilmo Leivo: None; Alena Skalova: None

Background: Oncocytomas (OC) are rare benign salivary gland tumors composed of the mitochondria-rich epithelial cells (oncocytes), mostly localized in the parotid gland. Malignant transformation is exceedingly rare. The treatment of choice is simple excision. Oncocytic

metaplasia is a well-known phenomenon in a variety of salivary gland tumors, including pleomorphic adenoma (PA) and myoepithelioma (ME). Extensive oncocytic transformation of PA/ME could be diagnostically challenging and may masquerade correct diagnosis. These tumors should be treated more aggressively compared to OC, given to the risk of frequent recurrences, and the possibility of malignant transformation to carcinoma ex PA/ME.

Design: A retrospective review of Salivary Gland Tumor Registry of the author's files (SA and MM) was conducted searching for “low grade/uncertain oncocytic tumor”, “oncocytoma” and “oncocytic PA/ME”. The search yielded 128 cases, including 78 OC, 49 oncocytic PA/ME and 1 oncocytic adenocarcinoma not otherwise specified (AdcaNOS). All these cases were investigated immunohistochemically (IHC) for S100 protein and SOX10. The tumors with IHC expression of one or both markers were tested by next-generation sequencing (NGS) using fusion-detecting panels. NGS results were confirmed by reverse transcription-polymerase chain reaction (RT-PCR) and/or fluorescence in situ hybridization (FISH).

Results: Ten cases originally diagnosed as benign OC (10/78) and one AdcaNOS (1/1) revealed nuclear-cytoplasmic and/or nuclear stain for S100 protein and SOX10, respectively. Fusion transcripts *GEM-PLAG1, FUS-PPARG* and *CHCHD7-PLAG1* were found in three cases (one fusion in each case), these were confirmed by FISH *PLAG1* break-apart probe. And the other seven cases were positive for *PLAG1* rearrangement by FISH. In the control group of 49 oncocytic ME/PA, 3 tumors (3/18 tested) harbored *NFT3-PLAG1*, *CHCHD7-PLAG1* and *CIC-TFG* fusions detected by NGS. The first two fusions were confirmed by RT-PCR, while *CIC* gene fusion was not analyzable by FISH break-apart probe.

Conclusions: SOX10 and/or S100 protein immunopositivity in conjunction with molecular profiling, particularly detection of rearrangement of the *PLAG1* gene, helps to reclassify subset of oncocytomas as oncocytic variants of PA and ME. Therefore, we recommend to include S100 protein and SOX10 into the investigative IHC panel when diagnosing tumors with predominant oncocytoma-like differentiation.

1243 Report of 20 Cases of Seromucinous Hamartomas and Respiratory Epithelial Adenomatoid Hamartomas with Dysplastic and Malignant Features

Martina Baneckova[1], Tomas Vanecek[2], Jan Laco[3], Martin Hyrcza[4], Stephan Ihrler[5], Niels Rupp[6], Fredrik Petersson[7], Olena Koshyk[8], Dominic Spagnolo[9], Manuel Schlageter[10], Ksenia Shelekhova[11], Alena Skalova[12], Michal Michal[2]
[1]Charles University, Faculty of Medicine in Plzen, Pilsen, Czech Republic, [2]Biopticka laborator s.r.o., Plzen, Czech Republic, [3]The Fingerland Department of Pathology, Charles University, Faculty of Medicine and University Hospital, Hradec Kralove, Czech Republic, [4]University of Calgary/Alberta Public Laboratories, Calgary, AB, [5]Dermpath, Muenchen, Germany, [6]Institute of Pathology and Molecular Pathology, University Hospital Zurich, Zurich, Switzerland, [7]National University Hospital, Singapore, Singapore, [8]CSD Health Care Pathology lab, Kyiv, Kyivska, Ukraine, [9]Path West Laboratory Medicine, Nedlands, WA, Australia, [10]Viollier AG, Allschwil, Baselland, Switzerland, [11]SPb Clinical Research and Practical Center for Specialized Oncological Care, Saint-Petersburg, Russian Federation, [12]Charles University, Faculty of Medicine in Plzen, Plzen, Czech Republic

Disclosures: Martina Baneckova: None; Tomas Vanecek: None; Jan Laco: None; Martin Hyrcza: None; Stephan Ihrler: None; Niels Rupp: None; Fredrik Petersson: None; Olena Koshyk: None; Dominic Spagnolo: None; Manuel Schlageter: None; Ksenia Shelekhova: None; Alena Skalova: None; Michal Michal: None

Background: Seromucinous hamartomas (SH) of the sinonasal tract are rare and underestimated lesions. They are separate entities among the group of epithelial hamartomas including respiratory epithelial adenomatoid hamartoma (REAH) and nasal olfactory hamartoma. The term hamartoma describes an indolent entity without neoplastic potential, however, SH does not behave accordingly.

Design: 20 cases of “dysplastic” polypoid lesions diagnosed as REAH and SH (13/20) (Fig.1), adenoid cystic carcinoma *ex* SH (Fig.2), and low-grade tubulopapillary adenocarcinoma *ex* SH were retrieved from the authors' files. Histology and immunohistochemical stains were reviewed by the authors, and seventeen cases were also examined by fluorescence in situ hybridization (FISH) and next-generation sequencing (NGS) using fusion-detecting panels.

Results: There were 13 males and 6 females, the median age was 58.4. The average size of the lesions was 28 mm. Cases were treated by polypectomy or endonasal resection, and in two cases by adjuvant radiotherapy. Recurrence occurred in three patients and pulmonary metastases in one. Seventeen SH gave rise to cystically dilated irregular glands lined by atypical irregular epithelium having luminal snouts, and secretory product, occasionally colloid-like, was present in 19 cases. The atypical glands arising from SH showed transitions to adenoid cystic carcinoma (AdC) (5/20) and low-grade tubulopapillary adenocarcinoma (2/20). Cartilaginous (1/20), osseous (2/20), adipose (2/20) or sebaceous (1/20) metaplasia occurred in 6 cases. Dense fibrous stroma occurred in all cases. Immunohistochemical expression of p63 marker was patchy or negative in SH but preserved in AdC. A biphasic phenotype was seen in S100 protein and SOX10 expression which were positive in the seromucinous component but negative in the AdC component. Three cases were positive for *MYB-NFIB*, one for *MYBL1-NFIB* and one for *EGFR-ZNF267* fusions, and one case was positive for low-risk HPV type 42.

Figure 1 - 1243

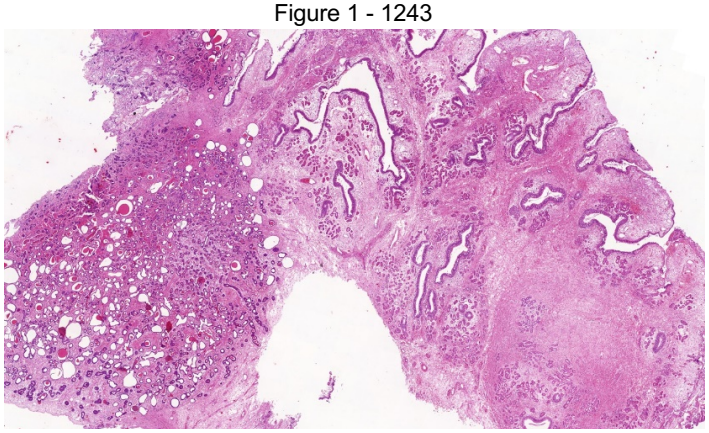

Figure 2 - 1243

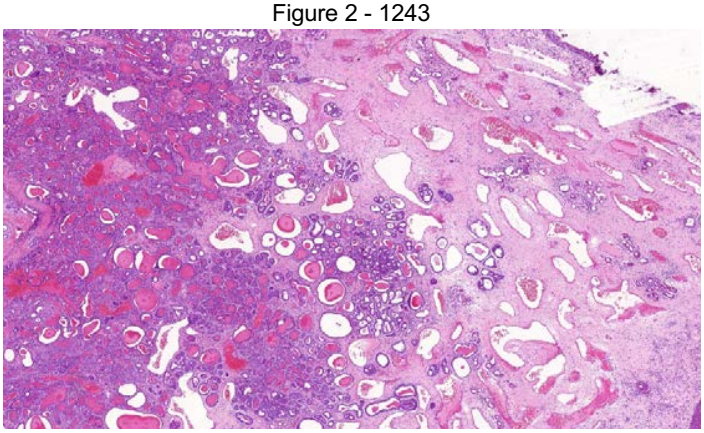

Conclusions: The term seromucinous hamartoma is a misnomer. Rather, it should be considered a benign neoplastic lesion having the potential for malignant transformation. This is supported histologically by the occurrence of various mesenchymal and epithelial metaplasias, glandular atypia and direct transitioning of SH into AdC or low-grade tubulopapillary adenocarcinoma, and immunohistochemically by virtue of complete or focal loss of the p63 positive myoepithelial layer and S100 protein expression in SH.

1244 Detection of High-Risk HPV (hrHPV) by P16 Immunohistochemistry (IHC) and In-Situ Hybridization (ISH) in Sinonasal Undifferentiated Carcinoma (SNUC)

Ezra Baraban[1], Ching Tong[2], Nithin Adappa[2], Kumarasen Cooper[1]
[1]University of Pennsylvania, Philadelphia, PA, [2]Hospital of the University of Pennsylvania, Philadelphia, PA

Disclosures: Ezra Baraban: None; Kumarasen Cooper: None

Background: SNUC is an aggressive high grade malignancy and a diagnosis of exclusion. Recent studies have shown SNUC to be a heterogeneous entity; careful attention to morphology and a complete IHC workup frequently enable more precise classification, often with important prognostic and therapeutic implications. Recent evidence strongly implicates hrHPV in the pathogenesis of sinonasal carcinomas, indicating that the sinonasal tract is a hotspot for hrHPV induced carcinogenesis. A small number of studies, none including more than 20 cases, have used a variety of methods to investigate SNUC for the presence of hrHPV, with rates of viral detection ranging from 0 to 64% across studies. We hypothesized that a subset of cases previously diagnosed as SNUC in our pathology archives may in fact represent hrHPV associated carcinomas. Using a simple reflex based approach, we tested all cases for P16 by IHC, and conducted ISH in all P16+ cases.

Design: P16 IHC (clone E6H4, Ventana 9517) was conducted on a representative whole-tissue section from 25 available SNUC cases. P16+ cases (defined by >70% nuclear and cytoplasmic staining) were selected for ISH using RNAScope (Leica DS9790) for 18 strains of hrHPV (ACD, Cat# 312598) according to manufacturer instructions.

Results: 12 of 25 cases were P16+ by IHC. Of these, 5 cases were positive for hrHPV by ISH. Thus, 20% of all SNUC cases (5/25) were positive for hrHPV by ISH, and 41% of P16 positive cases were positive for hrHPV by ISH. We acknowledge that our study may underestimate the true prevalence of hrHPV+ cases in our cohort, because we only performed ISH in cases that were P16+ by IHC.

Conclusions: We investigated the largest series to date of SNUC cases by P16 IHC and broad spectrum ISH covering 18 types of hrHPV, and identified hrHPV in a substantial percentage of cases (20%). Given the dramatic differences in biologic behavior and therapeutic responsiveness at other tissue sites between HPV associated and unassociated malignancies, we believe our findings may have important implications for future workup of sinonasal malignancies where the differential diagnosis includes SNUC. Our study establishes a significant prevalence of hrHPV in cases previously diagnosed as SNUC. Future work will investigate differences in clinical behavior and therapeutic responsiveness between HPV positive and negative cases.

1245 Nuclear NR4A3 Expression Distinguishes Low-Grade Acinic Cell Carcinoma from Anorexia/Bulimia-Related Sialadenosis of the Salivary Gland

Felicita Baratelli[1], Bonnie Balzer[2], Wonwoo Shon[2]
[1]UCLA-Olive View, Sylmar, CA, [2]Cedars-Sinai Medical Center, Los Angeles, CA

Disclosures: Felicita Baratelli: None; Bonnie Balzer: None; Bonnie Balzer: None; Wonwoo Shon: None

Background: Acinic cell carcinoma is a malignant salivary gland tumor recently characterized by recurrent chromosomal rearrangement, t(4;9)(q13;q31), which results in upregulation of the transcription factor NR4A3. A prior study using a monoclonal antibody NR4A3 (NOR-1) indicated that its nuclear staining is a sensitive and specific diagnostic marker for acinic cell carcinoma. Sialadenosis is a reactive process of the salivary gland and has been associated with eating disorders such as anorexia and bulimia. Given its significant histologic overlap with low-grade acinic cell carcinoma, anorexia/bulimia-related sialadenosis can be difficult to diagnose without appropriate clinical history. The purpose of this study was to evaluate NR4A3 nuclear immunoreactivity in a series of anorexia/bulimia-related sialadenosis and low-grade acinic cell carcinoma

Design: Formalin-fixed, paraffin-embedded whole tissue sections from 12 cases of low-grade acinic cell carcinoma and 5 cases of anorexia/bulimia-related sialadenosis were retrieved from our surgical pathology archives. An automated immunohistochemistry system (Bond-III, Leica) was used for the detection of NR4A3, using a commercially available antibody (sc-393902 [H-7], 1:100 dilution, Santa Cruz Biotechnology Inc.). Nuclear staining was scored as negative (<5%), or positive 1+ (5-25%), 2+ (26-50%), 3+ (>51%).

Results: Distinct nuclear staining for NR4A3 was observed in all 12 low-grade acinic cell carcinoma cases (3+: 11 cases and 2+: 1 case). Morphologically, anorexia/bulimia-related sialadenosis showed marked acinar cell enlargement with abundant granular-appearing cytoplasm; in many areas, they were closely resembling low-grade acinic cell carcinoma. NR4A3 expression was completely absent in all evaluated cases of anorexia/bulimia-related sialadenosis

Conclusions: Diagnostically challenging examples of anorexia/bulimia-related sialadenosis may be distinguished from low-grade acinic cell carcinoma by the use of NR4A3 immunohistochemistry, especially if there is limited clinical information.

1246 The Tumor Immune Contexture of Androgen-Resistant Salivary Duct Carcinoma

Diana Bell[1], Michael Tetzlaff[1], Michael Suchko[1], Ehab Hanna[1], Randal Weber[1], Renata Ferrarotto[1]
[1]The University of Texas MD Anderson Cancer Center, Houston, TX

Disclosures: Diana Bell: None; Michael Tetzlaff: *Speaker*, Nanostring; *Advisory Board Member*, Novartis LLC; *Advisory Board Member*, Myriad Genetics; *Advisory Board Member*, Seattle Genetics; Michael Suchko: None; Ehab Hanna: None; Randal Weber: None; Renata Ferrarotto: *Advisory Board Member*, Ayala, Sanofi-Regeneron, Medscape, Klus

Background: Salivary duct carcinoma (SDCa) is an aggressive malignancy, presenting de novo or as carcinoma transformation of pleomorphic adenoma in patients of both sexes. SDCa often presents with loco regionally advanced disease or distant metastases, and majority of patients succumb to treatment-resistant disease. Therapies such as androgen-deprivation therapy (ADT) and HER2 inhibition have achieved some promising clinical responses. However, intratumoral heterogeneity of both salivary duct carcinoma cells themselves and immune composition of the tumor microenvironment are important considerations for therapy.

Recently, it has been appreciated that immune cells within the tumor microenvironment (TIME) contribute to tumor progression and, importantly, to the tumor's response to therapy. The efficacy of immunotherapy for SDCa is incompletely understood and demands additional investigation. To understand the specific roles different immune cell types play, we profiled the immune cell composition of SDCa.

Design: We analyzed tumor-infiltrating immune cells (CD163, CD20, CD25, CD3, CD4, CD8, Lag3) by immunohistochemistry in a series of 18 SDCa. Automated image analysis quantified immune cell density at tumor periphery/center/hotspot.

Results: The clinicopathological characteristics of the cohort were the following: equal sex distribution(9 M, 9F), age 42-85 yo; 13 SDCa de novo, 5 SDCa-ex PA. Outcomes: 7 patients DOD, 5 deceased of unrelated causes, 6 NED. Her-2 neu was overexpressed (score 2-3) in 61% (11/18), negative in 28% (5/11), n/a 11% (2/18). AR status: expression: IHC- nuclear localization in 67% (12/18), nuclear/cytoplasmic in 16.5% (3/18), negative in 16.5% (3/18); isotype (PCR/WB)- WT in 39% (7/18); WT, v7 39% (7/18), WT, v45 6% (1/18), negative 16% (3/18). Detailed distribution of TIME according to AR splicing variants and outcomes in Table 1.

	CD163 %	CD20 %	CD25%	CD3%	CD4%	CD8%	Lag3%
AR-WT	13.01	2.4	1.42	3.78	6.35	5.58	6.68
AR-WT, v7	17.75	1.43	1.61	4.65	5.98	6.57	11.71
AR-Negative	27.3	2	2.6	14.2	10.83	20.36	4
DOD	14.75	1.60	1.35	2.98	6.57	5.35	7.9
NED	19.93	3.11	2.1	5.03	8.9	7.21	3.15
Deceased unrelated	18.74	1.58	1.7	10.46	6.82	11	12.52

Conclusions: SDCa immune subpopulation profiles, determined by IHC-based computer analysis, identify subtle differences between AR variants groups. Tumors from patients with poor outcomes exhibited lower densities of tumor associated CD20, CD3CD4, CD8, CD163 and enrichment of Lag3. Further understanding the crosstalk between immune cell distribution and AR variants may contribute to new immune and androgen-targeted therapies for SDCa.

1247 Pleomorphic Adenoma: Confirming Known and Novel Fusion Partners Using Diagnostic RNA-Sequencing

Justin Bubola[1], Christina MacMillan[1], Rose Chami[2], Elizabeth Demicco[1], Iona Leong[3], David Swanson[1], Ilan Weinreb[4], Brendan Dickson[3]
[1]Mount Sinai Hospital, Toronto, ON, [2]The Hospital for Sick Children, Toronto, ON, [3]Mount Sinai Health System, Toronto, ON, [4]University Health Network, Toronto, ON

Disclosures: Justin Bubola: None; Christina MacMillan: None; Rose Chami: None; Elizabeth Demicco: None; Iona Leong: None; David Swanson: None; Ilan Weinreb: None; Brendan Dickson: None

Background: Pleomorphic adenoma (PA) is the most common salivary gland tumor. A majority harbor fusion products involving *PLAG1*, which has numerous potential partners including: *CHCHD7*, *CTNNB1, FGFR1, LIFR*, and *TCEA1*. A minority have fusion products involving *HMGA2*, which likewise has multiple potential partners including: *FHIT*, *NFIB*, and *WIF1*. Given their morphologic heterogeneity, PAs occasionally pose a diagnostic challenge, particularly on limited sampling; in these situations molecular testing may be of potential diagnostic value. The intent of this study was to better define the diversity of molecular alterations in PA using targeted RNA sequencing (RNA-Seq).

Design: A retrospective archive review was performed for cases diagnosed as PA (2017-2019) The cases were re-reviewed to confirm the diagnosis. Those with a representative formalin-fixed paraffin-embedded tissue block containing adequate material for testing were selected for targeted RNA-Seq using the Illumina TruSight RNA Fusion panel (Illumina, CA).

Results: A total of 23 PA were identified, including 2 carcinoma ex-PA (carcinoma and adenocarcinoma, NOS). The average patient age was 48 years (range, 9-78), and included 15 females. The most common location was parotid (N=15), followed by submandibular (N=4) and minor salivary glands (N=2), and neck NOS (N=2). Known *PLAG1* partners included *ACTA2* (N=1 [previously described in a myoepithelial carcinoma]), *CTNNB1* (N=4) and *LIFR* (N= 1); known *HMGA2* partners included *NFIB* (N=1), and *WIF1* (N= 3). Novel *PLAG1* partners included *CALM2*, *DSTN*, *NCALD*, *NTF3,* and *MEG3* (N=1). In addition, two cases contained fusion products involving *PRB2*; however, both involved partial exons, thus their significance is currently uncertain. The remaining cases were technically successful but failed to show gene fusions (N=6). There was no apparent correlation between morphology, or anatomic location, with the fusion.

Conclusions: In this modest cohort of PA targeted RNA-Seq successfully confirmed multiple established fusion genes, in addition to revealing 5 novel *PLAG1* partners. Our observation that up to 35% of cases may lack a *PLAG1* or *HMGA2* rearrangement suggests a limitation of this assay that may be attributable to: (1) its limitation to detecting fusions, and not amplification events, and/or (2) the potential existence of fusion events beyond the genes covered by the assay.

1248 Osteoarthritis in the Head of the Stapes in Otosclerosis

Anna-Lee Clarke[1], Jerome Taxy[2]
[1]University of Chicago (Evanston-Northshore), Evanston, IL, [2]NorthShore University HealthSystem, Evanston, IL

Disclosures: Anna-Lee Clarke: None; Jerome Taxy: None

Background: Otosclerosis is a Pagetoid proliferation of bone affecting the otic capsule. This sclerotic process results in an ankylosis of the stapes footplate and a clinical mostly conductive hearing loss. The surgical treatment involves resection of the stapes above the level of the footplate with insertion of a prosthesis. Embroyologically, the 3 ear ossicles form through endchondral ossification, similar to long bones and interface with each other via articular cartilage. While the histologic changes of otosclerosis have not been described in stapedectomy specimens, given the mechanical rigidity affecting the stapedal head and its articulation with the incus, osteoarthritic changes might be

anticipated, similar to what is encountered in long bone joint replacements. This study examines:1)otosclerosis in the stapes 2)osteoarthritis related changes at the articular surface of the stapedal head.

Design: A retrospective search, for the period of 2008-19,of the NorthShore University HealthSystem surgical pathology accession system retrieved patients with a clinical and pathological diagnosis of otosclerosis. Of the 84 cases found,14 were excluded due to poor embedding or specimen orientation. H&E sections were reviewed. Histologic parameters recorded were: fissuring of the articular surface, irregularity of the osteochondral junction, cartilaginous erosion,subchondral cyst, osteophyte formation.

Results: In the remaining 70 cases, no changes of otosclerosis in the crura or head of the stapes were present. The bone/cartilage interface of the stapes head showed mild and marked irregularity in 51 & 6% of cases, respectively.47 & 6% of cases showed mild and marked cartilagenous erosion of the stapes head respectively. Other histological features included,70% surface fissuring with occasional osteophyte formation,8.5% (Fig.1).There were single cases of intracartinalginous cyst and subchondral histocytes.

Figure 1 - 1248

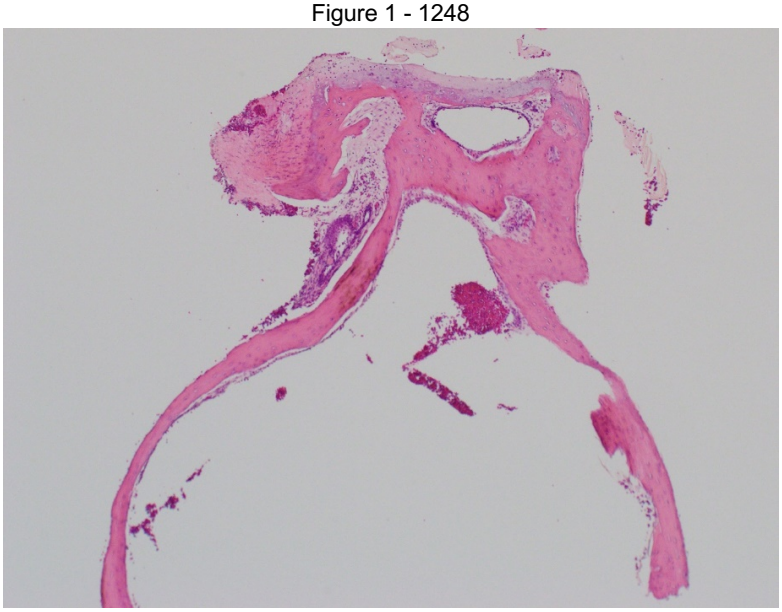

Conclusions: In this study, the sclerotic bony changes of otosclerosis did not involve the crura or subchondral head of the stapes. This may be related to the operative preservation of the foot plate, to accommodate the prosthesis. Mild changes of osteoarthritis affect the head of the stapes as it articulates with the incus. These changes include mild to marked fibrocartilaginous fissuring, erosions and interface change of the bone/cartilage interface and osteophyte formation. These changes are likely mechanical in origin.

1249 Oral Microbiome Changes Associated with Oral Squamous Cell Carcinoma and Salivary Gland Tumors

Katherine Cochrane[1], Mircea Podar[2], Eric Carlson[3], Zamin Yang[4], Laurentia Nodit[3]
[1]University of Tennessee Medical Center Knoxville, Knoxville, TN, [2]Oak Ridge National Laboratory, Oak Ridge, TN, [3]University of Tennessee Graduate School of Medicine Knoxville, Knoxville, TN, [4]Oak Ridge National Laboratory, Knoxville, TN

Disclosures: Katherine Cochrane: None; Mircea Podar: None; Eric Carlson: None; Zamin Yang: None; Laurentia Nodit: None

Background: The homeostasis of the oral microbiome is the result of interaction between host and a large variety of microbes; it plays a major role in the balance between health and disease with significant implications in preventive medicine, diagnostics and treatment. Known non-microbial risk factors for oral squamous cell carcinoma (SCC) and salivary gland tumors do not account for all disease cases; it is possible that specific oral pathogens, periodontal disease and overall poor oral health may play etiological roles. Bacteria are thought to contribute to carcinogenesis via inhibition of apoptosis, activation of cell proliferation, production of carcinogens and most importantly promotion of chronic inflammation. In this pilot study we make a comparative analysis on the potential role of oral salivary and biofilm microbiota in patients with SCC, salivary gland tumors, and healthy controls.

Design: Oral swabs from tumor surface and contra-lateral normal buccal mucosa, as well as tumoral tissue were collected intraoperatively from seven patients with benign salivary gland tumors (Warthin's and adenomas), nine patients with SCC, and seven healthy volunteers. Total genomic DNA was extracted using standard protocols, the V4 hypervariable region of the small subunit bacterial ribosomal RNA gene

was amplified using universal primers and sequenced on an Illumina MiSeq platform. Bacterial diversity was analyzed using the QIIME2 platform, looking at taxonomic classification, diversity indices and correlated with clinical parameters.

Results: Swabs from the tumor and overlying mucosae in SCC patients showed a greater diversity of microbes compared to that of the healthy group. Fusobacterium, Porphyromonas, and Parvimonas were increased compared to healthy or contralateral swabs. Streptococcus and Haemophilus were also decreased in SCC patients. Saliva samples and contralateral mucosal swabs of SCC patients revealed similar microbiota to those of healthy patients. In contrast, salivary gland tumors showed little bacterial DNA with decrease in Fusobacterium compared to healthy group or SCC cases.

Figure 1 - 1249

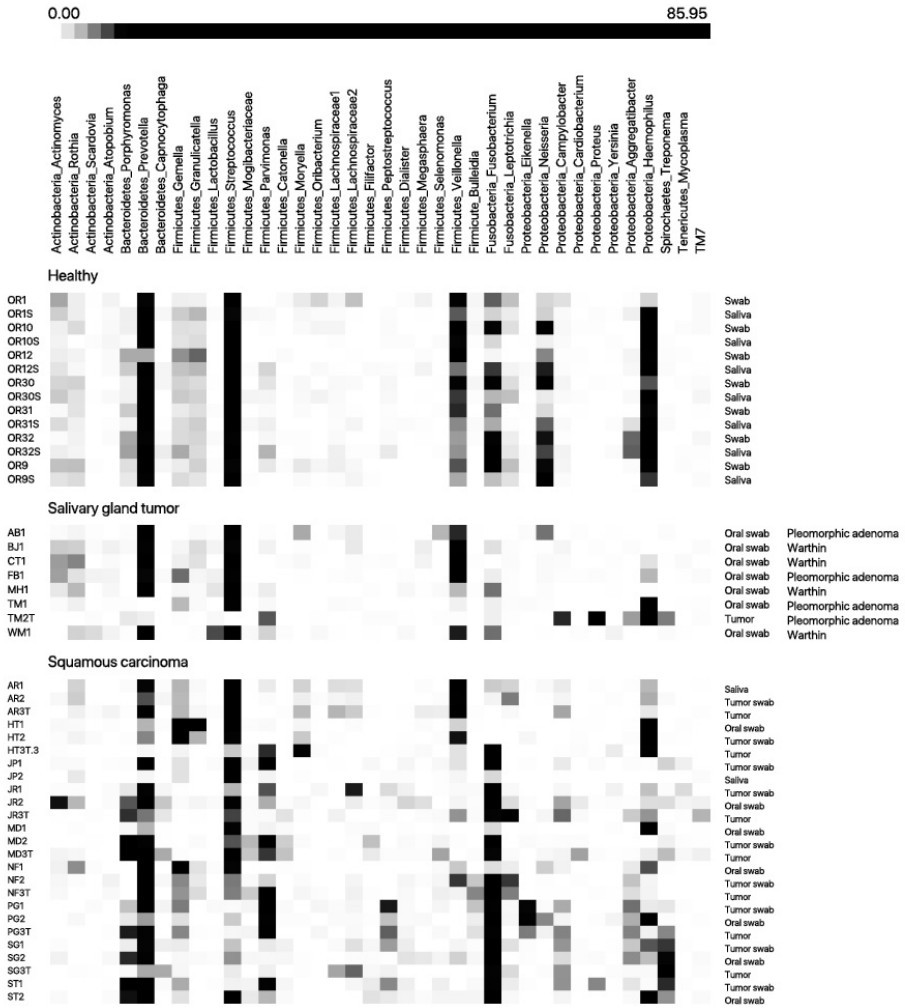

Conclusions: Microbiota appears to potentially play a greater role in the pathogenesis of SCC as compared to salivary gland tumors. Although a larger cohort will need to be analyzed to increase statistical robustness, the use of microbial biomarkers has emerged as a promising new approach for the development of novel diagnostic tools and therapeutic interventions.

1250 The Spatial Patterns of Tumor-Infiltrating Lymphocytes (TILs) are More Prognostic Than TIL Density in p16+ Oropharyngeal Squamous Cell Carcinoma Patients

German Corredor[1], James Lewis[2], Cheng Lu[1], Paula Toro[3], Pingfu Fu[4], Wade Thorstad[5], Justin Bishop[6], Farhoud Faraji[7], Anant Madabhushi[1]

[1]Case Western Reserve University, Cleveland, OH, [2]Vanderbilt University, Nashville, TN, [3]Bogotá, D.C., Colombia, [4]Broadview Heights, OH, [5]Washington University in St. Louis, St. Louis, MO, [6]University of Texas Southwestern Medical Center, Dallas, TX, [7]University of California San Diego, San Diego, CA

Disclosures: German Corredor: None; James Lewis: None; Cheng Lu: None; Paula Toro: None; Pingfu Fu: None; Wade Thorstad: *Employee*, Spouse works for Elekta, Inc; Justin Bishop: None; Farhoud Faraji: None; Anant Madabhushi: *Consultant*, Inspirata Inc.; *Stock Ownership*, Inspirata Inc

Background: Patients with p16+ oropharyngeal squamous cell carcinoma (OPSCC) are at high risk (up to 36%) of disease recurrence within 8 years of treatment. The density of tumor-infiltrating lymphocytes (TILs) on H&E-stained whole slide images (WSIs) has been shown to be prognostic in different types of cancer. Recent work has also suggested that spatial interplay between TILs and cancer nuclei may be even more prognostic than TIL density alone. In this work, we introduce and evaluate a new computerized strategy to capture the spatial arrangement and interplay between TILs & non-TILs (cancer cells, macrophages) on WSIs and evaluated the ability of this data in predicting disease-free survival (DFS) in OPSCC patients.

Design: WSIs from a cohort of 173 patients (treated at two independent institutions between 2009 and 2013) were retrospectively collected and used for this work. The cohort was split based on the institution into training (n=66) and validation (n=107) sets. Using a nuclei segmentation method in conjunction with a machine classifier, 4 types of nuclei (TILs and non-TILs in both stromal and epithelial regions) were identified. Cell clusters for each cell type were then constructed from which a set of features relating to neighborhood relationships, graph measures, and grouping degree were extracted. A linear discriminant classifier was trained to predict recurrence using the top 10 features identified via the Minimum Redundancy Maximum Relevance algorithm. For comparison, we also trained a model using only TIL-density-related features. Kaplan-Meier survival analysis was used to examine the difference of recurrence between different patient groups categorized by the classifiers.

Results: The TIL interplay and density models were applied on the validation set and achieved areas under the receiver operating characteristic curve of 0.68 and 0.49, respectively (Fig 1). Patients identified by the TIL interplay classifier as having recurrence had statistically significantly worse disease-specific survival (Fig 2). The hazard ratio was 2.88 (95% confidence interval: 1.07-7.74, p=0.03), so patients with high risk were approximately 3 times more likely to develop recurrence.

Figure 1 - 1250

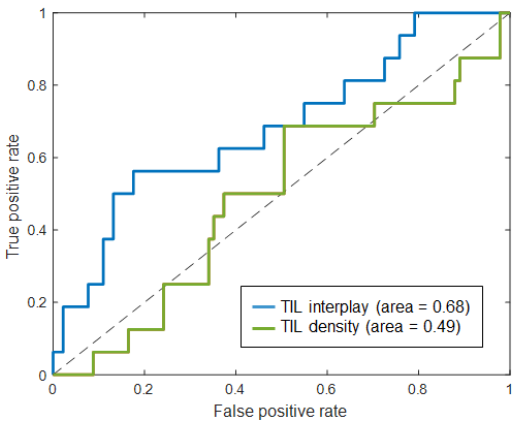

Figure 1. Receiver operating characteristic curves and corresponding areas under the curve for the TIL interplay and TIL density classifiers.

Figure 2 - 1250

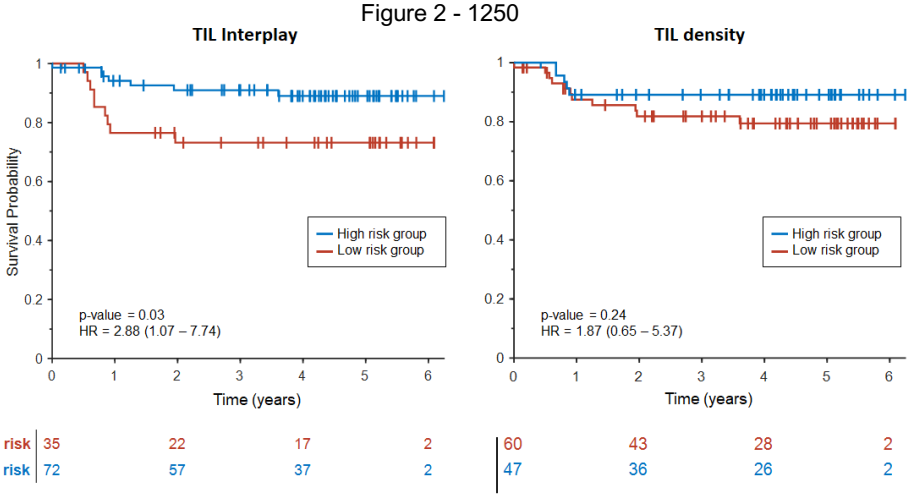

Figure 2. Kaplan-Meier plots, hazard ratios (HR), confidence intervals, and p-values for the TIL interplay and TIL density classifiers using DFS as endpoint. The number of cases in each category for different time instances is indicated at the bottom.

Conclusions: We present a prognostic model based on the automated quantification of interplay between tumor microenvironment cells that is able to help distinguish OPSCC patients with higher recurrence risk from those who will experience longer DFS. This method appears to be more prognostic than TIL density alone.

1251 SSTR2 Expression in Olfactory Neuroblastoma: Clinical and Therapeutic Implications

Vincent Cracolici[1], Eric Wang[1], Stacey Gargano[2], Aatur Singhi[3], Raja Seethala[4]
[1]University of Pittsburgh Medical Center, Pittsburgh, PA, [2]Thomas Jefferson University Hospital, Philadelphia, PA, [3]University of Pittsburgh Medical Center, Sewickley, PA, [4]University of Pittsburgh School of Medicine, Pittsburgh, PA

Disclosures: Vincent Cracolici: None; Eric Wang: None; Stacey Gargano: None; Aatur Singhi: None; Raja Seethala: None

Background: Somatostatin type 2 receptor (SSTR2) is expressed in a variety of neuroendocrine-type tumors including pancreatic neuroendocrine neoplasms, pheochromocytomas, and lung carcinoids. Expression may be associated with longer progression free survival. Additionally, ^{68}Ga labeled somatostatin analogs are now used to improve residual disease detection by imaging and radionuclide labeled somatostatin analogs may show therapeutic utility. To date, SSTR2 expression has not been well studied in olfactory neuroblastoma (ONB). We characterize SSTR2 expression in ONB and correlate staining results with clinicopathologic parameters.

Design: Fifty-eight tumors (35 primary biopsies/excisions, 23 recurrences/metastases) from 31 patients were stained for SSTR2 (Abcam: monoclonal rabbit UMB1) and reviewed by 2 authors. Staining was assigned an H-score based on intensity (0-3+) and percentage of tumor cells staining (PMID: 24070170). Pancreatic islet cells were used as an external control (considered 3+). When present, internal controls included: normal meningothelium (considered 3+) and normal olfactory neuroepithelium (considered 2+). Staining was correlated with clinicopathologic variables including modified Hyams grade (low grade = I-II, high grade = III-IV).

Results: All cases demonstrated SSTR2 staining (mean H-score: 188, range: 35-290). There were no significant differences in H-score between primaries and recurrences/metastases (mean H-score: 185 vs mean H-score: 193, Independent Samples T-test: p=0.467). Primary low-grade ONB had somewhat stronger staining than high grade tumors, but the difference was not quite significant (mean H-score: 207 vs mean H-score 173, p=0.069). SSTR2 staining had no prognostic value in terms of disease free survival (univariate Cox regression analysis: p=0.958) or disease specific survival (p=0.438).

Conclusions: SSTR2 is consistently expressed in all ONB suggesting a role for somatostatin analog based molecular imaging and therapy. However, this limited series shows no significant correlation between expression levels of SSTR2 and other clinicopathologic variables, though there is a trend towards decreased expression in high grade tumors.

1252 Histopathologic Determinants of Tumor-Immune Microenvironment in Head and Neck Squamous Cell Carcinoma (HNSCC)

Janis de la Iglesia[1], Juan Hernandez-Prera[1], Jude Masannat[1], Bruce Wenig[1], Robbert Slebos[1], Christine Chung[1]
[1]Moffitt Cancer Center, Tampa, FL

Disclosures: Janis de la Iglesia: None; Juan Hernandez-Prera: None; Jude Masannat: None; Bruce Wenig: None; Robbert Slebos: None; Christine Chung: None

Background: Immune checkpoint inhibitors are emerging treatment options for HNSCC. Pathologists are now commonly encountering requests for assessing the tumor immune microenvironment (TIME) and PD-L1 expression in HNSCC. We aim to identify histopathologic features that could be associated with TIME and PD-L1 expression in oral cavity SCC (OSCC).

Design: 35 OSCCs were subjected to multiplex immunofluorescence (mIF) using the BOND-RX autostainer (Leica Microsystem, Vista, CA) and antibodies for CD3, CD8, FOXP3, PD-L1, and AE1/AE3. 3 regions of interest in tumor core (TC) and tumor margin (TM) were analyzed. For the mIF analysis, the Vectra 3.0 spectral imaging system (PerkinElmer, Waltham, MA) was utilized. H&E sections of all cases were assessed for depth of invasion (DOI), worst pattern of invasion (WPOI), tumor budding, and eosinophilic infiltration at TM. Cases were subsequently sub-grouped as WPOI1-4 and WPOI5; < 5 buds/HPF and ≥ 5 buds/ HPF; < 7 mm DOI and ≥ 7 mm; < 20 eosinophils/HPF and ≥ 20 eosinophils/HPF. Kruskal-Wallis test was used to determine if there were statistically significant differences between the mIF results and the sub-groups of the aforementioned histopathologic features. The ratio of PD-L1 positive cells at the TC and TM (TC: TM) was also calculated.

Results: The overall number of CD3, CD8, FoxP3, and PD-L1 positive cells did not statistically differed between the sub-groups of DOI, WPOI, and tumor budding, neither did the CD3, CD8, and FoxP3 counts and the eosinophilic infiltration at TM. However, the overall expression of PD-L1 and the number of PD-L1 positive tumor cells were increased with a statistical significance at the TC and TM in cases with ≥ 20 eosinophils/HPF at the TM (p-value < 0.05). In 6 case the TC:TM ratio did not show difference in PD-L1 expression while in 29 cases the PD-L1 expression varied between the TC and TM (17 cases higher at TM and 12 case higher at TC).

Conclusions: TIME and PD-L1 expression in OSCC is not associated with DOI, WPOI, and tumor budding. Eosinophilic infiltration at TM is associated with PD-L1 expression in OSCC. This association warrants further investigations as eosinophils have important functions for tumor surveillance, and increased eosinophil counts have been associated with favorable outcome in melanoma patients receiving pembrolizumab. PD-L1 expression in OSCC shows spatial intra-tumoral heterogeneity between the TC and TM, which challenges interpretation and pathological reporting of this biomarker.

1253 Multimodal Analysis of 42 Patients with Head and Neck Squamous Cell Carcinoma with Node Metastasis at Diagnosis: A Focus on HPV and Mir200 Promotors' Methylation

Thomas Denize[1], Charles Lépine[2], Simon Garinet[3], Sophie Outh-Gauer[4], Camille Brochard[3], Yaelle Bellahsen-Harrar[3], Hélène Blons[5], Cecile Badoual[6]
[1]APHP.5 Hôpital Européen Georges Pompidou, boston, MA, [2]Hôpital Européen Georges Pompidou APHP, Paris, Ile de France, France, [3]APHP.5 Hôpital Européen Georges Pompidou, Paris, Ile de France, France, [4]Hôpital Européen Georges Pompidou, APHP, Paris, France, [5]Hôpital Européen Georges Pompidou, Paris, France, [6]G Pompidou Hospital, Paris, France

Disclosures: Thomas Denize: None; Charles Lépine: None; Simon Garinet: None; Sophie Outh-Gauer: None; Camille Brochard: None; Yaelle Bellahsen-Harrar: None; Hélène Blons: *Consultant*, AstraZeneca, MSD; Cecile Badoual: None

Background: Squamous cell carcinoma is the main histotype in the head and neck, with various risk factors and a poor 5-years survival. The majority present with lymph node metastasis at diagnosis. MicroARNs miR200 family have been showed to play an important role in the epithelial-mesenchymal transition in various cancer types. A major miR200 expression's regulatory mechanism is the hypermethylation of their promotor. The aim of this work was to characterize a cohort of head and neck squamous cell carcinomas with node metastasis at diagnosis, with a focus on mir200 family promotors' methylation.

Design: Every patient with Head and neck squamous cell carcinoma with node metastasis at diagnosis between 2013 and 2017 was included. Forty-two patients had sufficient material to perform the analysis. PDL1 IHC (22C3; Agilent) was performed on each tumor and node metastasis. It was evaluated by the percentage of positivity on tumor cells, inflammatory cells and by the combined positive score. DNA was extracted from every case using Maxwell® 16 FFPE Plus LEV DNA Purification Kit and analyzed by NGS with a 52 genes panel (Ion AmpliSeq™ Cancer Hotspot, Life Technologies™, France). DNA was also treated with bisulfite, amplified using specific probes for mir200 family promotors on chromosome 1 and 12 and subsequently analyzed by fragment analysis.

Results: Mean age at diagnosis was 61 years old. There was a strong male predominance (35M, 7F). The most frequent location was the oropharynx (25/42). Other included oral cavity, hypopharynx and larynx. Twenty-two cases were HPV related (18/24 in oropharynx, 4/17 in the other locations). PDL1 was variably expressed in 28 tumors and 23 metastases. NGS analysis was successful in 39 patients, 28 displayed at least 1 mutation. The more frequent alterations were TP53 (16/39) and PIK3CA (8/39). HPV status was associated with a

higher expression of PDL1 in both tumor and nodal metastasis (p <0.05). HPV positive tumors were also less likely to be mutated (p<0.05). No TP53 mutation was found in the HPV+ group. Levels of mir200 promotor's methylation on chromosome 1 and 12 were correlated (spearman correlation : 0.702 ; p<0.001) but not associated with any other variable.

Conclusions: In this series, HPV status is associated with the expression of PDL1 on both the tumor and the nodal metastasis and with fewer mutations, especially in TP53. Mir200 promotor's methylation was not associated with HPV or mutational status nor PDL1 expression.

1254 A Multicentre Study of Within-Stage Heterogeneity and Impact on Prognostic Performance in the AJCC Staging for Metastatic Head and Neck Cutaneous Squamous Cell Carcinoma

Ardalan Ebrahimi[1], Michael Veness[2], Lachlan McDowell[3], Peter Luk[4], Tsu-Hui (Hubert) Low[5], Matthew Magarey[3], Paul Smith[6], Diana Perriman[6], Jonathan Clark[5], Ruta Gupta[4]
[1]Chris O'Brien Lifehouse, Sydney, NSW, Australia, [2]Westmead Cancer Care Centre, Westmead Hospital, Westmead, NSW, Australia, [3]Peter MacCallum Cancer Center, Melbourne, VIC, Australia, [4]Royal Prince Alfred Hospital, Sydney, NSW, Australia, [5]Chris O'Brien Lifehouse, Camperdown, NSW, Australia, [6]Australian National University, Canberra, ACT, Australia

Disclosures: Ardalan Ebrahimi: None; Michael Veness: None; Lachlan McDowell: None; Peter Luk: None; Tsu-Hui (Hubert) Low: None; Matthew Magarey: None; Paul Smith: None; Diana Perriman: None; Jonathan Clark: None; Ruta Gupta: None

Background: Several studies have shown the AJCC staging system stratifies risk poorly for head and neck cutaneous squamous cell carcinoma (HNcSCC) with nodal metastases. We hypothesised that this may be due to the grouping of patients with widely disparate prognoses into the same risk category. The aim of this study was to investigate for sources of within-stage prognostic heterogeneity in the N and TNM stages based on established clinicopathological prognostic factors.

Design: Retrospective analysis of disease-specific survival (DSS) in a multicentre study of 1146 patients with nodal metastases from HNcSCC. Differences in survival were determined using Cox regression analyses, adjusted for treatment and stratified by institution to account for heterogeneity between centres.

Results: The majority of patients were classified as pN2a or pN3b (83.1%) and TNM Stage IV (90.6%), largely due to the presence of extranodal extension. Wide variation in DSS was noted in both pN2a and pN3b disease. Specifically, on multivariate analysis, there was significant prognostic heterogeneity between TNM Stage IV patients based on nodal metastasis number [(3-4 vs 1-2: HR, 1.56; 95% CI, 1.02-2.40; p=0.042) (≥5 vs 1-2: HR, 2.61; 95% CI, 1.78-3.82; p<0.001)] and size [(>3-6cm vs ≤3cm: HR, 1.36; 95% CI, 0.97-1.92; p=0.073) (>6cm vs >3-6cm: HR, 4.23; 95% CI, 2.37-7.54; p<0.001)], immunosuppression (HR, 2.10; 95% CI, 1.37-3.22; p=0.001) and perineural invasion (HR, 1.74; 95% CI, 1.26-2.41; p=0.001). When Stage IV patients were categorised into low, moderate and high-risk groups based on these features, there was wide variation in prognosis with 5-year DSS of 86.7%, 75.4% and 52.0%, respectively (p<0.001).

Conclusions: The AJCC staging system for HNcSCC performs poorly due to significant prognostic heterogeneity between patients assigned to the same stage category. This highlights the need to develop and validate a staging system specific to HNcSCC that reflects its distinct tumour biology.

1255 The Implications for Immunosuppression in Metastatic Head and Neck Cutaneous Squamous Cell Carcinoma: A Multicentre Study

Ardalan Ebrahimi[1], Michael Veness[2], Lachlan McDowell[3], Peter Luk[4], Tsu-Hui (Hubert) Low[5], Matthew Magarey[3], Paul Smith[6], Diana Perriman[6], Jonathan Clark[5], Ruta Gupta[4]
[1]Chris O'Brien Lifehouse, Sydney, NSW, Australia, [2]Westmead Cancer Care Centre, Westmead Hospital, Westmead, NSW, Australia, [3]Peter MacCallum Cancer Center, Melbourne, VIC, Australia, [4]Royal Prince Alfred Hospital, Sydney, NSW, Australia, [5]Chris O'Brien Lifehouse, Camperdown, NSW, Australia, [6]Australian National University, Canberra, ACT, Australia

Disclosures: Ardalan Ebrahimi: None; Michael Veness: None; Lachlan McDowell: None; Peter Luk: None; Tsu-Hui (Hubert) Low: None; Matthew Magarey: None; Paul Smith: None; Diana Perriman: None; Jonathan Clark: None; Ruta Gupta: None

Background: Patients with immunosuppression (IS) represent a unique cohort at markedly increased risk of head and neck cutaneous squamous cell carcinoma (HNcSCC) with a propensity for aggressive behaviour. Despite this, the AJCC omitted IS from the 8th edition staging due to a paucity of data confirming IS as an independent predictor of prognosis, heterogeneity of previous studies and lack of data on relative impact based on subtype of IS. The aim of this study was to address these issues.

Design: Multicentre retrospective study of 1301 patients with nodal metastases from HNcSCC. Differences in locoregional control (LRC), distant metastatic control (DMC), disease-specific (DSS) and overall survival (OS) were determined using multivariate Cox regression stratified by institution to account for heterogeneity between centres.

Results: IS was documented in 111 (8.5%) patients, including solid organ transplant in 28 (25.2%), haematological malignancy in 62 (55.9%), immunosuppressant medications in 16 (14.4%), immune disregulation in 2 (1.8%) and not specified in the remaining 3 (2.7%). Almost all IS patients (97%) were classified as TNM Stage IV. On multivariate analyses, IS was an independent predictor of reduced LRC (HR, 2.05; 95% CI: 1.36-3.09; p=0.001), DMC (HR, 2.47; 95% CI: 1.42-4.29; p=0.001), DSS (HR, 2.14; 95% CI: 1.42-3.22; p<0.001) and OS (HR, 2.33; 95% CI: 1.74-3.12; p<0.001). There were no differences in LRC (p=0.988), DMC (p=0.770), DSS (p=0.962) or OS (p=0.357) based on subtype of IS. Within the IS cohort, ≥5 nodal metastases and nodal size >6cm were the only significant predictors of outcome.

Conclusions: IS is an independent predictor of LRC, DMC, DSS and OS in HNcSCC with lymph node metastases and the prognostic impact appears not to be modified by the subtype of IS. Within the IS cohort, ≥5 nodal metastases and nodal size >6cm identify a particularly high-risk subset of patients. Consideration should be given to incorporating IS into future staging systems.

1256 Prognostic Assessment of Perineural Invasion Status and Extent in Oral Squamous Cell Carcinoma: Comprehensive Analysis Using Digital Whole Slide Images

Renee Eigsti[1], Kathryn Marcus[2], Andrew Davis[3], Anand Rajan KD[3]
[1]Iowa City, IA, [2]University of Iowa, Carver College of Medicine, Iowa City, IA, [3]University of Iowa Hospitals and Clinics, Iowa City, IA

Disclosures: Renee Eigsti: None; Kathryn Marcus: None; Andrew Davis: None; Anand Rajan KD: *Advisory Board Member*, Roche Diagnostics Corporation

Background: Perineural invasion (PNI) is a known prognostic factor that is linked to locoregional tumor recurrence and lymph node metastasis in oral squamous cell carcinoma (OSCC). However, PNI assessment is highly variable between pathologists and the extent (burden) of PNI is not a standardized part of OSCC resection reports or registry data. Previous studies have examined nerve size, count and extent in small cohorts of patients and the quantitative impact of the extent and nature of perineural invasion on clinical outcomes is poorly understood. We sought to address this in a large of cohort of well-characterized of OSCC treated surgically by quantifying PNI extent using HE whole slide image annotation.

Design: We identified consecutive patients with OSCC (n=274) spanning a 12-year period (2006-2018). Clinicopathologic variables (17) including disease-specific (DSS) and progression-free survival (PFS) time intervals were collected as outcome measures. Tumor-containing slides were digitized with a P1000 Pannoramic (3DHistech) whole slide scanner. Digital slides were meticulously examined and all nerves irrespective of size within 0.5 cm of invasive tumor were annotated. Involved nerves were tagged separately and nerve diameter (in mm) was measured for each.

Results: The follow-up duration ranged from 0.3 - 155.1 months. Nodal involvement, tumor grade, lymphovascular invasion and final margin status showed significant association with worse disease-specific survival (all $p<0.05$). Perineural invasion showed a significant association with worse DSS (Figure 1) as did the reported PNI status. Positive nerve counts (range; 1-59) and diameter (0.01 - 148 µm) showed an significant association with worse outcomes but study PNI status alone remained significant on multivariate Cox regression (HR: 1.18-1.95. $p = 0.001$). Nerve diameter showed a weak association with worse DSS and was not statistically significant in relation to worse DSS (HR: 0.98 - 10.1, $p = 0.8$).

Figure 1 - 1256

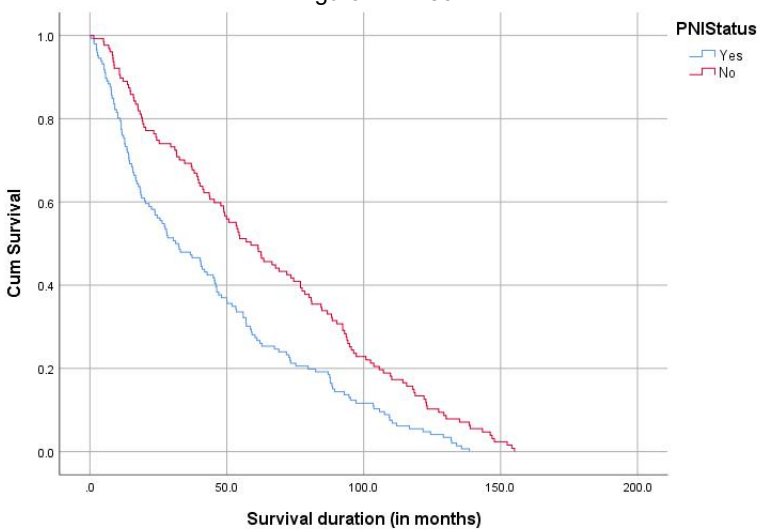

Conclusions: These results demonstrate that presence of perineural invasion (PNI) but not involved nerve count or size is correlated with worse disease specific survival in OSCC. The biologic behavior identified by presence of perineural invasion likely correlates with overall invasiveness (margin closeness, nodal spread) and thus the extent of PNI does not appear as an independent prognostic factor. Accurate and careful PNI assessment in routine reporting, regardless of size, will aid in accurate prognostication in OSCC.

1257 Choice of PD-L1 Scoring and Cutoff in Head and Neck Squamous Cell Carcinoma (HNSCC) Trials of Pembrolizumab

Kenneth Emancipator[1], Jonathan Juco[1], Lingkang Huang[2], Jared Lunceford[1], Jonathan Cheng[3], Joy Ge[3], Christine Gause[1], Ramona Swaby[1]
[1]Merck & Co., Inc., Kenilworth, NJ, [2]Merck & Co., Inc., Westfield, NJ, [3]Merck & Co., Inc., North Wales, PA

Disclosures: Kenneth Emancipator: *Stock Ownership*, Merck & Co., Inc., Kenilworth, NJ, USA; Johnson & Johnson; Bayer AG; Celgene; Jonathan Juco: *Employee*, Merck & Co., Inc.; *Stock Ownership*, Merck & Co., Inc.; *Stock Ownership*, Google; *Stock Ownership*, Illumina; *Stock Ownership*, Regeneron; Lingkang Huang: *Employee*, Merck; *Stock Ownership*, Merck; Jared Lunceford: *Employee*, Merck & Co., Inc.; *Stock Ownership*, Merck & Co., Inc.; Jonathan Cheng: *Employee*, Merck; Joy Ge: None; Christine Gause: *Employee*, Merck & Co., Inc., Kenilworth, NJ, USA; Ramona Swaby: *Employee*, Merck & Co., Inc., Kenilworth, NJ, USA

Background: TPS measures PD-L1 expression on tumor cells, and CPS measures PD-L1 expression on tumor and immune cells. Although TPS is successful at predicting response in NSCLC, emerging data in other solid tumors (gastric, bladder, breast, ovary) suggest the importance of immune cell PD-L1 expression to predict clinical outcomes with pembrolizumab (pembro). Data from KEYNOTE-012 (NCT01848834) and KEYNOTE-055 (NCT02255097) were used as training sets to determine PD-L1 scoring and cutoff for HNSCC.

Design: KEYNOTE-012, a multicohort phase 1b study of pembro, included 2 cohorts of pts with R/M HNSCC: cohort B in pts whose tumors expressed PD-L1 determined by a prototype assay and cohort B2 in pts regardless of PD-L1 status. Data from KEYNOTE-012 compared CPS vs TPS. Data from KEYNOTE-055, a phase 2 study of pembro in pts with platinum-refractory R/M HNSCC regardless of PD-L1 status, were combined with KEYNOTE-012 to determine the potential for a higher CPS cutoff for validation. ORR was assessed by central review per RECIST v1.1. Analysis of cutoffs included ROC and other clinical utility parameters.

Results: In nonenriched KEYNOTE-012 B2 (N=132), CPS ≥1 showed superior enrichment for ORR while maintaining higher sensitivity vs TPS. Other CPS cutoffs were evaluated in 296 pts (KEYNOTE-012, 148 [44 in B, 104 in B2]; KEYNOTE-055, 148). Response rate enrichment was observed from CPS ≥1 to ≥20 (range, 23%-29%) with reasonable preservation of sensitivity (93%-70%). Enrichment beyond CPS ≥20 was minimal with decreases in sensitivity. Of 60 responses, 40% (n=24) were positive at TPS ≥50%, 72% (n=43) at TPS ≥1%, and 93% (n=56) at CPS ≥1. The clinical utility profile for CPS vs TPS in the nonenriched KEYNOTE-012 B2 cohort and in KEYNOTE-055 (N=252; 51 responses) is shown (Table, Figure).

Scoring and Cutoff	Sensitivity, %	Specificity, %	YI, %	PPV, %	NPV, %	Prevalence, %
CPS ≥1	92.2	18.9	11.1	22.4	90.5	83.3
CPS ≥10	74.5	45.8	20.3	25.9	87.6	58.3
CPS ≥20	66.7	54.2	20.9	27.0	86.5	50.0
CPS ≥30	58.8	62.7	21.5	28.6	85.7	41.7
CPS ≥40	49.0	69.7	18.7	29.1	84.3	34.1
CPS ≥50	43.1	74.1	17.3	29.7	83.7	29.4
TPS ≥1%	74.5	32.3	6.8	21.8	83.3	69.0
TPS ≥10%	66.7	52.7	19.4	26.4	86.2	51.2
TPS ≥20%	62.7	59.2	21.9	28.1	86.2	45.2
TPS ≥30%	58.8	65.2	24.0	30.0	86.2	39.7
TPS ≥40%	45.1	71.6	16.7	28.8	83.7	31.7
TPS ≥50%	41.2	75.6	16.8	30.0	83.5	27.8

Figure 1 - 1257

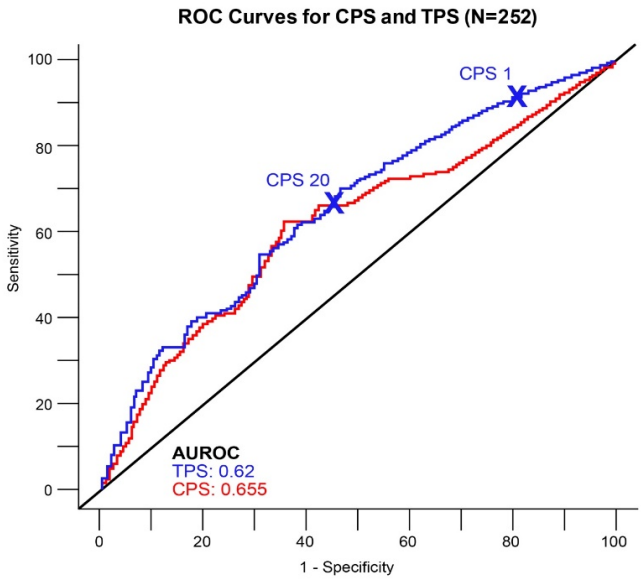

Conclusions: For pts with HNSCC, CPS was chosen as the scoring method because of its improved clinical utility profile vs TPS, with CPS ≥1 and CPS ≥20 selected for evaluation in the randomized setting.

1258 Comparison of Intrinsic PAM50 Gene Expression Analysis and Immunohistochemical Subtypes of Salivary Duct Carcinoma

Ramona Erber[1], Robert Stoehr[2], Florian Haller[3], Marlen Haderlein[4], Arndt Hartmann[5], Abbas Agaimy[6]
[1]University Hospital Erlangen, Erlangen, Bavaria, Germany, [2]Institute of Pathology, University Hospital, Erlangen, Erlangen, Germany, [3]University Hospital Erlangen, Erlangen, DE, Germany, [4]Radiation Therapy Clinic, Friedrich-Alexander University Erlangen-Nürnberg (FAU), Comprehensive Cancer Center (CCC) Erlangen-EMN, Erlangen, Erlangen, Bavaria, Germany, [5]Institut fur Pathologie, Erlangen, Germany, [6]Universitätsklinikum Erlangen, Germany, Erlangen, Germany

Disclosures: Ramona Erber: None; Robert Stoehr: None; Florian Haller: None; Marlen Haderlein: None; Arndt Hartmann: None; Abbas Agaimy: *Grant or Research Support*, Nanostring

Background: Already in the original description of salivary duct carcinoma (SDC) in 1968, the analogy to breast cancer has been raised and discussed. Later studies showed that SDC can be subdivided into luminal (androgen receptor/AR+), HER2-associated and basal (AR-/HER2-) subtypes using immunohistochemistry (IHC). Molecular profiling of invasive breast cancer using different methods of gene expression analysis (including the PAM50 classifier) has shown prognostic and predictive value. The aim of our study was to investigate whether mRNA-expression based PAM50 classifier initially established for breast cancer correlates with immunohistochemical subtypes of SDC.

Design: N=47 cases of malignant salivary tumors classified as SDC based on current WHO classification (irrespective of being de novo or ex pleomorphic adenoma) were included. All tumors were high grade. Immunohistochemical stains (AR, HER2) were used to subtype SDC according to Di Palma et al. A subset of cases was tested also for CK5, ER and PR. The IHC-based subtypes were defied as follows: luminal AR+/HER2 negative (HER2-), luminal AR+/HER2 positive (HER2+), non-luminal HER2+, and basal (double negative). Furthermore, PAM50 gene expression analysis was performed in cases with sufficient material left, and immunohistochemical and molecular subtypes were compared.

Results: PAM50 analysis was performed in 33 cases, intrinsic subtypes were n=9 basal-like, n=8 luminal A, and n=16 HER2-enriched. For 31 cases, both, IHC status (HER2 and AR), and PAM50 subtype, were known. Of the 9 PAM50 basal-like cases, 4 were also basal by IHC (double negative). The other 5 cases showed luminal AR+ IHC subtype (2 of them also HER2+). All 7 PAM50 luminal A cases were concordant by IHC (all AR+, 2 were also HER2+). Within the PAM50 HER2-enriched subgroup (n=15), only 6 cases showed concordant HER2 IHC (all were in addition to HER2 also AR+). The remainder (n=9) were IHC luminal AR+/HER2-.

Conclusions: In this small cohort of salivary duct carcinoma, immunohistochemical subtyping using AR and HER2 IHC did not correlate well with PAM50 gene expression analysis

1259 HER2 Gene Amplification and Protein Expression Assessment in 44 Salivary Duct Carcinomas

Donna Ferguson[1], Amir Momeni Boroujeni[2], Tao Zheng[1], Alan Ho[1], Maria Arcila[1], Dara Ross[1], Snjezana Dogan[1]
[1]Memorial Sloan Kettering Cancer Center, New York, NY, [2]Memorial Sloan Kettering Cancer Center, Brooklyn, NY

Disclosures: Donna Ferguson: None; Amir Momeni Boroujeni: None; Tao Zheng: None; Alan Ho: None; Maria Arcila: *Speaker*, biocartis; *Speaker*, Invovoscribe; Dara Ross: None; Snjezana Dogan: None

Background: Salivary duct carcinoma (SDC) is an aggressive malignancy that is morphologically and genetically similar to ductal breast carcinoma, has a dismal prognosis and limited therapeutic options. About 30% of SDCs harbor *HER2* amplification and these patients are reported to respond to HER2 inhibitor therapy (trastuzumab). However, a standardized diagnostic algorithm for *HER2* gene amplification assessment in SDC is lacking. Here, we evaluated three methods for *HER2* copy number (CN) status with an aim to identify SDC cases amenable to HER2 inhibition.

Design: A retrospective cohort of 44 SDCs (5 research, 39 clinical) including 18 primary and 26 metastatic tumors were analyzed with at least 2 methods: HER2 immunohistochemistry (IHC, n=29), a targeted exome massive parallel sequencing (MPS) assay (n=39), and/or fluorescence *in situ* hybridization (FISH, n=40). FACETS (Fraction and Allele-Specific Copy Number Estimates from Tumor Sequencing), an allele-specific CN analysis pipeline was used for *HER2* CN assessment on cases tested by MPS. Concordance between the three methods was evaluated.

Results: Of the 29 cases with IHC results, 3 (10%), 3 (10%), 11 (38%) and 12 (42%) of SDC specimens scored 0, 1, 2 and 3 by IHC, respectively. Of the 25 cases with IHC and FISH results, no cases scored 0 (n=3) or 1 (n=3), 2 (20%, n=10) cases scored 2, and all (100%, n=9) of cases scored 3 were amplified by FISH (ANOVA, post hoc Tukey test, p<0.0001, Figure 1). Receiver operating characteristic (ROC) analysis showed that the FACETS accurately predicted *HER2* amplification status by FISH (AUC 0.98). Using a CN cut off ≥5 FACETS had a sensitivity of 87% and specificity of 100% for FISH-detected *HER2* amplification.

Figure 1 - 1259

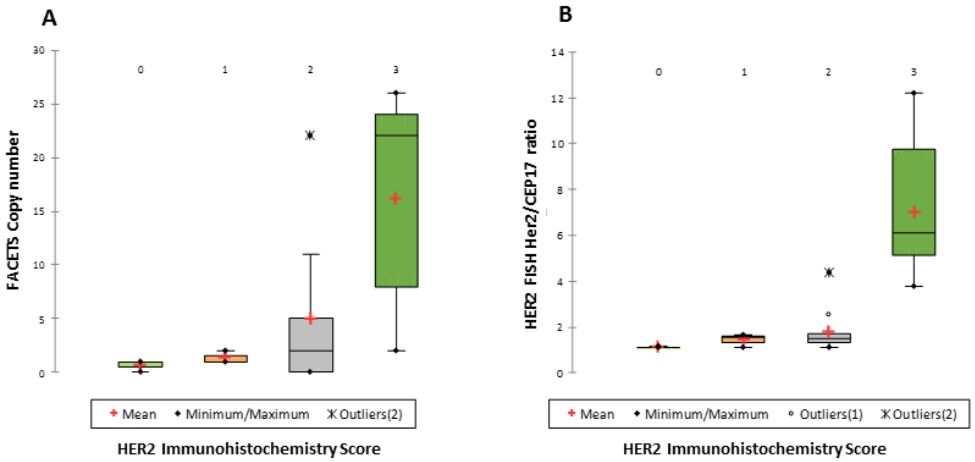

Conclusions: In SDC, HER2 IHC is an accurate predictor of *HER2* amplification in cases scored 0, 1 and 3. Similar to breast carcinoma, a minor subset of SDCs with HER2 IHC score 2 are *HER2* amplified warranting further evaluation by an alternate method. FACETS analysis is an accurate predictor of *HER2* gene amplification in SDC profiled by MPS and can be used as a reliable equivalent to FISH in equivocal cases.

1260 Histopathological and Molecular Immunophenotyping of Minor Salivary Glands from Patients Treated with Immune Checkpoint Inhibitors Presenting with Severe Sicca

Billel Gasmi[1], Astin Powers[2], Alan Baer[3], David Kleiner[4], Blake Warner[3]
[1]National Cancer Institute, National Institutes of Health, Bethesda, MD, [2]Bethesda, MD, [3]Salivary Disorders Unit, National Institute of Dental and Craniofacial Research, National Institutes of Health, Bethesda, MD, [4]National Cancer Institute, National Institutes of Health, Rockville, MD

Disclosures: Billel Gasmi: None

Background: Immune checkpoint inhibitors (ICI) have advanced the field of cancer therapeutics. By blocking the negative co-stimulation of T cells, ICI augment the anti-tumor immune response. However, ICI can elicit inflammatory reactions termed immune-related adverse

events (irAEs). In a previous published study, we demonstrated that ICI therapy is associated with an autoimmune-induced sicca syndrome distinct from Sjögren's syndrome, often abrupt in onset, usually developing within the first 3 months of treatment, and associated with sialadenitis and glandular injury. Herein, we characterize the inflammatory infiltrate of labial salivary gland biopsies (LSGB) patients with sicca diagnosed post ICI therapy

Design: We evaluated the surface area of Masson and Mucicarmine stains and density of CD45, CD20, CD3, CD4, CD8, PD-1, PD-L1 IHC stains in LSGB using QuPath 2.0 software. RNA expression of immune markers was also evaluated. Our aim is to immunophenotype the inflammatory infiltrate in patients with new-onset sicca post ICI therapy (ICI, n=21) compared to healthy volunteers (HV, n=9)

Results: The LSGB from ICI treated patients showed a lower acinar density (Mucicarmine, p=0.01) with destruction of PD-L1+ epithelia and dense sialadenitis composed chiefly of lymphocytes. but without increased fibrosis (Trichrome,p= 0.07) compared to the HV group that maintained normal glandular histology with minimal inflammation and epithelial damage. The inflammatory infiltrate was composed of T cells with a higher density of CD8 (p=0.039), CD4 (p=0.078), and CD3 (p=0.05) in the ICI vs HV group. The CD20 stain showed minimal scattered B-cells in both groups. The gene expression analysis showed a significantly higher PD-1 expression in the ICI treated vs HV (p=0.02) with higher CD39 expression (p=0.056). CD3, CD4, CD8, 4-1BB, TIM3, GzmB, FOXP3 and PDL1 were all upregulated in the ICI group vs HV but did not reach statistical significance. There was no difference in CD103, CD68, MPO and INOS RNA expression between the two groups.

Conclusions: The histopathology of ICI induced sialadenitis consists primarily of a T cell infiltrate with parenchymal destruction with mild fibrosis. The IHC analysis combined with the RNA data show the presence of cytotoxic T-cell population (CD8, PD1, 4-1BB, TIM3, GrzB) with a chronic antigen exposure phenotype (PD-1, CD39) in LSGB of ICI treated patients. Further investigation is necessary to determine if this T-cell population is causing the sicca or if it constitutes a reactive population

1261 Well-Differentiated/Dedifferentiated Liposarcoma Arising in the Upper Aerodigestive Tract Mimicking Non-adipocytic Lesions: A Series of 7 Cases

Toshi Ghosh[1], Anja Roden[1], Andrew Folpe[1], David Schembri-Wismayer[1], Karen Fritchie[1], Michael Rivera[1]
[1]Mayo Clinic, Rochester, MN

Disclosures: Toshi Ghosh: None; Anja Roden: None; Andrew Folpe: None; David Schembri-Wismayer: None; Karen Fritchie: None; Michael Rivera: None

Background: Well-differentiated (WDL) and dedifferentiated liposarcomas (DL) of the upper aerodigestive tract are rare, often mimicking benign lipomatous neoplasms or non-lipogenic mesenchymal tumors. We studied a series of WDL/DL in this anatomic region to better characterize their morphologic diversity and potential mimics.

Design: Cases of WDL/DL arising in the upper aerodigestive tract were obtained from our institutional and consultation archives from January 1, 1992 through May 1, 2019. Morphologic features were catalogued, and fluorescence in situ hybridization (FISH) studies for *MDM2* were performed on all specimens. Clinical and follow-up data were obtained from the patients' medical records.

Results: 7 WDL/DL (4 WDL, 3 DL; 5M, 2F) were identified in patients ranging from 32 to 77 years (median 50 years) with sites of origin including hypopharynx (5 cases), larynx (1 case) and oral cavity (1 case). 5 of the 7 cases were sent for expert consultation before final diagnosis, and the remaining 2 cases were initially misdiagnosed as benign lymphangiomatous or fibroepithelial polyps. 3 tumors had areas mimicking various non-lipomatous soft tissue tumors including nodular fasciitis, mammary-type myofibroblastoma and undifferentiated pleomorphic sarcoma, 2 cases simulated benign hypopharygeal polyps, and 1 lesion was notable for a dense lymphoplasmacytic infiltrate suggestive of hematolymphoid neoplasm or IgG4-related sclerosing disease. FISH showed amplification of *MDM2* (7/7 cases). All cases (3/3) with greater than one-year of follow-up recurred (at 7, 8 and 10 years) with one tumor showing progression to DL.

Conclusions: WDL/DL presenting in the upper aerodigestive tract are rare and diagnostically challenging. Awareness of the morphologic spectrum of WDL/DL coupled with appropriate use of *MDM2* FISH is essential for accurate classification and management, as these tumors appear to have a high risk for local recurrence and eventual dedifferentiation in these anatomical locations.

1262 Nanostring nCounter-Based Diagnostic Assay for Detection of Fusion-Associated Salivary Gland Tumors

Angela Goytain[1], Tony Ng[2]
[1]University of British Columbia/Vancouver General Hospital, Vancouver, BC, [2]Vancouver General Hospital, Vancouver, BC

Disclosures: Angela Goytain: None; Tony Ng: *Grant or Research Support*, Nanostring Technologies

Background: The majority of salivary gland tumors harbor gene fusions, the detection of which is useful for precise pathologic diagnosis to guide clinical management. Historically, the clinical utility of salivary gland tumor molecular diagnosis has been limited due to the availability of only laborious single-gene assays (e.g. FISH) or assays unable to detect fusions with highly variable partner genes (e.g. RT-PCR). Here, we report the development and early validation of a Nanostring-based assay for multiplexed detection of salivary gland tumor fusions.

Design: Nanostring nCounter is a fluorescence-barcoded hybridization method to detect gene expression that can be adapted for fusion gene detection using two different probe designs. Fusion-specific probes hybridize across the unique sequence at the fusion boundary. Alternatively, expression probes can determine expression of individual exons of fusion partner genes; imbalance in exon expression can be used to infer the presence of a fusion gene, while total gene overexpression is also used to infer fusion gene expression (presumably due to fusion breakpoint prior to the first exon). Prepared probe pools are hybridized to RNA extracted from formalin fixed paraffin embedded tissue. Excess probes and RNA are removed, and the remaining complexes of RNA/probes are digitally counted in an nCounter analyzer.

Results: We designed a panel with 67 fusion-specific probes and expression probes across 9 genes involved in salivary gland tumor fusions. Of the 74 excision and biopsy cases tested, 72 cases had sufficient RNA for analysis, of which 66 were expected to be fusion positive. A fusion was detected in all cases of pleomorphic adenoma, adenoid cystic carcinoma, secretory carcinoma, cribriform adenocarcinoma, low-grade intraductal carcinoma and NUT carcinoma, and two of three clear cell carcinomas. Fusions were detected in only 6 of 18 mucoepidermoid carcinoma cases, presumably due to fusion junction sequence variability in the negative cases, although orthogonal RT-PCR testing was only able to detect fusions in 6 of the 12 negative cases. Technical turnaround time from RNA isolation to reporting was 36 hours, and average reagent/technician cost per case was $300 when batched as 3-6 cases.

Tumor type	Fusion-specific probes	Exon expression imbalance probes	# of cases (positive/total)	Positive for fusion-specific or imbalance	Gene over-expression only
Fusion positive tumors					
Adenoid cystic carcinoma	MYB-NFIB, MYBL1 variants	MYB, MYBL1	15/15	12	3
Cribriform adenocarcinoma	PRKD1/2 variants	PRKD1, PRKD2, PRKD3	3/3	3	-
Hyalinizing clear cell carcinoma	EWSR1-ATF1, EWSR1-CREM	none	2/3	2	-
Low-grade intraductal carcinoma	none	RET	2/2	1	1
Mucoepidermoid carcinoma	CRTC1-MAML2 CRTC3-MAML2	none	6/18	6	-
NUT midline carcinoma	BRD3/4-NUTM1	NUTM1	1/1	1	-
Secretory carcinoma	ETV6-NTRK3	none	6/6	6	-
Pleomorphic adenoma/ carcinoma ex pleomorphic adenoma	PLAG1, HMGA2 variants	HMGA2, PLAG1	20/20	16	4
Fusion negative tumors					
High-grade salivary duct carcinoma			0/1		
Lymphoepithelial carcinoma			0/1		
Myoepithelial carcinoma			0/1		
Polymorphous adenocarcinoma			0/3		

Conclusions: The majority of salivary gland tumor fusions can be effectively detected with a Nanostring-based assay in a rapid and cost-efficient manner. Further validation is required to determine the utility of this assay in an active clinical setting.

1263 p16 Expression and High-Risk HPV Status of 18 Sebaceous Carcinomas of the Conjunctiva and Eyelid

Sarah Gradecki[1], Edward Stelow[2]
[1]Charlottesville, VA, [2]University of Virginia Health System, Charlottesville, VA

Disclosures: Sarah Gradecki: None; Edward Stelow: None

Background: Sebaceous carcinoma (SC) of the conjunctiva and eyelid is a rare entity, accounting for less than 1-5.5% of eyelid malignancies. While the etiology of this tumor is not fully understood, proposed risk factors include sun damage and human papillomavirus (HPV) infection, among others. While high-risk HPV (HRHPV) infection has been associated with other malignant and premalignant lesions of the conjunctiva and eyelid including squamous cell carcinoma in situ and nonkeratinizing squamous cell carcinoma, the role of HRHPV infection in SC is less clear. After clinically encountering a case of SC of the eyelid with metastasis to a parotid gland lymph node, both of which strongly expressed p16 and were HRHPV positive by in situ hybridization, the authors sought to determine the expression of p16 and HRHPV in SC of the eyelid and conjunctiva.

Design: Our archives were searched for all cases of conjunctival and primary eyelid SC between 2010-2019. Each tumor was stained with antibodies to p16, and chromogenic in situ hybridization was performed for RNA of the 18 most common high-risk HPV types. p16 staining was scored as negative, wild type, or positive, and HRHPV RNA ISH was scored as positive or negative.

Results: 18 cases of periocular SC (4 conjunctival and 14 eyelid) were identified from 11 female and 7 male patients, with an average age of 74.4 years (range 53 to 90). Two pathologists examined the cases to confirm diagnosis and presence of tumor in the tissue block, and IHC for adipophilin was reviewed to confirm sebaceous differentiation. 17/18 cases of SC showed positive expression of p16 (with the remaining case negative). 16/17 cases that showed p16 expression were negative for HRHPV RNA by in situ hybridization. The single case positive for HRHPV was a primary eyelid SC with metastasis to the parotid gland.<

Figure 1 - 1263

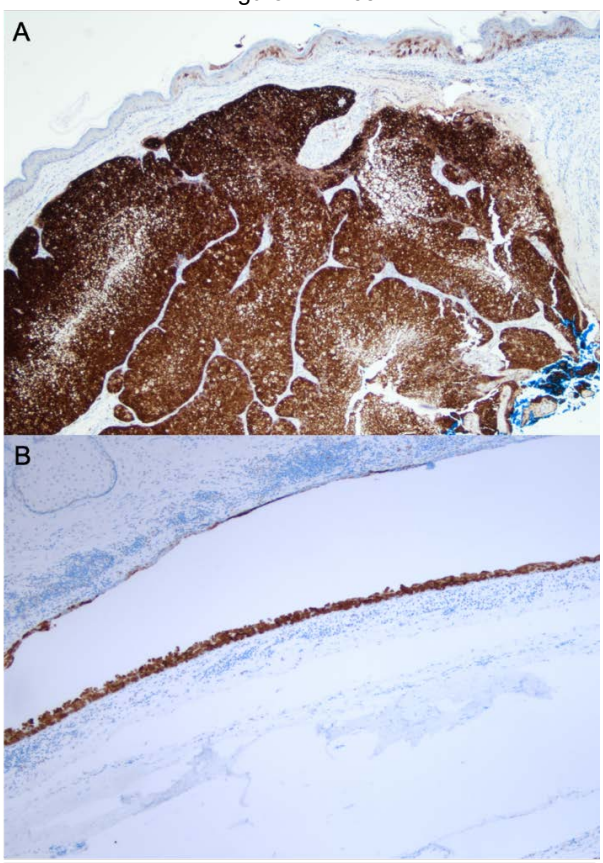

Figure 1: Strong, diffuse cytoplasmic expression of p16 in the invasive component of a primary eyelid SC (A) and in the in situ component of a primary conjunctival SC (B).

Conclusions: Strong, diffuse p16 expression was seen in 94% of SC cases (Figure 1). HRHPV was identified in only one SC, which was a primary eyelid lesion. Overall, no difference was observed in p16 expression or presence of HRHPV in conjunctival or primary eyelid lesions. These findings indicate that while some periocular carcinomas (nonkeratinizing SCC) have been reported to be associated with HRHPV, the identification of sebaceous differentiation makes infection by HRHPV extremely unlikely. Additionally, IHC for p16 in the setting of a tumor with sebaceous differentiation does not work as a surrogate for HRHPV testing, as is the case in other tumors.

1264 Increased IgG4-Positive Plasma Cells in Angiolymphoid Hyperplasia with Eosinophilia: A Potential Diagnostic Pitfall

Curtis Gravenmier[1], Rena Xian[2], Charles Eberhart[1], Lisa Rooper[3]
[1]Johns Hopkins University School of Medicine, Baltimore, MD, [2]Johns Hopkins Medical Institutions, Baltimore, MD, [3]The Johns Hopkins University School of Medicine, Baltimore, MD

Disclosures: Curtis Gravenmier: None; Rena Xian: None; Lisa Rooper: None

Background: Angiolymphoid hyperplasia with eosinophilia (ALHE), generally considered to be a subtype of epithelioid hemangioma, is a benign vascular proliferation which frequently arises in the head and neck and is associated with trauma to superficial blood vessels. Since ALHE demonstrates a dense lymphoplasmacytic infiltrate, fibrotic stroma with prominent eosinophils, and damaged blood vessels with luminal obliteration, it can be mistaken histologically for IgG4-related fibroinflammatory disease. This study aims to assess whether identification of IgG4-positive plasma cells and assessment of the IgG4/IgG ratio can help resolve this differential diagnosis.

Design: Nine cases of ALHE involving the head and neck were collected from the surgical pathology archives of a large academic medical center. Immunostains for IgG (Leica Biosystems, Buffalo Grove, IL) and IgG4 (Invitrogen, Carlsbad, CA) were performed on all cases. The maximum density of IgG4-positive cells per high-power field (HPF) and IgG4/IgG ratio were manually quantified by two independent pathologists. Clinical and demographic information was retrieved from the electronic medical record.

Results: The 9 cases of ALHE represented 6 men and 3 women with a median age of 22 years (range 16-84). Lesions presented as solitary superficial nodules on the forehead (n=3), orbit (n=3), eyebrow (n=1), temporal skin (n=1), and ear canal (n=1). The ALHE had a mean maximum density of 123 IgG4-positive plasma cells per HPF (range 20-262), with 6 cases (67%) exceeding the minimum of 50 cells per HPF recommended for a diagnosis of IgG4-related disease. Likewise, there was an average IgG4/IgG ratio of 62% (range 10-90%), and 7 cases (78%) surpassed the 40% threshold commonly used in IgG4-related disease. Although no serum IgG4 measurements were found in the electronic medical record, no patient had evidence of a systemic IgG4-related disease, consistent with the diagnosis of ALHE.

Conclusions: ALHE not only shows overlapping histologic features with IgG4-related fibroinflammatory disease, but it also frequently demonstrates a striking infiltrate of IgG4-positive plasma cells and increased IgG4/IgG ratio which pose a significant diagnostic pitfall. Although the role IgG4-positive cells play in ALHE is unclear, ALHE is not associated with systemic fibroinflammatory disease.

1265 High-Risk Human Papillomavirus (HR-HPV) Testing on Head and Neck Fine Needle Aspirations (FNA): Striving for a More Reliable Detection Method other than p16 Staining

Dominick Guerrero[1], Carmen Rivera[2], Helen Molina[1], Ravi Kothapalli[1], Dahui Qin[1], Jasreman Dhillon[1], Bruce Wenig[1], Juan Hernandez-Prera[1]
[1]Moffitt Cancer Center, Tampa, FL, [2]Moffitt Cancer Center, Odessa, FL

Disclosures: Dominick Guerrero: None; Carmen Rivera: None; Helen Molina: None; Ravi Kothapalli: None; Dahui Qin: None; Jasreman Dhillon: None; Bruce Wenig: None; Juan Hernandez-Prera: None

Background: The use of p16 immunohistochemistry (IHC) as a surrogate marker of HR-HPV in head and neck squamous cell carcinoma (HNSCC) has established] guidelines in surgical resection specimens. However, similar guidelines for interpreting p16 IHC in cytology specimens are not well established. Herein, we compare the performance of p16 IHC on cell blocks with two HPV-specific tests: HR-HPV E6/E7 messenger RNA by in situ hybridization (HR-HPV RNA ISH) and HR-HPV DNA genotyping by polymerase chain reaction (HR-HPV DNA PCR).

Design: Cell blocks from metastatic HNSCC were collected and reviewed. Cases were tested by p16 IHC, HR-HPV RNA ISH, and HR-HPV DNA PCR. For p16 IHC the E6H4 clone (CINtec Histology Kit) was utilized and its expression was evaluated for both distribution (nuclear and/or cytoplasmic) and quantity (manual morphometric assessment, assigned a percentage). The HR-HPV RNA ISH was performed using the RNAscope HPV kit (Advanced Cell Diagnostics, Inc) targeting HPV16, 18, 31, and 33. HR-HPV DNA PCR was analyzed by melting curve analysis (QuanDx's MeltPro HR-HPV Genotyping Assay) covering HPV strains 16, 18, 31, 33, 35, 39, 45, 51, 52, 56, 58, 59, 66, and 68.

Results: 27 cases were tested by the 3 methods. p16 IHC staining regardless of distribution and quantity of tumor cells was seen in 19 cases. HR-HPV RNA ISH was positive in 12 cases and HR-HPV DNA PCR was positive in 16. Concordance among the three methods

was observed in 12 cases. In these cases p16 expression varied from 5% cytoplasmic only to 100% nuclear and cytoplasmic. In the reminder 7 cases with p16 reactivity the pattern ranges from 5% nuclear and cytoplasmic to 85% cytoplasmic only. In the latter cases HR-HPV DNA PCR detected 2 HPV35, 1 HPV56 and 1 HPV59. Since these strains were not covered by the RNA ISH, the concordance between HR-HPV RNA ISH and DNA PCR was 100% for HPV16, 18, 31, and 33. The sensitivity, specificity, positive predictive value and negative predictive value of p16 IHC were calculated for different positivity cut-offs.

p16 IHC cut-off	Sensitivity %	Specificity %	PPV %	NPV %
Any staining	100	72.73	84.21	100
10%	93.75	81.82	88.24	90
50%	68.75	81.82	84.62	64.29
70%	56.25	90.91	90.00	58.82

Conclusions: p16 IHC as a marker of HR-HPV is suboptimal in cell blocks. This may represent an inherent problem in cell block preparation. HR-HPV RNA ISH and HR-HPV DNA PCR are more reliable methods for the identification of HR-HPV in cell blocks. In this study, HR-HPV DNA PCR performed better that RNA ISH due to the limited HPV strains covered by the latter test. Our results support HPV-specific tests as superior to p16 IHC in evaluating for the presence of HR-HPV in cytology material.

1266 Pathological and Clinical Analysis of Sinonasal Mucosal Melanoma with Emphasis on Prognosis Relevant Factors and Unusual Morphological Features: A Comprehensive Study of 45 Patients

Ruifeng Guo[1], Sarah Jenkins[1], Garret Choby[2]
[1]Mayo Clinic, Rochester, MN, [2]Department of Otorhinolaryngology – Head and Neck Surgery, Rhinology and Endoscopic Skull Base Surgery, Mayo Clinic, Rochester, MN

Disclosures: Ruifeng Guo: None; Sarah Jenkins: None; Garret Choby: None

Background: Sinonasal mucosal melanoma (SNMM) is a rare malignancy, accounting for less than 1% of all melanomas. Compared to its cutaneous counterpart, however, overall survival and treatment response are poor. The current study comprehensively evaluated the pathological and clinical features of SNMM with the aim of identifying pathological features of critical clinical significance.

Design: 45 patients with complete clinical records were included in the final analysis. These patients showed slight female predilection (F/M=28/17) with median age of 72 years (42-91). The median follow-up time was 37 months (6-271 months). The H&E slides of the primary excisions were reviewed to record the main pathological features, including morphology, mitoses (median 8/mm^2, ranging 1-61), ulceration and necrosis, in situ component, lymphovascular invasion (LVI), perineural invasion (PNI), tumor depth, and tumor infiltrating lymphocytes (TILs). In addition, onset clinical staging and surgical margin status were included. Associations between these features and clinical outcomes were performed with Cox Univariate Regression.

Results: The overall 3-year recurrence/metastasis-free survival was 0.35 (Kaplan-Meier estimate), and 22/45 (49%) patients died of disease within 5 years. 10 patients achieved complete clinical remission status. Pathologically, the majority of tumors showed at least partial epithelioid morphology (64.4%), while spindle cell morphology was not uncommon (31.1%). Other rare types of morphology were observed in small amount of cases. Perineural invasion was more common among tumors with spindle cell component (p=0.02). In addition, 7 cases with spindle cell morphology contained focal areas suggestive of precursor blue-nevus like component. Among all the pathological features, higher mitotic rate was the most significant factor associated with decreased survival (p=0.006). In addition, LVI (8/45) was associated with decreased survival (p=0.03) while brisk TILs (23/45) were associated with increased survival (p=0.01). Other pathological factors and margin status were not prognostically significant. Lastly, 8 patients received adjuvant PD-1 inhibitor and/or CTLA4 inhibitor, with only 1 demonstrated persistent clinical response.

Overall survival						
Variable	**N**	**Events**	**Median Days (95% CI)**	**3-Year Survival % (95% CI)**	**Cox Univariate Hazard Ratio (95% PLCI)**	**Cox Univariate LR p-value**
Mitoses (/mm2) category						0.0057
1) <10	26	11	2359 (1177-)	74.4% (56.6%, 92.2%)	--	
2) 10 to <20	10	8	1199 (218-4300)	60.0% (29.6%, 90.4%)	1.85 (0.71, 4.64)	
3) >=20	9	7	430 (187-824)	16.7% (0.0%, 44.4%)	5.99 (2.06, 16.66)	
LVI						0.0240
0 No	37	20	1819 (1028-4300)	65.4% (49.4%, 81.4%)	--	
1 Yes	7	5	430 (187-)	28.6% (0.0%, 62.0%)	3.85 (1.22, 10.36)	
Tumor infiltrating lymphocytes: any brisk vs non-brisk						0.0130
0 Non-brisk	19	12	824 (222-2359)	49.7% (25.9%, 73.5%)	--	
1 Brisk	23	12	2691 (1177-)	73.9% (56.0%, 91.9%)	0.33 (0.13, 0.79)	

Figure 1 - 1266

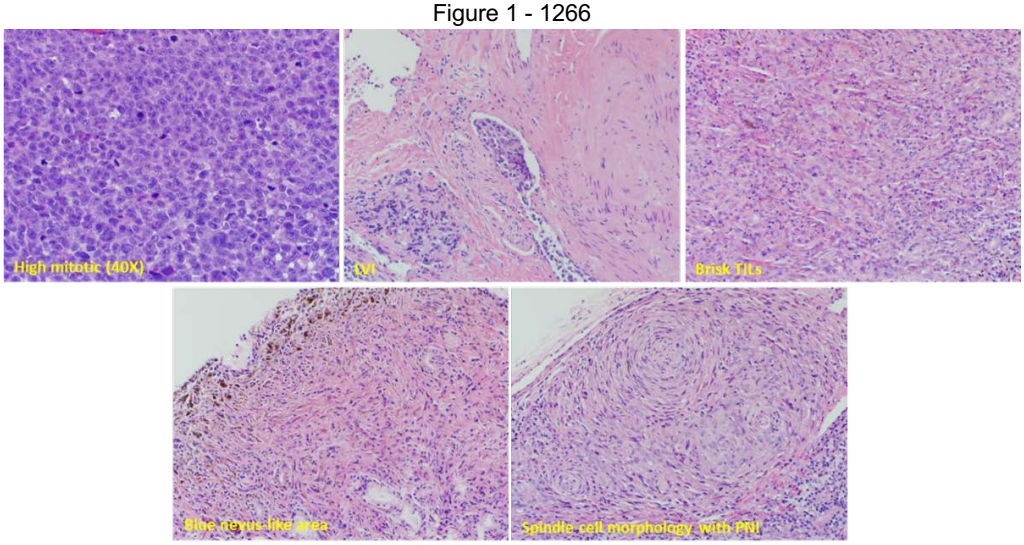

Conclusions: This study described some under-studied morphological features of SNMM and proposed the prognostically significant pathological features, including mitotic rate, LVI and TILs. A larger study to validate these findings is needed, and SNMM pathologic staging report could be potentially

1267 Epidermoid/Orthokeratotic Metaplasia of the Larynx: Toward a Unifying Concept for Pre-Dysplastic Lesions of the Upper Aerodigestive Tract

Danielle Hutchings[1], Annika Windon[2], Kevan Salimian[3], Naziheh Assarzadegan[4], Lysandra Voltaggio[5], Elizabeth Montgomery[6], Lisa Rooper[7]

[1]Johns Hopkins Medicine, Baltimore, MD, [2]Johns Hopkins Hospital, Baltimore, MD, [3]Johns Hopkins, Baltimore, MD, [4]Department of Pathology, The Johns Hopkins Medical Institutions, Baltimore, MD, [5]Baltimore, MD, [6]Johns Hopkins Medical Institutions, Baltimore, MD, [7]The Johns Hopkins University School of Medicine, Baltimore, MD

Disclosures: Danielle Hutchings: None; Annika Windon: None; Kevan Salimian: None; Naziheh Assarzadegan: None; Lysandra Voltaggio: None; Elizabeth Montgomery: None; Lisa Rooper: None

Background: In the esophagus and oral cavity, squamous mucosal lesions defined by hyperkeratosis and orthokeratosis with a granular cell layer have alternately been described as epidermoid metaplasia and orthokeratotic dysplasia. These lesions not only tend to occur in association with conventional squamous dysplasia and squamous cell carcinoma, but they also frequently harbor mutations implicated in squamous carcinogenesis. As such, they are increasingly regarded as precursor lesions for development of squamous neoplasia. In this study, we evaluated the incidence and significance of similar lesions in the larynx, termed here epidermoid/orthokeratotic metaplasia (EOM).

Design: We identified 242 consecutive laryngeal biopsies taken in an outpatient laryngology clinic at a large academic medical center between 2013 and 2015. All cases were reviewed for the presence of EOM, defined as hyperkeratosis and orthokeratosis with a granular cell layer. Any additional pathologic diagnoses were also confirmed. The frequency of squamous dysplasia or carcinoma was compared between cases with and without EOM using Fischer's exact test.

Results: The 242 specimens were taken from 205 patients including 123 men and 82 women with a median age of 58 years (range 19-88 years). EOM was found in 69 biopsies (29%) from 54 patients (26%). EOM was present in in association with 3 invasive squamous cell carcinomas (18%), 33 high-grade dysplasias/carcinomas in-situ (51%), 6 low-grade dysplasias/atypical squamous proliferations (60%), 11 vocal cord polyps (29%), and 16 other benign squamous lesions (14%). Overall, the presence of EOM was significantly associated with squamous dysplasia or carcinoma compared to larynx biopsies without EOM ($p<0.001$).

Conclusions: Similar to the esophagus and oral cavity, the presence of hyperkeratosis and orthokeratosis with a granular cell layer in the larynx occurs significantly more frequently with squamous dysplasia and squamous cell carcinoma than benign squamous lesions. These findings raise the possibility that EOM may represent a pre-dysplastic process throughout the upper aerodigestive tract. More consistent recognition of this entity in the larynx may facilitate better understanding of the role EOM plays in squamous carcinogenesis and prompt appropriate patient follow-up.

1268 SDHx Protein Expression and Mutation Analysis in Vagal Paragangliomas

Dmitry Kalinin[1], Anastasiya Snezhkina[2], Vladislav Pavlov[2], Maria Fedorova[2], Elena Pudova[2], Anastasiya Kobelyatskaya[2], George Krasnov[2], Anna Kudryavtseva[2]
[1]A.V. Vishnevsky National Medical Research Center of Surgery of the Russian Ministry of Healthcare, Moscow, MOS, Russian Federation, [2]Engelhardt Institute of Molecular Biology, RAS, Moscow, Russian Federation

Disclosures: Dmitry Kalinin: None; Anastasiya Snezhkina: None; Vladislav Pavlov: None; Maria Fedorova: None; Elena Pudova: None; Anastasiya Kobelyatskaya: None; George Krasnov: None; Anna Kudryavtseva: None

Background: Vagal paraganglioma (VPGL) accounts for about 13% of all head and neck paragangliomas (HNPGLs) and arises from the vagus nerve paraganglia. VPGL occur as both sporadic and hereditary tumors; mutations in *SDHx* genes are often associated with hereditary VPGL. However, molecular mechanisms behind the VPGL development and progression is not clear. There is no data on distinct diagnostic and prognostic markers for VPGL, as well as potential targets for tumor therapy. VPGL biology has poorly been studied due to rare disease cases.

Design: We performed a comparative analysis of *SDHx* mutation status and their protein expression in vagal paragangliomas. Identification of pathogenic/likely pathogenic mutations in *SDHx* genes (*SDHA*, *SDHB*, *SDHC*, and *SDHD*) and genes, encoding for SDH complex assembly factors (*SDHAF1-4*), were carried out using whole-exome analysis. Exome libraries were prepared with Nextera Rapid Capture Exome Kit (Illumina, USA) and sequenced on a NextSeq 500 System (Illumina) with paired-end mode, 76x2 cycles. The protein expression was assessed using immunohistochemistry.

Results: In five of seven patients with VPGLs, we found pathogenic/likely pathogenic mutations in the studied genes: *SDHB* (3), *SDHD* (1), *SDHAF3* (1), and *SDHAF4* (2) (Table). Negative or weak diffuse SDHB staining was observed in all VPGLs with variants in *SDHB/D* and *SDHAF3/4* genes. In samples without any mutations, weak positive SDHD expression or weak diffuse SDHB staining were detected.

Patient	*SDHx/SDHAF1-4* gene mutated	Pathogenic/likely pathogenic mutation in *SDHx/SDHAF1-4* genes	Immunohistochemistry			
			SDHA	SDHB	SDHC	SDHD
Pat1	No	-	+	+	+	+ (weak)
Pat2	*SDHB*	NM_003000 (*SDHB*): c.A307G, p.M103V (chr1: 17355211, rs140178341) NM_003000 (*SDHB*): c.308_309insTAAG, p.M103fs (chr1: 17355209) NM_003000 (*SDHB*): c.304_305insATGAT, p.A102fs (chr1: 17355213)	+	-	+	+
Pat3	*SDHAF3* *SDHAF4*	NM_020186 (*SDHAF3*): c.T157C, p.F53L (chr7: 96747192, rs62624461) NM_145267 (*SDHAF4*): c.C223T, p.P75S (chr6: 71298323, rs146446063)	+	*	+	+
Pat4	No	-	+	*	+	+
Pat5	*SDHB* *SDHAF4*	(*SDHB*): (chr1: 17350571, rs786201161) NM_145267 (*SDHAF4*): c.C223T, p.P75S (chr6: 71298323, rs146446063)	+	-	+	+
Pat6	*SDHD*	NM_003002 (*SDHD*): c.A305G, p.H102R (chr11: 111959726, rs104894302)	+	*	+	+ (weak)
Pat7	*SDHB*	NM_003000 (*SDHB*): c.C79T, p.R27X (chr1: 17371377, rs74315369)	+	-	+	+ (weak)

(+) - positive staining; (-) – negative staining; (*) - weak diffuse staining.

Conclusions: Negative and weak diffuse SDHB staining correlates with the presence of mutations in *SDHB* and *SDHD* genes, respectively, in VPGLs that is in concordance with the literature data (previous results were obtained for all types of paragangliomas).

However, weak diffuse SDHB immunoreactivity was firstly detected in VPGLs with likely pathogenic mutations in *SDHAF3* and *SDHAF4* genes showing their important role in SDH complex stability. Moreover, the fact that weak diffuse SDHB staining can be seen in VPGLs without any mutations in *SDHx* and *SDHAF1-4* genes indicates other molecular mechanisms (not only pathogenic mutations), which can lead to SDH complex disruption.

This work was financially supported by the Russian Science Foundation, grant no. 19-15-00419.

1269 PD-L1 Combined Positive Score (CPS) Scoring in p16+ Oropharyngeal Squamous Cell Carcinoma (OPSCC): A Comparison of Scoring in Paired Primary Tumors and Lymph Node Metastases

Amandeep Kaur[1], Pouya Jamshidi[2], Ajit Paintal[3]
[1]University of Chicago at NorthShore HealthSystem, Evanston, IL, [2]University of Chicago - Northshore, Chicago, IL, [3]NorthShore University HealthSystem, Glenview, IL

Disclosures: Amandeep Kaur: None; Pouya Jamshidi: None; Ajit Paintal: None

Background: Pembrolizumab, a PD-1 inhibitor, was recently approved by the FDA for use as first line monotherapy in patients with metastatic head and neck squamous cell carcinoma whose tumors demonstrated a PD-L1 CPS score of >=1 by immunohistochemistry (IHC). Patients whose tumors demonstrated CPS scores of >=20 were found to respond particularly well. Prior work has demonstrated frequent discordance in PD-L1 expression by tumor cells in primary versus metastatic sites in non small cell lung cancer. Our goal was to compare PD-L1 CPS scores derived from paired primary tumors (PT) and metastatic cervical lymph nodes (LM) in patients with p16+ OPSCC.

Design: We identified 30 resected p16+ OPSCC cases where concurrent material from both the PT as well as a LM were present. In each case, PD-L1 IHC using the SP263 antibody clone (Ventana) was performed on whole sections from both the PT as well as the LM. CPS scoring was performed by a single experienced observer on all sections and data was analyzed both as a continuous variable and as a dichotomous variable using Cohen's kappa (k) at the CPS>=20 cutpoint.

Results: A CPS<1 was seen in 2 (7%) PT and 2 (7%) LM. A score between 1% and 20% seen in 20 (66%) PT and 17 (56%) LM. 8 (27%) PT and 11 (37%) CM node metastases had CPS>= 20. As a continuous variable, CPS scoring in paired PT and LM showed poor agreement (ICC=.24). Using the CPS>=20% cutpoint, there was a discrepancy between paired specimens in 5 cases (83%) (k=.62). In 4 of the 5 discrepant cases, the LM demonstrated a CPS>=20, while the PT had a CPS score between 1 and 20. At the CPS>=1 cutpoint, there was a discrepancy between the paired specimens in 2 cases (7%). In 1 case, the PT CPS score was >=1 while the LM score was <1. In 1 case the LM CPS score was >=1 while the PT score was <1. As the frequency of cases with CPS<1 was low, inter specimen reliability was not assessed. Discrepant cases variably showed differences in staining of immune cells (Figure 1) and tumor cells (Figure 2).

Case Summary								
Case Number	**Primary Tumor CPS**	**Lymph Node CPS**						
1	25	20						
2	7	5						
3	20	25						
4	10	20						
5	15	15						
6	10	7						
7	25	20			**Case distribution**	**Lymph node CPS**		
8	7	2				<1	>=1, <20	>=20
9	4	<1		**Primary Tumor CPS**	<1	1	1	0
10	2	10			>=1, <20	1	15	1
11	10	100			>=20	0	4	7
12	30	20						
13	5	2						
14	15	30						
15	5	3			**CPS1 Cutpoint**	**Agreement: 93%**		
16	25	20			Agree positive	27		
17	2	1			Agree negative	1		
18	15	15			LN positive, PT negative	1		

19	10	15			PT positive, LN negative	1		
20	15	2						
21	35	20			**CPS20 Cutpoint**	**Agreement: 83%**	**k=.62**	
22	40	10			Agree positive	7		
23	15	15			Agree negative	18		
24	10	25			LN positive, PT negative	4		
25	<1	<1			PT positive, LN negative	1		
26	7	10						
27	10	7						
28	15	15						
29	30	50						
30	<1	1						

Figure 1 - 1269

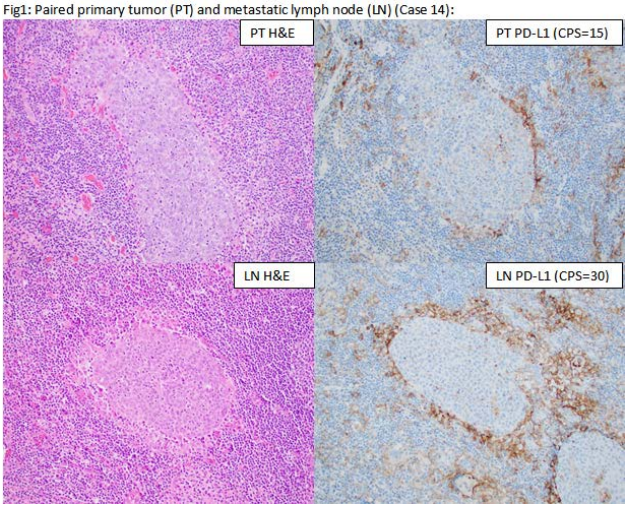

Figure 2 - 1269

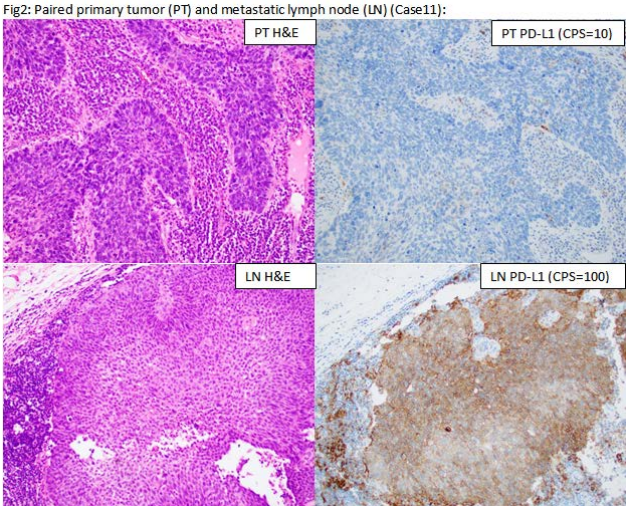

Conclusions: Poor agreement was seen between CPS scores as a continuous variable in PT and LM (ICC=.24). At the CPS>=1 cutpoint, negative cases were uncommon in both PT and LM in p16+ OPSCC and, as a dichotomous variable, CPS scores in PT and LM agreed in 93% of cases. At the CPS>=20 cutpoint, CPS scores in PT and LM agreed in 83% of cases with only moderate interspecimen reliability (k=.62). In most discrepant cases, the LM CPS was greater than the PT CPS.

1270 Expanding the Clinicopathologic and Genomic Characterization of Inflammatory Myofibroblastic Tumors of the Head and Neck: Identification of a Novel Fusion Partner and a Potential Diagnostic Pitfall

Darcy Kerr[1], Lester Thompson[2], Laura Tafe[3], Vickie Jo[4], Azfar Neyaz[5], Ivy John[6], Claudia Salgado[7], Vikram Deshpande[8], Julia A. Bridge[9], Iva Brcic[10], Konstantinos Linos[3]

[1]Dartmouth-Hitchcock Medical Center and Geisel School of Medicine at Dartmouth, Lebanon, NH, [2]Southern California Permanente Medical Group, Woodland Hills, CA, [3]Dartmouth-Hitchcock Medical Center, Lebanon, NH, [4]Brigham and Women's Hospital, Harvard Medical School, Boston, MA, [5]Massachusetts General Hospital, Malden, MA, [6]University of Pittsburgh, Pittsburgh, PA, [7]Children's Hospital of Pittsburgh, Pittsburgh, PA, [8]Massachusetts General Hospital, Boston, MA, [9]Translational Genomics Research Institute/University of Nebraska Medical Center, Phoenix, AZ, [10]Medical University of Graz, Graz, Austria

Disclosures: Darcy Kerr: None; Lester Thompson: None; Laura Tafe: None; Vickie Jo: *Employee*, Merck and Co; Azfar Neyaz: None; Ivy John: None; Claudia Salgado: None; Vikram Deshpande: *Grant or Research Support*, Advanced Cell Diagnostics; *Advisory Board Member*, Viela Bio; *Grant or Research Support*, Agios Pharmaceuticals; Julia A. Bridge: None; Iva Brcic: None; Konstantinos Linos: None

Background: Inflammatory myofibroblastic tumor (IMT) is a rare, distinctive (myo)fibroblastic neoplasm that may recur locally and rarely metastasizes. IMTs harbor frequent tyrosine kinase fusions, most often *ALK*. They are uncommon in the head and neck area (HN-IMT) comprising ~16% of extra-pulmonary IMTs. Herein, we describe the clinicopathologic and molecular features of a HN-IMT cohort.

Design: HN-IMTs were identified from archives of 5 institutions. Slides and available clinicopathologic data were centrally reviewed. Genomic characterization was performed (Archer® Sarcoma or Ashion® GEM ExTra™). While 13 cases met preliminary inclusion criteria, 1 was reclassified after further molecular analysis for a final cohort of 12.

Results: Patients were 7 males (M) and 5 females (F) aged 7-69 years (median 25.5). Median tumor size was 1.5 cm (range 0.6-10.6); locations were: larynx (6), oral cavity (3), pharynx (2), and mastoid bone (1). Histologically, tumors showed a storiform proliferation of spindle cells comprising 10-90% (mean 60%) of tumor cellularity with an associated mixed inflammatory infiltrate. Mitoses ranged from 0-5 per $2mm^2$; no case had malignant histology. By immunohistochemistry (IHC), 10/12 cases were ALK+, 6/10 were SMA+, and 0/10 expressed keratin. *ALK* partner genes were identified in 9/12 cases (1 had poor RNA quality but was *ALK*+ by fluorescence *in situ* hybridization (FISH)). The most common rearrangement was *TIMP3-ALK* (5); remaining *ALK* fusion partners were (1 case each): *TPM3, KIF5B, CARS* and *THBS1*. One ALK- case showed a novel *SLC12A2-ROS1* fusion (28M, hypopharynx), and 1 was fusion negative (46F, mastoid). Most (11/12) patients were treated surgically. Two patients received crizotinib, and both showed treatment response. All 11 patients with clinical follow up (mean 2.8 years) were alive without metastasis. One developed local recurrence after 3 years and is now disease-free 5.3 years from presentation. The excluded case was ALK+ by IHC; however, it was reclassified as a spindle cell rhabdomyosarcoma (RMS) after identification of a *FUS-TFCP2* fusion and demonstration of desmin and MyoD1 expression by IHC.

Conclusions: In our cohort, HN-IMTs often involve the larynx, show a range of neoplastic cellularity and most (92%) harbor a driver molecular abnormality, commonly *ALK*. Tumors tend to have indolent biology, though may recur locally. Our experience highlights the identification of *SLC12A2-ROS1*, a novel fusion in IMT, and a potential diagnostic pitfall with ALK+ spindle cell RMS.

1271 Association of HPV In Nasopharyngeal Carcinoma In Caucasian-Americans: An Intuitional Experience

Binny Khandakar[1], Jihong Sun[2], Shengje Cui[3], Lingjia Liu[4], Margaret Brandwein-Weber[5]
[1]Mt Sinai St Luke's Roosevelt Hospital, New York, NY, [2]Mount Sinai West, New York, NY, [3]Mount Sinai St Luke's Roosevelt Hospital, New York, NY, [4]NewPath Diagnostics, Flushing, NY, [5]Icahn School of Medicine at Mount Sinai, New York, NY

Disclosures: Binny Khandakar: None; Jihong Sun: None; Shengje Cui: None; Lingjia Liu: None; Margaret Brandwein-Weber: None

Background: Nasopharyngeal carcinoma (NP-Ca) is a tumor arising from the epithelial cells ling the surface of the nasopharynx. Annual incidence in the United States (US) is <1/ 100,000; it is commoner in Asia. Epstein-Barr virus (EBV) has been proven as a known causative agent in Asian population. Human papilloma virus (HPV) may play a role in Caucasian-American population. The association of HPV and NP-Ca in Caucasian-Americans is not well established. The current study aims to explore the association of HPV and NP-Ca in Caucasian-Americans.

Design: This retrospective study [2012-2019] including all nasopharyngeal cancers diagnosed at the institution, which are tested for EBV-in-situ hybridization (EBER-ISH) and p16 immunohistochemistry. Cases without an EBER-ISH result were excluded. All EBER-ISH negative and p16 positive cases were tested for HPV DNA by polymerase chain reaction (PCR) method. Clinic-pathologic features were noted and the data was symmetrically analyzed.

Results: Cohort (n=27) comprised of Caucasian-Americans (n=16), Asian (n=8), & African-American (n=3). 21 cases were male (M: F = 21:6). Mean age of entire cohort was 53-years; mean age was 59-years in Caucasian-Americans (table1). 89% tumor was non-keratinizing squamous carcinoma. P16 was expressed in 13; all p16 positive were tested for HPV by PCR. 8 cases were positive for HPV (n=8, Caucasian-American; n=0, Asian/Chinese; n=0, African–American). 50% of the Caucasian-American patients were positive for HPV. Most common subtype of HPV was 16 (n=4), followed by 45 (n=3) & 18 (n=1). 38% (n=5/13) of p16-positive cases were negative for usual HPV subtype (16, 18 and 45). Overall 52 % cases were positive for EBV (n=14). EBV was positive in all NP-ca from Asian/Chinese population (n=8), while only 25% cases in the Caucasian-Americans was positive for EBV (n=4). There was no co-expression of EBV & HPV (table1).

Characteristics	**Ethnic Groups**			
	Caucasian-American (n=16)	Chinese/Asian (n=8)	African-American (n=3)	Overall (n=27)
Age [mean (range), years]	59 (40-83)	43 (16-64)	52 (47-56)	53 (16-83)
Gender (M: F)	12:4	7:1	2:1	21:6
Tumor type (n)				
Non-keratinizing SCC (n)	14	8	2	24
Papillary SCC (n)	1	0	0	1
Keratinizing SCC (n)	1	0	1	2
EBV [positive, n]	4	8	2	14
P16 [positive, n]	11	1	1	12
HPV [positive, n]	8	0	0	8

HPV subtypes (n)	16 (4) 45 (3) 18 (1)	-	-	16 (4) 45 (3) 18 (1)	
P16 & HPV co-expression	8	0	0	8	
P16 & EBV co-expression	0	1	0	1	
EBV & HPV co-expression	0	0	0	0	

Conclusions: NP-Ca is historically described as an EBV-associated/driven tumor; however, there is a difference in pathogenesis in different ethnic group. Based on our series, in the US, majority of the NP-Ca in the Caucasian-Americans are HPV-positive and P16 may be helpful as a surrogate marker for HPV-driven NP-ca as in these cases in other sites. In the Chinese/Asian population, NP-ca is EBV-positive. Not all P16 positive cases were positive for the commonly tested HPV subtype, which may indicate additional/unknown HPV subtypes may be responsible for HPV-associated NP-Ca.

1272 Evaluation of Phenotypic Differences as a Function of HPV Genotype in a Large Experience of Head and Neck Cancers: HPV 18 Strongly Correlates with the Small Cell Phenotype

Binny Khandakar[1], Simran Mashiana[2], William Westra[3]
[1]Mt Sinai St Luke's Roosevelt Hospital, New York, NY, [2]University of Nebraska Medical Center, Omaha, NE, [3]Icahn School of Medicine at Mount Sinai, New York, NY

Disclosures: Binny Khandakar: None; Simran Mashiana: None; William Westra: None

Background: Of the more than 200 known HPV genotypes, type 16 dominates the oncologic landscape when it comes to head and neck carcinomas (HNC). Current clinical practice algorithms advocating non-discriminant HPV testing by way of p16 immunohistochemistry makes no effort to discern the impact of variant (i.e. non-16) HPV genotypes. As a result, virtually everything known about the pathology and behavior of HPV-HNC is based on HPV16. The purpose of this study was to challenge the prevailing assumption of HPV equivalency across all high-risk HPV genotypes.

Design: As of 2012, it has been the practice of our institution to provide HPV genotype information for those HNCs cancers undergoing HPV testing using a PCR-based approach combined with Sanger's sequencing. Following histologic evaluation of the HPV positive cases, we compared the phenotypic features of HPV-positive HNCs as a function of HPV genotype.

Results: A total of 1058 cases from 964 patients with head and neck cancer were tested over a 7 year period. 655 (68%) patients had HPV positive cancers. The preponderance of these HPV-related carcinomas arose from the oropharynx (n=565, 86%) and the sinonasal tract (n=30, 5%). The most frequently detected genotype was 16 (n=551, 84.1%) followed by 35 (n=37, 5.6%), 33 (n=27, 4.1%), 18 (n=18, 2.7%), 45 (n=7, 1.1%), 69 (n=5, 0.8%), 56 (n=4, 0.6%), 67 (n=2, 0.3%), 58 (n=1, 0.2%) and 59 (n=1, 0.2%). Comparing the phenotypic features of HPV16 and HPV-variant carcinomas, there were no significant differences with respect to anaplasia, mitotic activity, basaloid features or morphologic variant forms (e.g. lymphoepithelial variant) with the notable exception of the small cell variant. Of the 5 patients with HPV-positive small cell carcinomas, HPV18 was detected in 4 cases, HPV69 in 1 case, and HPV16 in none. HPV18 (4 of 18 cases, 22%) and HPV69 (1 of 5 cases, 20%) cases were strikingly associated with small cell transformation, but HPV16 cases (0 of 551, 0%) were not ($p < 0.0001$).

Conclusions: HPV genotyping across a large experience of HNCs promises to provide some resolution in pathologic and behavioral differences among the various HPV genotypes associated with head and neck cancer. As one important example, variant HPV types, particularly HPV18, strongly correlate with the small cell phenotype – a highly aggressive form of HPV-HNC. This observation may explain in part the more aggressive behavior of HPV variant-HNC that has been consistently noted in clinical outcome studies.

1273 Predictive Value of the Depth of Invasion for Cervical Lymph-Node Involvement in Squamous Cell Carcinoma of the Oral Cavity: A 10-Year Retrospective Analysis

Erisa Kola[1], Berdica Leart[2], Mehdi Alimehmeti[3]
[1]Mother Teresa University Hospital Center, Tirane, Tirane, Albania, [2]Mother Teresa University Hospital Center, Tirana, Albania, Albania, [3]Mother Teresa University Hospital Center, Tirana, Tirana, Albania

Disclosures: Erisa Kola: None

Background: Oral and maxillofacial malignancies consist of a wide range of lesions with squamous cell carcinoma (SCC) being the most common type. Oral SCC has a high metastatic potential with a predilection to spread to regional lymph nodes. Most patients present at advanced stage disease, because it is difficult to detect the disease clinically at an early stage.

Design: The aim of this study is to provide information about epidemiological data of the disease in Albania, to explore the effect of the depth of invasion for predicting metastases in pT1-T2 OSCC and to determine the optimal cut-off depth for performing an elective neck dissection.

Materials and methods
Records of malignant tumors of oral and maxillofacial regions were retrospectively analyzed from January 2009 to January 2019. Microscopic slides of patients diagnosed with primary oral SCC were reviewed following the criteria such as depth of invasion using an ocular micrometer, histological grade and cervical nodal metastases in subjects who had undergone elective neck dissection. Correlation analyses were made studied by the Chi-square test. P-value <0.05 was accepted as the level of statistical significance.

Results: A total of 1,159 cases were diagnosed as malignant tumors of the oral and maxillofacial region, from which 61% were diagnosed as squamous cell carcinoma, salivary gland cancer (17%) with mucoepidermoid carcinoma being the most common type, metastasis (7%), lymphoma (3%), sarcoma (3%) and other tumors (9%). 108 patients with OSCC pT1-T2 were selected and 56 of them had undergone neck dissection. Evaluation of the relationships of nodal stage with histologic grade and depth of invasion using the Chi-Square test showed statistical significance with P-values of <0.003 and <0.005 respectively.

	Total patients included
Total Oral and Maxillofacial Malignancies	1159
Oral SCC	698
Primary OSCC pT1-T2	234
Male	464
Female	234
Mean Age at Diagnosis	61
Median	63
Range	19-92
Site:	123
Lip	8
Floor of mouth	49
Cheek mucosa	39
Tongue	8
Retromolar area	7
Others	
Depth of invasion	108 pts
Mean	4.76 (108 pts)
Range	0.5-10 mm (108 pts pT1-2)
Neck dissection	56 pts (N0=28, N1=28)

Figure 1 - 1273

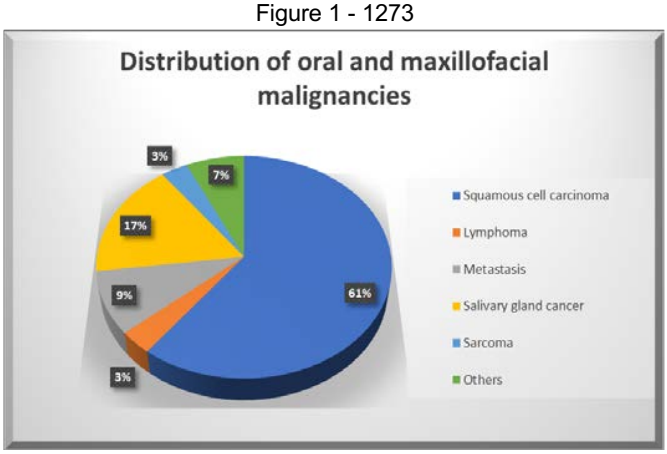

Figure 2 - 1273

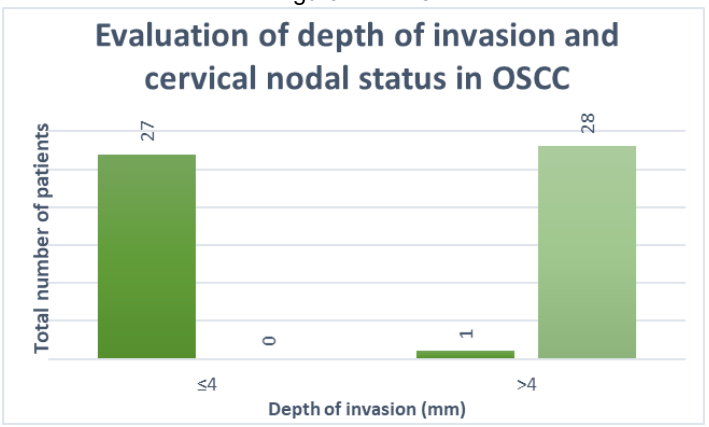

Conclusions: Oral SCC is the most frequent head and neck cancer. Our analysis revealed a statistically significant relationship among histological grade, depth of invasion and lymph node involvement underscoring the importance of reporting these tumor features and their effect in predicting the outcome of patients with oral SCC. This emphasizes the significance of constructing a method to identify high risk versus low risk patients, thereby to reduce unnecessary neck dissections. According to that an infiltration depth of ≥4 mm is an indication for high risk positive nodal metastasis. A larger sample size and additional well-designed prospective randomized controlled trials would enable better understanding of this association.

1274 Predicting HPV Status of Oropharyngeal Squamous Cell Carcinoma Patients Using Handcrafted Histomorphometric and Deep Learning Features

Can Koyuncu[1], Cheng Lu[1], Dibson Gondim[2], Kaustav Bera[1], Lester Thompson[3], James Lewis[4], Anant Madabhushi[1]
[1]Case Western Reserve University, Cleveland, OH, [2]University of Louisville, Louisville, KY, [3]Southern California Permanente Medical Group, Woodland Hills, CA, [4]Vanderbilt University, Nashville, TN

Disclosures: Can Koyuncu: None; Cheng Lu: None; Dibson Gondim: None; Kaustav Bera: None; Lester Thompson: None; James Lewis: None; Anant Madabhushi: *Consultant*, Inspirata Inc; *Stock Ownership*, Inspirata Inc.

Background: Human papillomavirus (HPV) accounts for 70 to 80 percent of oropharyngeal squamous cell carcinoma (OPSCC) cases in North America and Europe [1]. The HPV status is critical for staging, treatment, and prognosis. There are numerous tests on different specimens to determine HPV status. In this study, we developed and compared two computer-aided approaches for predicting p16/HPV status using H&E stained primary tumor slides.

Design: A cohort of 50 patients with primary OPSCC, including 25 p16+ and p16-, were used to build the classifiers. H&E slides from the primary tumors (biopsy or resection) were digitally scanned at 40x magnification. Handcrafted and DL features were extracted from tumor regions identified using a neural network-based strategy. For the computational histomorphometric classifier, features related with the spatial arrangement of nuclei on H&E images, proposed in [2], were extracted and the top three features were selected (Wilcoxon test) to build the final classifier (LDA classifier). 3-fold cross validation was applied 100 times. For the DL based classifier, a patch-wise ResNet architecture was employed. 3142 patches (2048*2048 at 40x magnification) were extracted (n_{pos} = 1812, n_{neg} = 1330). Patches were separated into training and validation sets. The DL model was built using the training set and validated on the validation set. The majority voting approach was employed to assign the final label of patients. To validate and compare our classifiers on an independent set, we utilized another cohort of 35 patients with OPSCC, of which 16 and 19 were p16- and p16+, respectively.

Results: Area under the ROC curve (AUC) for the handcrafted and the DL models were 75.66 and 80.59 respectively, on the independent test set (N=35) (Table 1). 62.86% of the cases were accurately classified correctly by both methods.

Table 1: AUC, accuracy, sensitivity, and specificity results of the two classifiers on the independent test set.

	AUC	Accuracy	Sensitivity	Specificity
Histo. classifier	75.66	80.00	94.74	62.50
DL classifier	80.59	80.00	84.21	75.00

Conclusions: This study compares two different computational feature engineering approaches for p16 prediction from H&E images of OPSCC patients. Both approaches show promise in predicting the HPV status of patients using only H&E slides. Future work will entail combining the two approaches and comparing it with human visual HPV status prediction as well as gold standard HPV-specific testing.

1275 Tumor Cell Multinucleation is More Frequent in African-American Oropharyngeal Squamous Cell Carcinoma Patients Than Caucasian-American Ones – Implications for Outcome Differences

Can Koyuncu[1], Cheng Lu[1], Zelin Zhang[2], Pingfu Fu[3], Dibson Gondim[4], Jun Xu[2], Kaustav Bera[1], James Lewis[5], Anant Madabhushi[1]

[1]Case Western Reserve University, Cleveland, OH, [2]Nanjing University of Information Science and Technology, Nanjing, China, [3]Broadview Heights, OH, [4]University of Louisville, Louisville, KY, [5]Vanderbilt University, Nashville, TN

Disclosures: Can Koyuncu: None; Cheng Lu: None; Zelin Zhang: None; Pingfu Fu: None; Dibson Gondim: None; Jun Xu: None; Kaustav Bera: None; James Lewis: None; Anant Madabhushi: *Consultant*, Inspirata Inc.; *Stock Ownership*, Inspirata Inc

Background: Human papillomavirus-related (p16+) oropharyngeal squamous cell carcinoma (OPSCC) patients have improved prognosis but can have major morbidity from current treatment regimens and data have suggested poorer survival for African-American (AA) patients with this cancer type compared to Caucasians (CA). Tumor cell multinucleation (MN) by image analysis has been shown to be an independent prognostic factor in p16+ OPSCC patients [1]. In this study, we analyzed the differences of computer detected MN index between patients of these different races.

Design: Three independent cohorts (totaling 544 patients, 28 AA and 516 CA) with primary p16+ OPSCC were utilized. Each patient had one representative H&E slide from their primary tumors (biopsy or resection) digitally scanned at 40x magnification. We used a pretrained deep learning (DL) model to automatically detect epithelial cells and stroma on the image. MN index was then calculated within the epithelium, which is the ratio of the number of MNs to the number of cells. The two groups (CA vs AA) were compared under Mann Whitney U-Test. Since MN index is very skewed in the entire dataset, 40 of the 516 CA patients were randomly selected and the MN index was compared to the entire AA group (28 patients). The step was repeated 200 times using a bootstrapping method, and the associated p-values were recorded for each iteration for the analysis.

Results: Among the 200 comparisons, 63% and 79% of the p-values were less than 0.05 and 0.1, respectively. The histogram of these collected p-values is shown in Figure 1. This experiment indicates that the difference in MN indices of the CA and AA groups is statistically significant.

Figure 1 - 1275

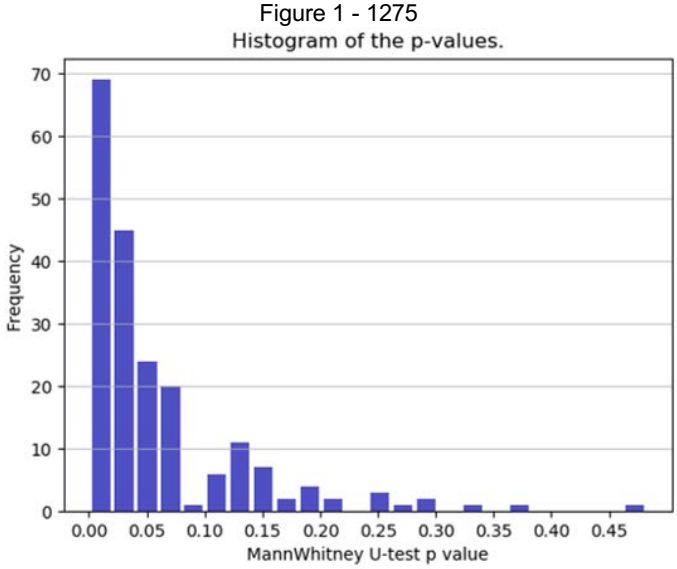

Figure 2 - 1275

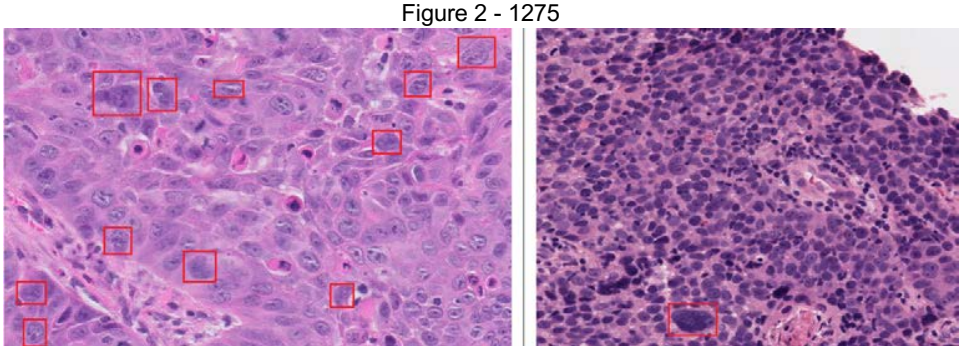

Conclusions: This study validates that the computer-extracted MN index of p16+ AA OPSCC patients is significantly higher than for CA patients (see example images in Fig. 2). Multinucleation in OPSCC is known to be correlated with the tumor aggressiveness and shows promise as a biomarker for disease prognosis. This study suggests that MN may help explain why AA patients with p16+ OPSCC have poorer survival. Investigation of the underlying mechanisms of MN may be useful.

1276 Small Biopsy Samples- Are They Representative for the Biphenotypic Sinonasal Sarcoma? - Proposed Diagnostic Algorithm Based on Immunohistochemical and Molecular Tests

Olga Kuczkiewicz-Siemion[1], Aneta Wojnowska[2], Maciej Rysz[3], Monika Durzyńska[2]
[1]Maria Sklodowska-Curie Cancer Center - Institute of Oncology, Warsaw, Poland, [2]Maria Sklodowska-Curie Institute - Oncology Center, Warsaw, Poland, [3]Maria Sklodowska-Curie Institute - Oncology Center, Warszawa, Poland

Disclosures: Olga Kuczkiewicz-Siemion: None; Aneta Wojnowska: None; Maciej Rysz: None; Monika Durzyńska: None

Background: Biphenotypic sinonasal sarcoma (BSNS) is a rare entity initially described in 2012 by Lewis et al. This low-grade (LG) spindle cell sarcoma of the upper sinonasal tract is characterized by specific rearrangements of *PAX3* gene and both myogenic and neural differentiation, which can be demonstrated by co-expression of S100 and myogenic markers. However, the available IHC stains are relatively nonspecific and can show only focal or patchy pattern. Additionally, due to histologic similarities to other sinonasal sarcomas BSNS is a diagnostic challenge, especially from small biopsy specimen.

The aim of our study was to evaluate the utility of small biopsy examination in diagnosis of BSNS and establish the diagnostic algorithm for sinonsal LG spindle cell sarcomas.

Design: We searched our clinical cohort of solid tumor patient samples from sinonasal tract area (January 2009 to August 2019). H&E stained slides, whenever tissue material were available, were re-evaluated and only LG spindle cell sarcomas (lack of: high-grade atypia, necrosis or atypical mitoses) with paired biopsy and subsequent resection specimens were included to the study. Osteosarcomas and chondrosarcomas were excluded. Both biopsy and surgical specimens were stained for: S100, SMA, desmin, caldesmon, SOX10, MyoD1, STAT6, CD34, CKAE1\3, EMA. Further FISH for *PAX3* was performed on resection specimens. In some cases TLE-1 (IHC) and *SS18* (FISH) were done. Diagnostic algorithm (Figure 1) was established based on morphology, IHC and molecular findings.

Results: Six small biopsies with surgical specimens were included to the study. BSNS diagnosis was made in 4 cases and confirmed by *PAX3* rearrangement in 3 specimens. Among 4 BSNS cases all patients were females with a mean age of 67 years. Average diameter of BSNS biopsy samples was 0,8 cm, which accounted for 32% of H&E stained slide average diameter of subsequently resected tumor. IHC panel was identical for paired samples apart from 1 BSNS case. IHC for TLE-1 was diffusely positive in 1 paired BSNS specimen, however FISH for SS18 was negative (Table 1).

No.		**1**	**2**	**3**	**4**	**5**	**6**
Age (years)		68	62	45	62	70	75
Sex		F	F	M	F	M	F
IHC	S100	(+) focal*	(+) focal*	(-)*	(+)*	(-)*	(+) focal*
		(+) focal	(+) focal	(-)	(+)	(-)	(+) focal
	SMA	(+) focal*	(+) focal*	(+) focal*	(+) focal*	(-)*	(-)*
		(+) focal	(+) focal	(+) focal	(+) focal	(-)	(+) patchy
	desmin	(-)*	(-)*	(-)*	(-)*	(-)*	(-)*
		(-)	(-)	(-)	(-)	(-)	(-)
	caldesmon	(-)*	(-)*	(-)*	(-)*	(-)*	(-)*
		(-)	(-)	(-)	(-)	(-)	(-)
	MyoD1	(-)*	(-)*	(-)*	(-)*	(-)*	NA
		(-)	(-)	(-)	(-)	(-)	NA
	SOX10	(-)*	(-)*	(-)*	(-)*	(-)*	NA
		(-)	(-)	(-)	(-)	(-)	NA
	STAT6	(-)*	(-)*	(-)*	NA	NA	NA
		(-)	(-)	(-)*	NA	NA	NA
	CD34	(-)*	(-)*	(-)*	(-)*	(-)*	(-)*
		(-)	(-)	(-)	(-)	(-)	(-)
	CKAE1/3	(-)*	(-)*	(-)*	(-)*	(-)*	(-)*
		(-)	(-)	(-)	(-)	(-)	(-)
	EMA	(-)*	(-)*	(-)*	(-)*	(-)*	(-)*
		(-)	(-)	(-)	(-)	(-)	(-)
	TLE-1	NA	NA	NA	(+)*	NA	NA
		NA	NA	NA	(+)	NA	NA
FISH	PAX3	(+)	(+)	(-)	(+)	(-)	ND
	SS18	(-)	NA	(-)	(-)	ND	NA

Diagnosis	BSNS	BSNS	LGMS	BSNS	LG MPNST	BSNS
*- biopsy speimen; NA- not available; ND- non diagnostic; LGMS- low- grade myofibroblastic sarcoma; LG MPNST- low-grade malignant peripheral nerve sheath tumour						

Figure 1 - 1276

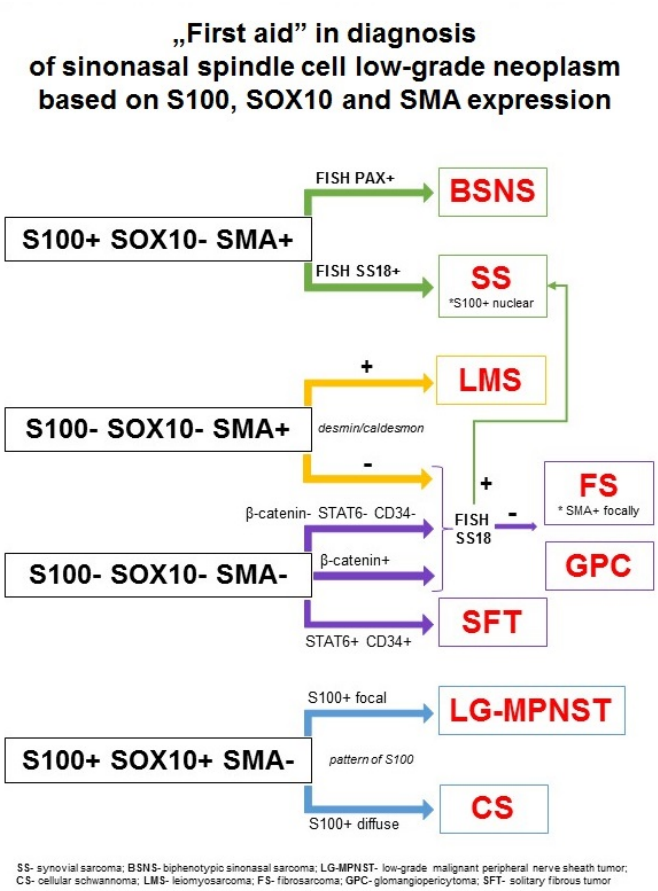

Conclusions: Diagnosis of LG sinonasal sarcoma is relatively rare, however BSNS is a quite common finding in this group. The biopsy is appropriate method to establish BSNS diagnosis in most cases. *PAX3* rearrangement is specific for BSNS. We encourage to use our algorithm for sinonasal small biopsies in the morphological spectrum of LG spindle cell sarcomas.

1277 Immunoprofiling of Salivary Duct Carcinoma in a Large Cohort Retrospective Study of 170 Patients from Japan: Significances of p53 and MUC6

Kimihide Kusafuka[1], Satoshi Baba[2], Matsuyoshi Maeda[3], Koji Yamanegi[4], Hiroshi Inagaki[5], Yoshiro Otsuki[6], Naoto Kuroda[7], Junya Itakura[8], Yoshiaki Imamura[9]
[1]Shizuoka General Hospital, Shizuoka city, Shizuoka, Japan, [2]Hamamatsu University School of Medicine Hospital, Hamamatsu, Shizuoka, Japan, [3]Toyohashi Municipal Hospital, Toyohashi, Japan, [4]Hyogo College of Medicine, Nishinomiya, Japan, [5]Nagoya City University, Nagoya, Japan, [6]Seirei Hamamatsu General Hospital, Hamamatsu, Shizuoka, Japan, [7]Kochi Red Cross Hospital, Kochi City, Kochi, Japan, [8]Kurashiki Central Hospital, Kurashiki, Okayama, Japan, [9]Fukui University, Yoshida-gun, Fukui, Japan

Disclosures: Kimihide Kusafuka: None; Satoshi Baba: None; Matsuyoshi Maeda: None; Koji Yamanegi: None; Hiroshi Inagaki: None; Yoshiro Otsuki: None; Naoto Kuroda: None; Junya Itakura: None; Yoshiaki Imamura: None

Background: Salivary duct carcinoma (SDC) is a relatively rare high-grade malignancy of the salivary glands, but it is frequently seen as a carcinomatous component of carcinoma ex pleomorphic adenoma (CXPA). We aim to subclassify SDC cases and to elucidate the relationship with its outcomes, and also to find a new bio-marker for SDC.

Design: We re-estimated SDC cases from 10 institutions during 1990-2019, immunostained them for SDC bio-markers, and according to modified Katase's classification (Oncotarget 2017), we subclassified them into 7 subtypes: apocrine A(AR+/HER2-/Ki-67^{low}), apocrine B(AR+/HER2-/Ki-67^{high}[>40%]), apocrine-HER2(AR+/HER2+), HER2-enriched(AR-/HER2+), basal-like(EGFR+ and/or CK5/6+), HER2-

basal(HER2+/EGFR+ or CK5/6+) and unclassified. We also examined the expression status of p53 in all cases and the expression status of MUC1, MUC2, MUC5AC, and MUC6 in 102 cases. We examined them with statistical analysis using STATA ver. 13.

Results: One hundred seventy cases were finally diagnosed as SDC: 101 cases of CXPA, including 24 cases of intracapsular type; 65 cases of *de novo* cancer; unknown, 4 cases. The mean age of the patients was 65-years-old, and M/F ratio was 3.9:1. The parotid gland, submandibular gland, other sites and unknown were 130, 34, 4, and 2 cases, respectively. pN(+) cases showed worse outcome, and pT3/T4 cases were also similarly worse. Apocrine A, apocrine B, apocrine-HER2, HER2-enriched, basal-like, HER2-basal, and unclassified were 18, 42, 50, 25, 15, 10, and 10 cases, respectively. In the cases in which we could follow up, the rates of the patients, who died of disease and were alive with disease, were 38%, 52%, 45%, 58%, 40%, 40%, and 50% in apocrine A, apocrine B, apocrine-HER2, HER2-enriched, basal-like, HER2-basal, and unclassified, respectively. Strong positivity and entire negativity for p53, which corresponded to the point mutation and the deletion of *TP53* gene, respectively, were frequently observed in apocrine B (60%) and apocrine-HER2 (62%). MUC1 was expressed in almost cases (95%), examined, whereas MUC6 expression (30%) was frequently observed in non-dead and non-relapsed cases, despite of subtypes.

Results of clinicopathological analysis				
	DOD/AWD	**AWOD**	**lost/DOAD**	**total**
Gender				
M	55	49	31	135
F	9	14	12	35
Age				
<= 66 y/o.	25	38	15	79
> 66 y/o.	42	30	19	91
Site				
parotid gland	45	50	36	131
submandibular gland	17	12	4	33
others	2	1	1	4
unknown	0	0	2	2
pT factor				
pT1/T2	16	35	21	72
pT3/T4	38	30	21	89
pN factor				
pN0	11	31	15	57
pN+	45	25	17	87
CXPA vs *de novo* ca.				
CXPA(intracapsular)	3	11	10	24
CXPA(minimally invasive)	3	3	6	12
CXPA(widely invasive)	24	28	13	65
de novo ca.	25	27	11	63
SDCIS	0	1	1	2
unknown	2	0	2	4
Immuno-subtypes				
apocrine A	5	8	5	18
apocrine B	16	15	11	42
apocrine-HER2	17	21	12	50
HER2-enriched	11	8	6	25
basal-like	4	6	5	15
HER2-basal	4	6	0	10
unclassified	3	3	4	10
p53 status				
p53(++)[Mutation pattern]	13	15	7	35
p53(-)[Deletion pattern]	20	17	5	42
p53(weakly+)[Wild type pattern]	35	26	23	84
MUC expression				
MUC1	38	45	14	97
MUC2	5	3	1	9
MUC5AC	3	3	4	10
MUC6	15	31	12	58

Figure 1 - 1277

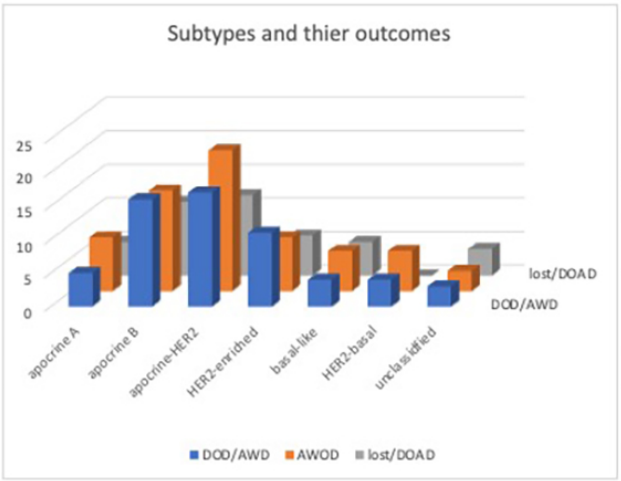

DOD, dead of disease; AWD, alive with disease; AWOD, alive without disease; DOAD, dead of another disease

Figure 2 - 1277

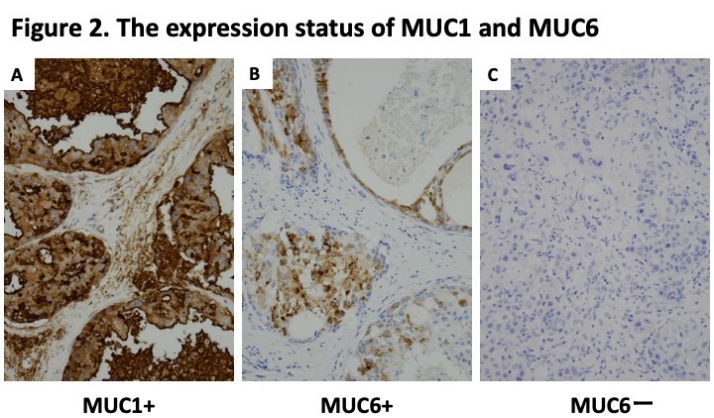

Conclusions: HER2-enriched and apocrine B subtypes statistically showed worse outcomes rather than other subtypes, whereas apocrine A subtype showed better outcome. Apocrine-HER2 subtype was related to the abnormal status of p53. As MUC6 was mainly expressed in the cases with good outcome despite subtypes, it may be a new prognostic marker for SDC.

1278 Ligation-Dependent RT-PCR: A New Specific and Low-Cost Technique to Detect Gene Fusion in Salivary Gland Tumors

Marie Delphine Lanic[1], Michel Wassef[2], Rene Guerin[1], Didier Meseure[3], Fabrice Jardin[1], Philippe Ruminy[1], Marick Lae[4]
[1]Centre Henri Becquerel, Rouen, France, [2]Hopital Lariboisiere, Paris, France, [3]Curie Institute, Paris, France, [4]Paris, France

Disclosures: Marick Lae: None

Background: Gene fusion have become central to the characterization of salivary gland tumors including MASC-mammary analog secretory carcinoma, HCCC-hyalinizing clear cell carcinoma, MEC –mucoepidermoid carcinoma, AdCC-adenoid cystic carcinoma, IC-salivary gland intraductal carcinoma and ACC-acinic cell carcinoma. We developed a multiplex Ligation-dependent reverse transcription polymerase chain reaction (LD-RTPCR) technique, applicable to FFPE samples, able to detect these rearrangements using oligonucleotide probes which specifically hybridized to either side of the break point on fusion mRNAs. After ligation and PCR amplification, these probes are then sequenced by next-generation sequencing (NGS) in order to identify the two genes involved.

Design: 50 salivary gland tumors known to be associated with a gene fusion (31 MASC, 9 HCCC, 5 IC, 2 MEC, 2 adenocarcinomas NOS, 1 AdCC) were reviewed by pathologists from the French Rare Head and Neck Tumors Group (REFCOR) and tested by FISH with break apart probes. LD-RTPCR with a mix containing 336 probes allowing the detection of fusion genes involving more than 180 genes, 12 of which are recurrent in these tumors was performed, in all cases starting from RNA extracted from FFPE blocks.

Results: Among 26 MASC, 23 presented an *ETV6* rearrangement (FISH). LD-RTPCR identified *ETV6-NTRK1*(n=20) or *ETV6-RET (n=3)* fusions. In 3 cases with non interpretable *ETV6* FISH, LD-RTPCR identified an *ETV6-NTRK1* fusion. These tumors were definitely classified as MASC. None of the cases diagnosed as “suspicion of MASC” (n=5) harbored *ETV6* rearrangement (FISH). LD-RTPCR identified 5 *NCOA4-RET* fusions allowing their reclassification as IC. One IC was also confirmed to harbor a *NCOA4-RET* fusion. 9 HCCC presented *EWSR1* gene rearrangement (FISH). The LD-RTPCR assay confirmed the presence of *EWSR1-ATF1* (n=8) and *EWSR1-CREM (n=1)* fusion. 2 adenocarcinomas NOS were reclassified by LD-RTPCR: one MASC with *ETV6-NTRK1*, one IC with *NCOA4-RET fusion*. 2 MEC harbored a *CRTC1-MAML2 (n=1) and CRTC3-MAML2 (n=1)* fusion, 1 AdCC a *MYB-NFIB*

Conclusions: Ligation-dependent RT-PCR is a new specific and low-cost technique to detect a large spectrum of gene fusion in salivary gland tumors. It is easily applicable on FFPE tissue sections (even biopsies and cell blocks). By allowing the identification of a large panel of recurrent genetic alterations, it is a powerful diagnostic tool which can provide therapeutic and prognostic informations and help to reclassify some adenocarcinomas NOS.

1279 Exploring the Microenvironment of Head and Neck HPV-Related Squamous Cell Carcinoma with Multiparametric Fluorescent Immunolabelling according to Location and HPV RNA Hybridization In Situ Stratification

Charles Lépine[1], Marine Nervo[2], Marion Mandavit[3], Sophie Outh-Gauer[4], Marc Rassy[5], Thomas Denize[6], Eric Tartour[4], Cecile Badoual[7]

[1]Hôpital Européen Georges Pompidou APHP, Paris, Ile de France, France, [2]INSERM U970, Université Paris Descartes Sorbonne Paris-Cité, Paris, France, [3]Inserm U970, Paris, France, [4]Hôpital Européen Georges Pompidou, APHP, Paris, France, [5]INSERM U970, Université Paris Descartes Sorbonne Paris-Cité, Puteaux, Ile de France, France, [6]APHP.5 Hôpital Européen Georges Pompidou, boston, MA, [7]G Pompidou Hospital, Paris, France

Disclosures: Charles Lépine: None; Marine Nervo: None; Marion Mandavit: None; Sophie Outh-Gauer: None; Marc Rassy: None; Thomas Denize: None; Eric Tartour: None; Cecile Badoual: None

Background: Human papillomavirus (HPV)-related head and neck squamous cell carcinoma (HNSCC) is a distinct entity from HPV-unrelated HNSCC. HPV-related HNSCC are mainly located in the oropharynx (OPSCC). Compared with patients with HPV-negative SCC, patients with HPV-related SCC tend to have a better overall survival. This phenomena may rely on modifications of the microenvironment following HPV infection. Among HPV-related OPSCC, our team found a difference in prognosis based on the level of expression in chromogenic *in situ* hybridization (CISH) of HPV mRNA E6 and E7 proteins.

Design: Our goal is to explore the immune microenvironment of HPV-related HNSCC and to explain their prognosis heterogeneity.

We selected 69 patients with HPV-related HNSCC of which 53 are located in the oropharynx, 2 in the oral cavity, 2 in the hypopharynx and 12 in the larynx. Collected data included demographic characteristics, clinical status and treatment. CISH with a probe against mRNA of HPV E6 and E7 proteins was performed on FFPE sections. CISH staining strength was divided in two categories: 1+ (weak) and 2+ (strong). As well we performed a multiparametric fluorescent immunolabelling using tyramide signal amplification with antibodies against PD-1/PD-L1/CD68/CD3/cytokeratin. A spectral digital analysis was performed to quantify the tumor and stroma distribution of T cells and macrophages and their expression of PD-1 and PD-L1.

Results: Patient with OPSCC had an higher infiltration of T cells in the stroma and in the tumor compared to other locations (p=0,001 for stroma and p=0,011 for tumor). Density of T cells expressing PD-1 was higher in the stroma and in the tumor in patients with OPSCC compared to other locations (p=0,021 for tumor and p=0,009 for stroma). There was no difference in survival between patients with OPSCC and SCC in other locations (p=0.246 ; LogRank test). Interestingly, repartition of the density of T cells expressing PD-1 was bimodal among patients with OPSCC : one group had < 100 cells/mm2 and one group had > 500 cells/mm2. Finally, there was no difference in the density of the studied cell populations between patients with a weak and strong CISH score.

		Oropharynx (n=53)			Other location (n=16)			
	Phenotype	**Median (cells/mm²)**	**Min**	**Max**	**Median (cells/mm²)**	**Min**	**Max**	**p**
Stroma	**CD3+**	4470	261	10513	2045	142	6669	**0.001**
	CD3+ PD1+	117	0	6148	18	0	4050	**0.009**
	CD68+	124	10	999	222	15	942	0.125
	CD68+ PDL1+	390	0	1919	164	0	836	0.174
	CD3+ PD1+ PDL1+	0	0	33	0	0	6	0.951
	CD3+ PDL1+	0	0	19	0	0	6	0.810
Tumor	**CD3+**	1076	22	4145	304	19	1868	**0.011**
	CD3+ PD1+	28	0	940	2	0	1418	**0.021**
	CD68+	81	4	976	69	7	306	0.460
	CD68+ PDL1+	190	2	1742	267	0	1340	0.921
	CD3+ PD1+ PDL1+	0	0	48	0	0	12	0.536
	CD3+ PDL1+	0	0	3	0	0	2	0.727

Figure 1 - 1279

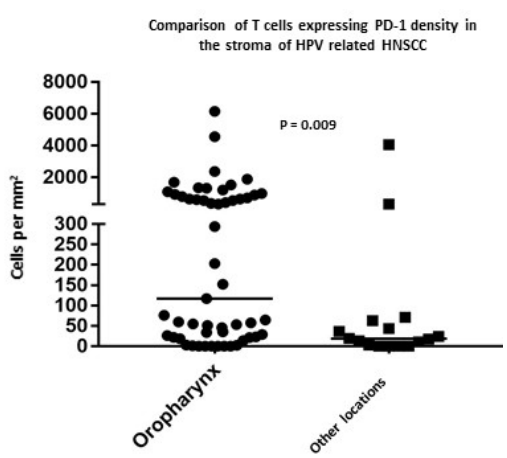

Figure 2 - 1279

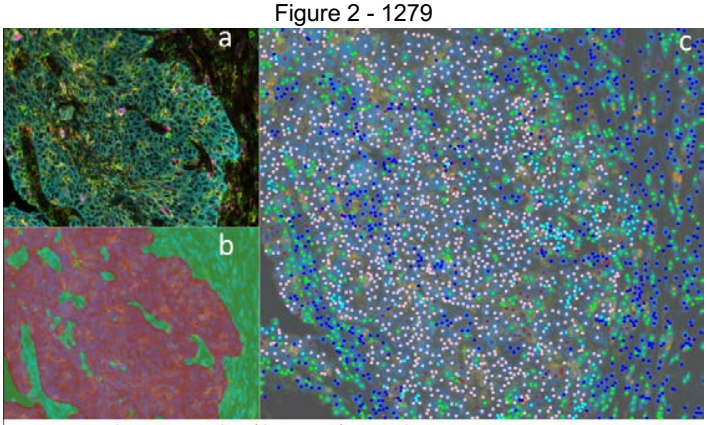

Computer-assisted immunophenotyping process :
a. Sample with fluorescent immunolabelling
b. Tissue segmentation (stroma VS tumor)
c. Results of computer-assisted immunophenotyping

Conclusions: This work contributes to a better understanding of the microenvironment of HPV-related HNSCC. Further studies will be needed to explore the micro-environment more accurately in order to explain the difference in prognosis between patients with a weak and strong CISH score.

1280 Next Generation Sequencing Assay Demonstrated Frequent Mutation in PI3K3CA, PI3R1 and p53 Gene in Clinically Aggressive Head Neck Squamous Cell Carcinoma

Rusella Mirza[1], Aliaksandr Aksionau[2], Eric Wei[2]
[1]Louisiana State University Shreveport, Shreveport, LA, [2]LSU Health Sciences Center Shreveport, Shreveport, LA

Disclosures: Rusella Mirza: None; Aliaksandr Aksionau: None

Background: The Phosphoinositide-3-kinase catalytic alpha polypeptide (PIK3CA) is an important regulator of cell signaling pathways in human cancers. *PIK3CA* mutations activate the PI3K-PTEN-AKT pathway, which is downstream from both the EGFR and the RAS-RAF-MAPK pathways. *PIK3CA* mutations may cause oncogenic transformation independent of *RAS* or *RAF* mutations. The *PIK3R1* gene is important to regulate PI3K enzyme activity. Promising data have been published regarding the PI3K inhibitor, PI3K/mTOR inhibitor and PI3K/HDAC inhibitor. Few phase I/II clinical trials are also going on. Here we are presenting Cancerplex (a comprehensive next generation sequencing system) data from clinically aggressive head neck squamous cell carcinoma (HNSCC). We have observed frequent mutation in PIK3CA, PIK3R1 and in p53 gene together with few new gene mutations.

Design: The patients have been selected for Cancerplex assay (Kew, Inc., Waltham, MA) based on their clinically aggressive behavior such as rapid disease progression and non-responsiveness to conventional treatment. Formalin fixed tissue from 13 patients had been used for the assay. Most exons of 435 genes were sequenced via Cancerplex platform. Tumor areas were circled on H&E slides and cut from formalin fixed paraffin embedded tissues. Neoplastic tissues with tumor content higher than 20% were microdissected form the blocks and NGS was performed on materials with at least 50 ng DNA content. 435 genes were sequenced with a limit of detection of 10% mutant alleles. The depth of coverage was 500, and the size of the targeted region was 2.8 Mb. Results were compared with published databases.

Results: We have observed mutation in PIK3CA and PIK3R1in 54% cases which has been reported as actionable variants and actionable copy number variants. P53 mutation was found in 100% cases. Interestingly, no mutation in PIK3CA, PIK3R1or p53 is found in two cases of HPV16 positive HNSCC. The result has been summarized in a table.

Patient ID	Actionable variants	Actionable CNVs	P53 variants	Other variants
1	PIK3CA, T1025T			
2	TSC1, p.S836X	CCND1+, CDKN2A-, CDKN2B-	TP53, p.R202fs	PBRM1, p.E457X
3	PIK3CA, p.E545K	CCND2, gain, KRAS, gain, PIK3CA, gain	TP53, splice variant	
4	CDKN2A, p.R80X, HRAS, p.G12S, PIK3CA, p.E545K, TERT, promoter variant	FGFR4, gain, PDGFRB, gain	TP53, p.G244S	
5		CDKN2B, loss, PIK3R1, loss	TP53, p.R156fs	NFE2L2, p.D29H
6	HRAS, p.Q61H, TERT, c.C-124T		TP53, p.R273C	FAT1, p.G3953fs, FAT1, p.Q3968X
7		CDKN2A-, CDKN2B-, PIK3R1-, PTEN-	TP53, p.L348fs	
8	CDKN2A, p.R80X, PIK3CA, p.E545K		TP53, p.M246L	TERT, splice variant
9	ARID1B, p.A276G			
10	PIK3CA, p.E542K	CDKN2A-, CDKN2B-, PIK3R1-	TP53, p.C275Y	TGFBR2, p.S199X
11			TP53, c.G994-1A, splice variant	BRAF, p.D287N
12		CCND1+, CDKN2B-, ERBB2+, PIK3CA+, PIK3R1-	TP53, splice variant	
13			TP53, p.R202fs	PBRM1, p.E457X
14 HPV16 positive	FBXW7, p.R479Q			
15 HPV 16 positive	FBXW7, p.R479P	STK11-		

Conclusions: Based on studies conducted on HNSCC cell lines of different manufacturers, PI3K inhibitors (PI-828, PI-10, PX-866) slow down the growth and proliferation of cancer cells and decrease the invasiveness. However, this antitumor effect of PI3K inhibitors varies from one HNSCC cell line to another. The reason may be due to variations of the mutation site. Thus, the development of individual chemotherapy requires a correlation of the gene mutation with the clinical outcome of the patient.

1281 (Hyalinizing) Clear Cell Carcinoma Of The Head And Neck Region: A Tertiary Care Cancer Center Experience

Neha Mittal[1], Swapnil Rane[2], Munita Bal[2], Asawari Patil[3]
[1]Tata Memorial Hospital, Mumbai, Maharashtra, India, [2]Tata Memorial Centre, Mumbai, India, [3]Tata Memorial Centre, Thane (west), Maharashtra, India

Disclosures: Neha Mittal: None; Swapnil Rane: None; Munita Bal: None; Asawari Patil: None

Background: (Hyalinizing) Clear cell carcinoma(CCCa) of the salivary gland comprises <1% of all salivary gland neoplasms and is characterized by clear cells with low grade histology, with or without hyalinization.

Design: A detailed retrospective review of clinical and histological parameters of cases diagnosed from 2014 till date was undertaken.

Results: A total of 14 cases (9 males, 5 females, with a M:F ratio of 1.8:1) of CCCa were retrieved. The mean age of the patients was 48.3 years (median; 52 years). Six out of 14(42.9%) patients were habitual tobacco users. Minor salivary gland involvement was seen in 92.9% (13 out of 14) with hard palate being the most common site (28.9%), followed by base of tongue region (21.4%). Tumor size varied from 1.2-5cm with a mean size of 2.97cm. Tumour borders were well-defined in 5 cases (35.7%). Small nests of tumour cells with clear cytoplasm, round, monomorphic nuclei, and hyalinization which was more in the center of the tumour than at the periphery, were the hallmark features seen in all cases. PNI was seen in 35.7%, and bone involvement in 7.1% cases. Necrosis, atypical mitoses, squamous differentiation, and LVI were not seen. All the tumours were positive for keratins and p63 on immunohistochemistry. Ki-67 index was <5% in all but two cases. Regional nodal metastasis was seen in 21.4% cases, distant metastasis in 7.1%, and recurrence in 7.1% cases, with interval to recurrence being 36 months. Interphase FISH identified EWSR1 gene rearrangement in both the cases in which it was done. Surgery was the only modality of treatment in 63.6% patients. All the patients were alive at the time of last follow up (2-36 months).

Parameter	Results
Epidemiology	
Age range	28-66 years
M:F	1.8:1 (9 males, 5 females)
Tobacco user	6/14
Site of tumour	
Hard palate	4 cases
Base of tongue	3 cases
Oropharynx	1 case
Nasopharynx	1 case
Vallecula	1 case
Submandibular gland	1 case
Lateral border of tongue	1 case
Soft palate	1 case
Gross tumour characteristics	
Circumscribed	5
Infiltrative	10
Cannot be evaluated	1 (only biopsy)
Tumour size	1.2-5cm
Histology	
Nests	All cases
Cords	All cases
Cribriform architecture	1/14
Hyalinization	All cases
Round, monomorphic nuclei	All cases
Clear cells	All cases
Atypical mitosis	none
Necrosis	1/14(in the lymph node metastasis of recurrent tumour)
Perineurial invasion (PNI)	5/14
Lymphovascular invasion (LVI)	None
Immunohistochemistry	
CK7	13 cases diffuse positive, one case focal positive
P63/p40	Diffusely positive in all cases
S100	Negative in all cases (n=14)
GFAP	Negative (n=10)
Calponin	Negative (n=10)
Pax8	Negative (n=4)
Ki67 <5%	6 cases
Ki67 of 5-10%	2 cases
Molecular testing	
EWSR1 gene rearrangement by FISH (n=2)	Positive
Treatment	
Surgery alone	8 cases
Surgery+RT	3 cases
Surgery+CTRT	1 case
No details of treatment	2 cases
Follow up	
Alive without disease	11 cases
Alive with disease	1 case
Not known	2 cases

Conclusions: CCCa of salivary glands is a rare low grade salivary gland tumour with an excellent prognosis with surgical resection alone. Small, but definite risk of nodal and distant metastasis warrants appropriate imaging studies. Potential misdiagnosis as squamous cell carcinoma or other clear cell tumours of the head and neck region necessitates an accurate histological diagnosis, especially in small biopsies, supported by molecular confirmation to avoid potential overtreatment.

1282 Clinicopathologic Characteristics of Young Patients with Oral Squamous Cell Carcinoma (OSCC)

Wadad Mneimneh[1], Bin Xu[2], Bayan Alzumaili[3], Shenon Sethi[2], Anjanie Khimraj[2], Snjezana Dogan[2], Ronald Ghossein[2], Nora Katabi[2]
[1]University of South Alabama, Mobile, AL, [2]Memorial Sloan Kettering Cancer Center, New York, NY, [3]Mt Sinai St Luke's Roosevelt Hospital, New York, NY

Disclosures: Wadad Mneimneh: None; Bin Xu: None; Bayan Alzumaili: None; Shenon Sethi: None; Anjanie Khimraj: None; Snjezana Dogan: None; Ronald Ghossein: None; Nora Katabi: None

Background: OSCC most commonly occurs in the fifth and sixth decades of life with smoking being the most important etiologic factor. However, OSCC occasionally occurs in young non-smoker patients and may be distinct from OSCC in older patients. In this study, we aimed to describe the clinicopathologic features of OSCC in young patients.

Design: A retrospective cohort of 73 OSCCs that were diagnosed in patients of 40-year-old or younger was retrieved. HPV positive oropharyngeal SCCs were excluded. Details of the clinical presentation, histopathologic features, and outcome were reviewed.

Results: The median patient's age at presentation was 35 (range: 18-40). The male to female ratio was1.5:1. The patients were Caucasian in 79%, non-smoker in 69% and non-drinker in 74%. Autoimmune diseases, prior malignancies and Fanconi anemia were noted in 15%, 12%, and 5.5%, respectively. The tumors were mostly located in the oral tongue (n=66, 90%), whereas the remaining affected buccal mucosa (n=3), lip (n=1), gingiva (n=1), retromolar trigone (n=1), and base of tongue (n=1).

All OSCCs were of keratinizing type. High risk HPV status was tested in 17 cases, all of which were negative. There were no significant pathologic differences between oral tongue and non-oral tongue tumors ($p>0.05$).

Twenty-six (36%) OSCCs occurred in patients 30 years or younger. Compared with patients 31 to 40-year-old, OSCC in the younger group was associated with significant less alcohol consumption ($p=0.011$) and greater tumor thickness (median 9.6 mm vs. 4.2 mm, $p=0.006$). The remaining characteristics did not differ between the two age groups.

The 1-year, 3-year, 5-year, and 10-year disease specific survival (DSS) were 94%, 88%, 85%, and 78% respectively. Univariate analysis showed that younger age at presentation, higher histologic grade, larger tumor size, higher cT stage, nodal metastasis, and the presence of extranodal extension (ENE) were associated with decreased DSS. History of smoking and positive margin predicted worse local recurrence free survival; whereas younger age at presentation and ENE correlated with distant metastasis.

Conclusions: OSCC in young patients does not always occur in genetic predisposition syndromes, e.g. Fanconi anemia and most cases occur in non-smokers. Age at presentation, T and N stage, histologic grade, and ENE are important prognostic factors in young patients with OSCC.

1283 Claudin-4 Immunohistochemistry Differentiates SMARCB1-Negative Skull Base Tumors

James Nix[1], Murat Gokden[2], Justin Bishop[3], Lisa Rooper[4]
[1]Johns Hopkins Hospital, Baltimore, MD, [2]University of Arkansas for Medical Sciences, Little Rock, AR, [3]University of Texas Southwestern Medical Center, Dallas, TX, [4]The Johns Hopkins University School of Medicine, Baltimore, MD

Disclosures: James Nix: None; Murat Gokden: None; Justin Bishop: None; Lisa Rooper: None

Background: SMARCB1-deficient sinonasal carcinoma (SDSC) is a recently described tumor that frequently presents with extensive sinonasal and skull base involvement. While namesake loss of SMARCB1 (INI1) expression differentiates this entity from overlapping sinonasal small round blue cell tumors, it can be challenging to distinguish from other aggressive, SMARCB1-negative skull base tumors. The rare subsets of atypical teratoid rhabdoid tumors (ATRTs) that arise in the sella of adults and poorly differentiated chordomas that occur in the clivus of children not only show SMARCB1 loss but also pancytokeratin positivity and rhabdoid morphology that can mimic SDSC. Claudin-4 is a protein involved in tight junctions of epithelial cells which has proved useful in differentiating other carcinomas and sarcomas in the SWI/SNF family. This study aims to evaluate whether Claudin-4 can help distinguish SDSC from ATRT and poorly differentiated chordoma.

Design: We identified 8 SDSCs, 4 ATRTs, and 1 chordoma from the surgical pathology archives of 2 large academic medical centers between 1998 and 2019. Loss of SMARCB1 expression was previously confirmed in all cases. Immunohistochemical staining for Claudin-4

(1:100 dilution; clone 3E2C1, Thermo Fisher Scientific, Waltham, MA) was performed on whole slide sections of 2 SDSCs, 4 ATRTs, and 1 chordoma; 6 SDSCs were stained as part of an existing tissue microarray. >5% membranous Claudin-4 reactivity was considered positive.

Results: 8 SDSCs (M:F=4:4; age range: 33-79 years), 4 ATRTs (M:F=1:3; age range: 11 months-48 years), and 1 poorly differentiated chordoma (M, 5 years) were identified. All 8 SDSCs involved multiple sinonasal and skull base subsites with intracranial extension in 3 cases. The 1 chordoma also extensively involved the skull base and nasopharynx. Locations for ATRTs included 2 brain, 1 brainstem, and 1 spinal cord. Claudin-4 was positive in all SDSCs and negative in all ATRTs and the chordoma (sensitivity=100%; specificity=100%).

Conclusions: Pilot data suggests Claudin-4 is a sensitive and specific marker that is consistently positive in SDSC and negative in a small sample of ATRT and chordoma. Claudin-4 may be helpful in distinguishing SDSC from other SMARCB1-negative skull base tumors in rare cases of clinical and demographic overlap.

1284 Tumor Microenvironmental Factors of Tongue Squamous Cell Carcinoma Predict Invasion Depth, Nodal Metastasis and PD-L1 Expression

Harim Oh[1], Bokyung Ahn[2], Eojin Kim[3], Yang-Seok Chae[4], Chul Hwan Kim[2], Jeong Hyeon Lee[4], Yoo Jin Lee[5], Youngseok Lee[6]
[1]Seoul, Seoul, Korea, Republic of South Korea, [2]Korea University Anam Hospital, Seoul, Korea, Republic of South Korea, [3]Korea University Anam Hospital, Seoul, Seongbuk-gu, Korea, Republic of South Korea, [4]Korea University Medical Center, Anam Hospital, Seoul, Korea, Republic of South Korea, [5]Korea University Anam Hospital, Seoul, Gangnam-gu, Korea, Republic of South Korea, [6]Seoul, Korea, Republic of South Korea

Disclosures: Harim Oh: None; Bokyung Ahn: None; Eojin Kim: None; Yang-Seok Chae: None; Chul Hwan Kim: None; Yoo Jin Lee: None; Youngseok Lee: None

Background: Tongue squamous cell carcinoma is the most common head and neck malignancy with poor prognosis. Many studies have reported the limitation of conventional clinicopathologic parameters and emphasized the need for more accurate risk stratification for appropriate treatment and better prognosis.

Design: We evaluated the prognostic significance of tumor microenvironmental elements (TME) using the tumor stroma percentage (TSP), Klintrup-Mäkinen (KM) grade; the density of inflammatory cells at the most invasive margin, and Glasgow microenvironment score (GMS); the combination of TSP and KM grade, in total 70 cases of tongue squamous cell carcinoma. Moreover, we evaluated the significance of pattern of invasion including tumor budding (TB) and worst pattern of invasion (WPOI)-5. Lastly, we evaluated the PD-L1 expression and correlated with TME and other clinicopathologic factors.

Results: Low KM grade (25 cases) (HR, 2.836; 95% CI: 1.171-6.870, p=0.021) and higher GMS (GMS0, 45; GMS1, 12; GMS2, 13 cases) (HR, 4.350; 95% CI: 1.670-11.330, p=0.003) showed shorter disease free survival (DFS). High TSP (35 cases) was significantly correlated with deeper DOI (p=0.025), higher pN stage (p=0.034), lymph node metastasis (p=0.006), and high tumor budding (p=<0.001). Higher GMS was significantly correlated with deeper DOI (p=0.044), and high tumor budding (p=0.011). Higher TB (33 cases) was significantly correlated with deeper DOI (p=0.004), lymphovascular invasion (p=0.022), and lymph node metastasis (p=0.035). Lastly, high PD-L1 expression was correlated with deeper DOI (p=0.032), higher TNM stage (p=0.010), high TSP (p=0.027), higher GMS (p=0.013), and high TB (p=0.026).

Conclusions: Assessing the TME and tumor invasion pattern in the deepest invasive part were more sensitive markers of predicting prognosis than the preexisting staging system in tongue squamous cell carcinoma. These can be cost-effective way, and helpful in deciding the extent of surgical resection and additional lymph node dissection. Furthermore, these factors can suggest the possibility of anti PD-L1 therapy in tongue squamous cell carcinoma especially in the group with factors of worst prognosis such as deeper invasion depth, higher TNM stage, high TSP, higher GMS and high TB.

1285 Characterization of the Salivary Gland Immune Microenvironment in Tumor-Associated Lymphoid Proliferation, Immune Stroma, and Sialadenitis

Ankit Rajgariah[1], Lisa Rooper[1]
[1]The Johns Hopkins University School of Medicine, Baltimore, MD

Disclosures: Ankit Rajgariah: None; Lisa Rooper: None;

Background: Tumor-immune cell interactions play an important role in tumorigenesis and are increasingly exploited for treatment. In the salivary glands, immune cells are seen in a broad range of lesions, including tumor-associated lymphoid proliferation (TALP) that occurs in reaction to a subset of carcinomas, lymphoid stroma that is an intrinsic component of certain benign and malignant tumors, and various types of sialadenitis. While these immune infiltrates are usually non-clonal, their constituent cells have not been well-characterized. This study aims to compare the immune microenvironment across the spectrum of immune-rich salivary lesions.

Design: Immune-rich salivary lesions were identified at a large academic medical center between 1999 and 2019, including mucoepidermoid carcinoma with TALP (n=10), acinic cell carcinoma with TALP (n=9), lymphoepithelial carcinoma (n=3), Warthin tumor (n=10), lymphadenoma (n=6), lymphoepithelial sialadenitis (n=3), lymphoepithelial cyst (n=10), and chronic sialadenitis (n=17). Immunostains for CD3, CD8, CD20, FoxP3, PD1, and PD-L1 were performed on tissue microarrays containing all cases. Immune cell density was quantified using Halo image analysis software. Percentages of epithelial and immune cell PD-L1 expression was manually counted.

Results: As shown in table 1, most lesions had more CD20+ B-cells than CD3+ T-cells. Although density of each immune cell type varied between diagnoses, benign and malignant neoplasms did not differ overall in density of CD3+ (p=0.41), CD8+ (p=0.15), CD20+ (p=0.70), or FoxP3+ (p=0.94) cells. Similarly, although tumors with immune stroma had a higher density of immune cells than TALP, these lesions had equal CD3:CD20 ratios (p=0.47) and proportion of CD8+ cells (p=0.32). Virtually all tumors and inflammatory processes showed a low degree of PD-L1 expression on epithelial and immune cells, although activated PD1+ cells were more frequent in malignant than benign processes (p=0.06).

Diagnosis	CD3/mm2	CD8/mm2	CD20/mm2	PD1/mm2	FoxP3/mm2	PD-L1 % Epithelium	PD-L1 % Immune
Acinic Cell Carcinoma	2753 (747-5899)	596 (119-1455)	1695 (347-4412)	68 (4-205)	670 (216-1368)	4 (0-10)	19 (5-40)
Chronic Sialadenitis	2251 (355-4893)	585 (56-2491)	3307 (513-6497)	157 (0-766)	374 (118-767)	0 (0-0)	7 (0-30)
Lymphadenoma	4686 (1035-7666)	396 (55-1011)	3558 (767-5237)	46 (3-87)	863 (117-1685)	9 (0-50)	12 (0-30)
Lymphoepithelial Cyst	4119 (82-7211)	1054 (103-3981)	6036 (15-10487)	326 (2-780)	675 (91-1357)	1 (0-5)	8 (0-20)
Lymphoepithelial Carcinoma	6553 (5004-7822)	2088 (522-5031)	9858 (9481-10491)	341 (46-775)	1323 (1061-1719)	17 (0-30)	17 (5-40)
Lymphoepithelial Sialadenitis	9510 (8207-12053)	2462 (1185-4129)	9455 (6772-12358)	356 (9-867)	789 (593-1071)	3 (0-10)	30 (30-30)
Mucoepidermoid Carcinoma	2570 (512-6938)	360 (38-1200)	4327 (529-11331)	243 (2-898)	542 (137-1787)	1 (0-5)	6 (0-30)
Warthin Tumor	3339 (990-8418)	318 (133-522)	4809 (2066-7450)	92 (16-495)	622 (153-1442)	1 (0-10)	16 (5-30)

Conclusions: This is the first study to analyze the composition of immune infiltrates across the spectrum of salivary lesions. Overall, the immune cell composition was similar in benign and malignant salivary tumors and lesions that showed TALP and had intrinsic immune stroma. These findings suggest that the immune cell population in salivary tumors may be more a function of the inherent glandular microenvironment than specific tumor characteristics.

1286 Intraoperative Primary Tumor Identification and Margin Assessment in Head and Neck Unknown Primary Tumors: Utility and Accuracy of Frozen Sections and Comparison with Final Pathology

Priyanka Ravi[1], Matthew Rigby[2], Jasmijn Herruer[1], S.Mark Taylor[1], Colin MacKay[1], Martin Corsten[1], Jonathan Trites[1], Martin Bullock[2]

[1]Queen Elizabeth II Health Sciences Centre and Dalhousie University, Halifax, NS, [2]Dalhousie University, Halifax, NS

Disclosures: Priyanka Ravi: None; Matthew Rigby: None; Jasmijn Herruer: None; Colin MacKay: None; Martin Corsten: None; Martin Bullock: None

Background: Four percent of head and neck squamous cell carcinomas (HNSCC) present as unknown primary (UP) neck mass; >90% are HPV-mediated oropharyngeal cancers. At our institution, oropharynx SCC is treated with transoral laser microsurgery (TLM) +/- adjuvant (chemo) radiation. Positive margin after resection is a major predictor of recurrence and mortality. Our study assesses utility of frozen section (FS) during TLM in diagnosis and margin assessment for UPHNSCC, following a localizing PET-CT scan. We correlated FS diagnosis with final pathology and margin status, determined FS turn-around time (TAT) and estimated FS cost.

Design: 61 UPHNSCC were included from Jan 2013- Aug 2018. Patients had a PET-CT followed by oropharynx TLM, using a standard protocol. When possible, the primary tumor was identified and margins assessed by a FS pathologist (n=13). In many cases, resection specimens were submitted in toto for FS. Positive margin on FS resulted in re-resection. Results were confirmed during final pathology by a head and neck pathologist. Decision for adjuvant therapy was based on positive margins, extranodal extension and >1 positive node. TAT and FS cost-analysis were calculated.

Results: The primary tumor was identified intraoperatively in 82% (n=50). Margins were considered negative in 49 (98%) cases, but were reversed in four cases on final pathology. Five more tumors were identified only on final pathology, for a total detection of 90% (n=55). 18 patients avoided adjuvant therapy. Concordance of 93% (n=57) was achieved between FS and final pathology. Four cases had a major FS-final discrepancy. Three were sampling errors (tumor not present in FS slides); one was an interpretive error. The negative predictive value of FS in UPHNSCC was 91.8% (45/49). The average number of tissue sections submitted/case was 9 (2-16). Intraoperative TAT averaged 2.0 hours (0.5-4.1), greater than for known primary HNSCC, using a defect-driven or specimen-driven protocol (0.75 hrs and 0.83 hrs respectively). The average cost of FS analysis alone was 490CAD$ (N=44), negligible compared to the cost and morbidity associated with adjuvant treatment.

Conclusions: The accuracy of FS for detection and margin analysis of UPHNSCC is high despite rare sampling/interpretative errors. In some cases, the UP is not identified. The protocol is intense on pathology resources, with slower TAT than for known primary tumors. The procedure is beneficial as it saves patient morbidity and costs associated with adjuvant therapy.

1287 Does Immunohistochemical Combined Positive Score of PDL-1 Reflect the Genetic and Transcriptomic Profile of CD274 and its Regulators in Oral Squamous Cell Carcinoma

Jessica Reagh[1], Laveniya Satgunaseelan[2], Dario Strbenac[3], Kitty Lo[4], Carsten Palme[5], Jean Yang[3], Jonathan Clark[6], Ruta Gupta[7]
[1]NSW Health Pathology, Royal North Shore Hospital, St Leonards, NSW, Australia, [2]Royal Prince Alfred Hospital, Camperdown, NSW, Australia, [3]School of Mathematics and Statistics, The University of Sydney, Sydney, NSW, Australia, [4]University of Sydney, Sydney, NSW, Australia, [5]Missenden Road, NSW, Australia, [6]Chris O'Brien Lifehouse, Camperdown, NSW, Australia, [7]Royal Prince Alfred Hospital, Sydney, NSW, Australia

Disclosures: Jessica Reagh: None; Laveniya Satgunaseelan: None; Dario Strbenac: None; Kitty Lo: None; Carsten Palme: None; Jean Yang: None; Jonathan Clark: None; Ruta Gupta: None

Background: There are limited treatments available in patients with metastatic or recurrent oral squamous cell carcinoma (OSCC). The immune modulatory therapies offer a new therapeutic option by suppressing the PD-1/PDL-1 axis. The recent KEYNOTE-048 trial has shown overall survival of 14.7 months following immunotherapy in patients with immunohistochemical PDL-1 combined positive score (CPS) $\geq$ 20 versus 11months following chemotherapy in head and neck squamous cell carcinoma. In this study, we investigate whether PDL-1 expression on tumor cells and the CPS reflect the genomic and transcriptomic profile of *CD274* (gene encoding PDL-1) and its putative regulators (*PIK3CA, PTEN, AKT1, JAK1, JAK2, STAT1, STAT3* and *STK11*) in OSCC.

Design: Tumor samples from 16 OSCC patients were obtained for PDL-1 (22C3) immunohistochemistry, whole genome and RNA sequencing. CPS for PDL-1 immunohistochemical expression was derived through assessment of tumor cells and tumor infiltrating cells.

Results: The study includes 9 males and 7 females. The median tumour mutation burden (TMB) was 3.8Mut/Mb. The CPS ranged from 0-65; 9 patients had CPS $\geq$ 1 and 6 patients had CPS $\geq$ 20. Strong membranous PDL-1 expression on tumour cells was seen in only 4 patients, in others the immune milieu contributed to the CPS. There was high correlation between CPS and *CD274* RNA abundance. There was no correlation between CPS at thresholds of 1 and 20 with tumour mutation burden or CNV of *CD274* and its putative regulators.

Complete lack of staining in the tumor cells was observed in 11 cases, 3 of these demonstrated *CD274* deletion. A trend was observed between the membranous PDL-1 staining on the tumour cells and *CD274* RNA profile. Analysis of Single nucleotide variants (SNV) in *CD274* and its regulators is being performed.

Conclusions: While a larger cohort and SNV analyses are essential, our preliminary findings indicate that PDL-1 immunohistochemical expression and CPS correlates with the transcriptomic profile of *CD274* but not with CNV of *CD274* or its regulators in OSCC.

1288 Recurrent Loss of SMARCA4 in Sinonasal Teratocarcinosarcoma

Lisa Rooper[1], Jeffrey Gagan[2], Lodewijk Brosens[3], Lester Thompson[4], Justin Bishop[5]
[1]The Johns Hopkins University School of Medicine, Baltimore, MD, [2]University of Texas Southwestern, Dallas, TX, [3]University Medical Center Utrecht, Utrecht, Netherlands, [4]Southern California Permanente Medical Group, Woodland Hills, CA, [5]University of Texas Southwestern Medical Center, Dallas, TX

Disclosures: Lisa Rooper: None; Jeffrey Gagan: None; Lodewijk Brosens: None; Lester Thompson: None; Justin Bishop: None

Background: Teratocarcinosarcoma (TCS) is a rare and aggressive sinonasal tumor defined by the presence of immature or malignant epithelial, mesenchymal, and primitive neuroepithelial elements. This distinctive multilineage differentiation has engendered persistent controversy as to whether TCS is of germ cell or somatic origin. Furthermore, its morphologic heterogeneity can create significant diagnostic challenges in small biopsies when only one or two components are sampled. This study aims to evaluate the molecular underpinnings of TCS in hopes of clarifying its pathogenesis and facilitating more specific diagnosis.

Design: All available cases of sinonasal TCS were identified from the surgical pathology archives of two large academic medical centers and the authors' consultation files. Next generation sequencing (NGS) was performed on an index case. Based on these NGS results, immunohistochemistry for SMARCA4 (BRG1) was performed on all cases.

Results: There were 9 cases of sinonasal TCS identified in 6 males and 3 females with a mean age of 53 years. Next generation sequencing identified biallelic somatic loss of *SMARCA4* in one case without other known driver mutations. Immunohistochemistry confirmed loss of SMARCA4 expression in 6 cases (67%) including the index case, with consistent lack of staining across epithelial, mesenchymal, and primitive neuroepithelial tumor components despite retained endothelial expression.

Conclusions: A significant subset of sinonasal TCS demonstrate immunohistochemical loss of SMARCA4 expression with corresponding NGS evidence of biallelic loss of *SMARCA4*. These findings not only point to somatic histogenesis for TCS but also suggest that it may exist on a spectrum with SMARCA4-deficient sinonasal carcinomas, which have previously been reported with mixed neuroendocrine, squamous, and glandular features. Additionally, SMARCA4 immunohistochemistry may provide a useful adjunct for confirming a diagnosis of TCS in limited material.

1289 MYB Overexpression by RNA In-Situ Hybridization Facilitates Sensitive and Specific Diagnosis of Adenoid Cystic Carcinoma Regardless of Translocation Status

Lisa Rooper[1], Kara Lombardo[2], Patrick Ha[3], Justin Bishop[4]
[1]The Johns Hopkins University School of Medicine, Baltimore, MD, [2]Johns Hopkins Medical Institutions, Baltimore, MD, [3]University of California San Francisco, San Francisco, CA, [4]University of Texas Southwestern Medical Center, Dallas, TX

Disclosures: Lisa Rooper: None; Kara Lombardo: None; Patrick Ha: None; Justin Bishop: None

Background: Adenoid cystic carcinoma (ACC) can demonstrate significant morphologic overlap with a wide range of benign and malignant salivary gland tumors, especially in small biopsy specimens. While molecular identification of the characteristic MYB-NFIB fusion is diagnostic for ACC, this rearrangement is only present in 50-80% of cases, and testing can take weeks to complete. Furthermore, most immunohistochemical stains (IHC), including those for MYB protein expression, have limited specificity for ACC. Because MYB RNA is overexpressed in the vast majority of ACC regardless of translocation status, we sought to determine whether chromogenic RNA in-situ hybridization (ISH) for MYB could provide a rapid diagnostic adjunct for differentiating ACC from its mimics.

Design: We identified 61 ACC, 16 polymorphous adenocarcinomas (PACs), 16 epithelial-myoepithelial carcinomas (EMCs), 3 basal cell adenocarcinomas (BCACs), 24 pleomorphic adenomas (PAs), and 24 basal cell adenomas (BCAs) from the surgical pathology archives of a large academic medical center between 1999 and 2018. All tumors were evaluated as part of existing tissue microarrays. MYB rearrangement status had previously been determined in 57 ACC via FISH. We performed MYB RNA ISH and IHC on all cases. MYB RNA ISH overexpression was defined by the presence of >5 punctate nuclear signals in >50% of tumor cells. MYB IHC was considered positive if >5% of tumor cells showed nuclear reactivity.

Results: There were 56 ACC (92%) that demonstrated MYB RNA ISH overexpression, including 34 MYB-rearranged cases (97%) as well as 18 tumors without MYB rearrangement (82%). Only 4 non-ACC (5%) also showed MYB RNA ISH overexpression, including 1 BCAC (33%) and 3 PACs, all cribriform type (19%). In contrast, MYB immunohistochemistry was positive in 54 ACC (89%) but 35 non-ACC (42%), including 9 EMCs (56%), 12 BCAs (50%), 7 PACs (44%), 1 BCAC (33%), and 6 PAs (25%). Overall, MYB RNA ISH overexpression had 92% sensitivity and 95% specificity for the diagnosis of ACC, compared with 89% sensitivity and 58% specificity with MYB IHC and 61% sensitivity and 100% specificity with MYB FISH.

Conclusions: Detection of MYB overexpression via chromogenic RNA in-situ hybridization provides superior sensitivity for the diagnosis of ACC compared to MYB FISH and superior specificity compared to MYB IHC. This assay could provide a useful tool for rapidly confirming the diagnosis of ACC on small biopsy material.

1290 High Grade Neuroepithelial Carcinoma of the Sinonasal Tract: A Distinctive Entity at the Intersection of Olfactory Neuroblastoma, Neuroendocrine Carcinoma, and Sinonasal Adenocarcinoma

Lisa Rooper[1], Gary Gallia[2], Lester Thompson[3], Justin Bishop[4], William Westra[5]
[1]The Johns Hopkins University School of Medicine, Baltimore, MD, [2]Johns Hopkins University School of Medicine, Baltimore, MD, [3]Southern California Permanente Medical Group, Woodland Hills, CA, [4]University of Texas Southwestern Medical Center, Dallas, TX, [5]Icahn School of Medicine at Mount Sinai, New York, NY

Disclosures: Lisa Rooper: None; Gary Gallia: None; Lester Thompson: None; Justin Bishop: None; William Westra: None

Background: Olfactory neuroblastoma (ONB), sinonasal neuroendocrine carcinoma (NEC), and sinonasal adenocarcinoma (ACA) are regarded as biologically and clinically distinct entities. However, a unique subset of high grade neoplasms that show histologic and immunohistochemical features of all three tumor types has persistently created confusion for diagnosis and management. Such tumors have alternately been termed ONB with epithelial differentiation, combined ONB-ACA, and olfactory carcinoma. This study aims to characterize the clinicopathological features of these perplexing lesions.

Design: We identified 7 sinonasal tumors that demonstrated mixed histologic and immunohistochemical features of ONB, NEC, and ACA from two large academic medical centers and the authors' consultation files. All available histologic slides and immunohistochemical stains were reviewed. Clinical and demographic information was obtained from the electronic medical record.

Results: The 7 tumors were taken from 5 men and 2 women with a median age of 47 years (range 19-63 years). All 7 were centered in the superior nasal cavity with intracranial extension in 2 cases. Histologically, tumors showed nests and sheets of round to angulated cells embedded in vascular stroma. Well-developed glandular structures were present in all 7 cases with prominent cilia in 3 cases. No neuropil or squamous or sarcomatoid elements were present. Immunohistochemically, tumors were diffusely positive for AE1/AE3 (6/6) and Cam 5.2 (3/3). They also showed patchy positivity for neuroendocrine markers synaptophysin (6/7), INSM1 (2/2), and CD56 (3/3). S100 did not highlight a sustentacular network (0/4). The Ki67 index ranged from 50-80% in 4 cases. In median follow-up of 26 months, 2 patients developed local recurrence at 5 and 12 months.

Conclusions: High grade sinonasal tumors with mixed features of ONB, NEC, and ACA represent a distinctive clinicopathological group. While their localization to the superior nasal cavity, nested growth, and ciliated morphology are suggestive of olfactory neuroepithelial origin, they demonstrate more diffuse cytokeratin expression than is acceptable for ONB and can show rapid progression that is more in keeping with a carcinoma. We propose that classifying these tumors as high grade neuroepithelial carcinomas may best reflect their unique histological, immunohistochemical, and clinical features and facilitate improved recognition and understanding of their pathogenesis.

1291 Adenoid Cystic Carcinoma of the Trachea: A Comparative Comprehensive Genomic Profiling Study

Jeffrey Ross[1], James Corines[1], Jo-Anne Vergilio[2], Keith Killian[2], Douglas Lin[2], Erik Williams[3], Natalie Danziger[4], James Haberberger[5], Julie Tse[3], Shakti Ramkissoon[5], Eric Severson[5], Amanda Hemmerich[5], Naomi Lynn Ferguson[5], Claire Edgerly[5], Daniel Duncan[5], Richard Huang[6], Jon Chung[2], Russell Madison[2], Siraj Ali[7], Venkataprasanth Reddy[2], Kimberly McGregor[2], Julia Elvin[2]

[1]Upstate Medical University, Syracuse, NY, [2]Foundation Medicine, Inc., Cambridge, MA, [3]Boston, MA, [4]Foundation Medicine, Inc., Somerville, MA, [5]Foundation Medicine, Inc., Morrisville, NC, [6]Foundation Medicine, Inc., Cary, NC, [7]Cambridge, MA

Disclosures: Jeffrey Ross: *Employee*, Foundation Medicine; James Corines: None; Jo-Anne Vergilio: *Employee*, Foundation Medicine, Inc; *Employee*, Foundation Medicine, Inc; Keith Killian: *Employee*, FMI; Douglas Lin: *Employee*, Foundation Medicine; Erik Williams: *Stock Ownership*, F. HoffmanLa Roche, Ltd.; *Employee*, Foundation Medicine, Inc.; Natalie Danziger: *Employee*, Foundation Medicine Incorporated; James Haberberger: *Employee*, Foundation Medicine Inc.; Julie Tse: *Employee*, Foundation Medicine, Inc.; *Consultant*, Pathology Watch, LLC.; Shakti Ramkissoon: *Employee*, Foundation Medicine/Roche; Eric Severson: *Employee*, Foundation Medicine; Amanda Hemmerich: *Employee*, Foundation Medicine, Inc; Naomi Lynn Ferguson: *Employee*, Foundation Medicine; Claire Edgerly: *Employee*, Foundation Medicine, Inc.; Daniel Duncan: *Employee*, Foundation Medicine; Richard Huang: *Employee*, Roche/Foundation Medicine; Jon Chung: *Employee*, Foundation Medicine; *Stock Ownership*, Roche; Russell Madison: *Employee*, Foundation Medicine Inc.; *Stock Ownership*, Roche; Siraj Ali: *Employee*, Foundation Medicine; *Advisory Board Member*, Incysus therapeutics; *Consultant*, Takeda; Venkataprasanth Reddy: *Employee*, Foundation Medicine; Kimberly McGregor: *Employee*, Foundation Medicine; Julia Elvin: *Employee*, Foundation Medicine, Inc; *Employee*, Hoffman La Roche

Background: Among the primary sites of adenoid cystic carcinoma (ACC), salivary gland (SG) origin predominates. Although ACC of the trachea (TACC) is the most frequent primary carcinoma of the trachea, it represents well less than 4% of all ACC. In the following comparative comprehensive profiling study (CGP), we compared the genomic alterations (GA) in TACC with SGACC.

Design: Comprehensive genomic profiling (CGP) was performed on FFPE samples from 14 cases of clinically advanced tracheal adenoid cystic carcinoma (TACC) and 405 cases of salivary gland ACC (SGACC). Tumor mutational burden (TMB) was determined on 0.8-1.1 Mbp of sequenced DNA and microsatellite instability (MSI) was determined on 114 loci. PD-L1 expression in tumor cells (Dako 22C3) was measured by IHC.

Results: TACC and SGACC featured a similar median age and gender distribution. The genomic alterations (GA) per tumor were similar in both tumor types although slightly higher in the TACC cases. MSI high status was virtually unidentified in TACC and SGACC and the TMB levels for both tumor types were extremely low. The frequencies of untargetable GA differed between the groups with *TERT*, *TP53* and NOTCH1 mutations higher in TACC than SGACC. The ability to identify the characteristic *NFIB-MYB* fusion was limited by the ability to target the introns in this DNA sequencing only assay. *MYB* fusions were identified in 17% of the SGACC and was not identified in any of the TACC. The groups differed significantly in the identification of potentially targetable genomic alterations. TACC featured higher frequency of potential targets including *KIT*, *PDFRA*, and *NTRK1* compared to the low frequencies of targetable GA in SGACC.

	Trachea ACC		Salivary Gland ACC	
Cases	14		405	
Gender	Male 57%; Female 43%		Male 50%; Female 50%	
Median Age/Range (years)	53 (40-76)		57 (11-89)	
GA/tumor	3.4		2.9	
Most Frequently Altered Genes	*TERT* *NOTCH1* *TP53* *KDR* *MYB*	60% 36% 29% 21% 0%	*NOTCH1* *MYB* *KDM6A* *TERT* *BCOR* *TP53*	22% 17% 15% 14% 13% 9%
Potential Targeted Therapy Impacting Alterations	*KIT* *PDGFRA* *NTRK1* *PIK3CA*	21% 21% 7% 7%	*PIK3CA* *FGFR2* *PDGFRA* *PTEN* *KIT*	7% 4% 3% 3% 3%
MSI High Status	0%		0.3%	
Median TMB (mut/Mb)	1.7		1.7	
TMB > 10 mut/Mb	0%		0%	
TMB > 20 mut/Mb	0%		0.3%	
PD-L1 IHC Low	NA		1%	
PD-L1 IHC High	NA		0%	

Conclusions: Although they feature a similar histology, TACC and SGACC vary significantly at the molecular level. *TERT* ($p<0.05$), *TP53* ($p<0.05$) and *NOTCH1* mutations were higher in TACC than SGACC. TACC featured a greater frequency of potential genomic targets including GA's in *KIT*, *PDFRA*, and *NTRK1* compared to the lower frequencies of targetable GA in SGACC.

1292 Papilloma-Like Invasive Non-Keratinizing Squamous Cell Carcinoma (PLINKS): A Comparison Study of Five Cases of a Unique, Low Grade Carcinoma of the Sinonasal Tract

Mario Saab-Chalhoub[1], Qiuying (Judy) Shi[2], James Lewis[3]
[1]Vanderbilt University Medical Center, Nashville, TN, [2]Emory University, Atlanta, GA, [3]Vanderbilt University, Nashville, TN

Disclosures: Mario Saab-Chalhoub: None; Qiuying (Judy) Shi: None; James Lewis: None

Background: Numerous benign and malignant tumors arise in the sinonasal tract, most of which can be separated easily based on their histopathology. We previously reported an entity termed low-grade papillary Schneiderian carcinoma that blurs that distinction between benign and malignant because it is invasive, but deceptively bland, with potential for recurrence and metastasis. Here, we report a series of 5 such tumors and compare them to classic inverted papillomas (IP) and to non-keratinizing squamous cell carcinomas (NKSCC).

Design: We gathered 5 sinonasal PLINKS cases and also randomly retrieved 8 cases each of sinonasal IP and NKSCC for comparison. All cases underwent review of their H&E slides, electronic medical record review, and immunohistochemistry (IHC) for the following: mitotic rate per 10 high power fields (HPF), degree of atypia, clinical features, treatment, clinical outcomes, p16, p53, and Ki-67 percentage. Four of the 5 PLINKS cases were immunostained for p40 or p63.

Results: PLINKS showed papillary architecture, infiltrative growth, and no (to very minimal) cytologic atypia but lacked other features of IP such as ciliated or mucus secreting cells. Mitotic activity averaged 9.2 per 10 HPF compared to only 1.1 per 10 HPF for IP and a staggering 76.4 per 10 HPF for NKSCC ($p = 0.013$ and 0.016, respectively). The average Ki-67 fraction was 27% for PLINKS compared to 13.7% for IP and 63.5% for NKSCC ($p = 0.019$ and 0.0101, respectively). p53 IHC averaged 43% for PLINKS compared to 9% for IP and 39% for NKSCC ($p = 0.002$ and 0.85, respectively). p16 was negative in all of the PLINKS and IPs while strongly and diffusely positive in 6 of the 8 NKSCC. All PLINKS that underwent staining for p40 or p63 were diffusely positive, confirming the squamous phenotype. Two of the 5 PLINKS had been initially misdiagnosed as benign. Clinical features were notable for an aggressive presentation with multiple recurrences, nodal metastasis, and even death in 1 PLINKS patient.

	Mitotic count/10HPF	Ki-67	p53	p16 positivity
IP	1.1	13.70%	9%	0/8
PLINKS	9.2	27%	43%	0/5
NKSCC	76.4	63.50%	39%	6/8

Table 1. Average mitotic count/10HPF, Ki-67 positivity and p53 positivity, and number of cases positive for p16 in IPs, PLINKS, and NKSCCs.

Conclusions: PLINKS appear to be a rarely reported, distinct type of sinonasal carcinoma. Our series of 5 PLINKS shows that there is potential for misdiagnosis as a papilloma due to the papillary architecture and bland cytology. While they resemble IP, the morphology, mitotic and Ki67 rates fall clearly in between IP and NKSCC while p53 is similar to NKSCC. Familiarity with these features is essential for appropriate diagnosis of PLINKS as malignant and for proper management and counseling.

1293 Application of Morphometry for Labial Salivary Gland Biopsy Interpretation in Primary Sjögren Syndrome: An Institutional Experience

Mukund Sable[1], Anirban Kundu[2], Gaurav Chhabra[2], Pritinanda Mishra[1], Amit Adhya[2]
[1]All India Institute of Medical Sciences, Bhubaneswar, Odisha, India, [2]All India Institute of Medical Sciences, Bhubaneswar, Bhubaneswar, Odisha, India

Disclosures: Mukund Sable: None; Anirban Kundu: None; Gaurav Chhabra: None; Pritinanda Mishra: None; Amit Adhya: None

Background: Labial salivary gland (LSG) biopsy plays a major role in diagnosis of primary S*jögren* syndrome (pSS) as per American-European Consensus Group classification criteria. Assessment of focal lymphocytic sialadenitis (FLS) and focus score (FS) is very critical for interpretation of LSG biopsy. Focus showing >50 lymphocytes is usually taken for focus scoring and FS >1 has been considered as diagnostic. However, no further guidelines exist on reporting of foci sizes, ratio of total focus area with glandular tissue, nature of lymphocytes, fibrosis, atrophy, and lymphoepithelial lesions in LSG.

Design: It is a retrospective observational study of 16 LSG biopsies reported in a patient of pSS, from Jan 2018 to Sept 2019. Additional serial deep cuts were performed on biopsy-negative cases. Morphometrical evaluation of total glandular area, FLS, FS, number of ducts, intraepithelial lymphocytes, and atrophy was done (Figure 1). The goal of the study is to apply consensus guidelines with morphometry in LSG biopsies, which may further help to improve reporting and reduce the interobserver variability. Imaging analysis was done on ZEN 2.3 lite software.

Results: On initial evaluation, 5/14 cases were interpreted as histological negative. However, after serial sectioning & morphometric evaluation of FS, additional one case showed FS <1. Total 8 cases fulfilled the criteria FS> 1. Morphometrical details are mentioned in Table 1. Glandular area was ranging from 2.843 mm^2 to 42.22 mm^2 (mean- 24.06 mm^2). FS was ranging from 0 to 1.38. Average number of ducts examined were 10. On histology, all cases with FS>1 showed glandular atrophy (mild – 3; moderate - 2 and marked - 2 cases) and fibrosis (mild – 4; moderate- 3 and marked - 1 cases). Ratio of total area of FLS and total glandular area was ranging from 7.02 to 30.05.

Sr No	Age	Sex	HP diagnosis	No of Foci	FS	Area(mm2)	Size of foci	Total area of FLS (mm2)	Area of smallest foci	Aera of Largest foci	Ratio	Apoptosis	Fibrosis	Atrophy	Dilated ducts	IL	chronic sailadenitis
1	34	F	Negative	2	0.6	13.3	0.084	0.138	0.064	0.074	96.37	Absent	0	0	0	0/100	Absent
2	32	F	Positive	13	1.23	42.22	0.301	3.913	0.133	0.522	10.78	Occasional	2+	1+	1+	2/100	Present
3	26	F	Negative	0	0	23.86	NA	NA	NA	NA	NA	NA	0	0	0	0/100	NA
4	60	M	Negative	0	0	2.843	NA	NA	NA	NA	NA	Ab	0	0	0	0	Absent
5	48	M	Negative	3	0.42	28.05	0.58	0.77	0.159	0.325	36.42	Absent	1+	1+	1+	1/100	Present
6	30	M	Negative	0	0	7.55	NA	NA	NA	NA	NA	Absent	0	0	0	0	Present
7	78	M	Negative	4	0.56	28.58	0.321	1.287	0.217	0.448	22.206	Occasional	3+	3+	2+	1/100	Present
8	35	F	Positive	10	1.38	28.79	0.4	4	0.168	0.468	7.1975	Marked	1+	2+	2+	7/100	Present
9	38	F	Positive	8	1.24	25.4	0.19	1.52	0.12	0.21	16.71	Absent	2+	3+	2+	2/100	Present
10	70	F	Positive	3	1.17	10.24	0.163	0.49	0.12	0.24	20.89	Absent	2+	2+	1+	4/100	Present
11	40	F	Positive	7	1.24	22.51	0.28	1.978	0.07	0.524	11.42	Occasional	3+	3+	3+	3/100	Present
12	25	F	Positive	9	1.11	32.16	0.55	4.58	0.37	0.808	7.02	Occasional	1+	1+	1+	2/100	Present
13	36	F	Positive	8	1.09	29.35	0.19	0.96	0.093	0.26	30.5	Absent	1+	1+	1+	2/100	Present
14	19	M	Positive	12	1.14	42.1	0.24	2.97	0.187	0.613	14.17	Occasional	1+	1+	1+	4/100	Present

Figure 1 - 1293

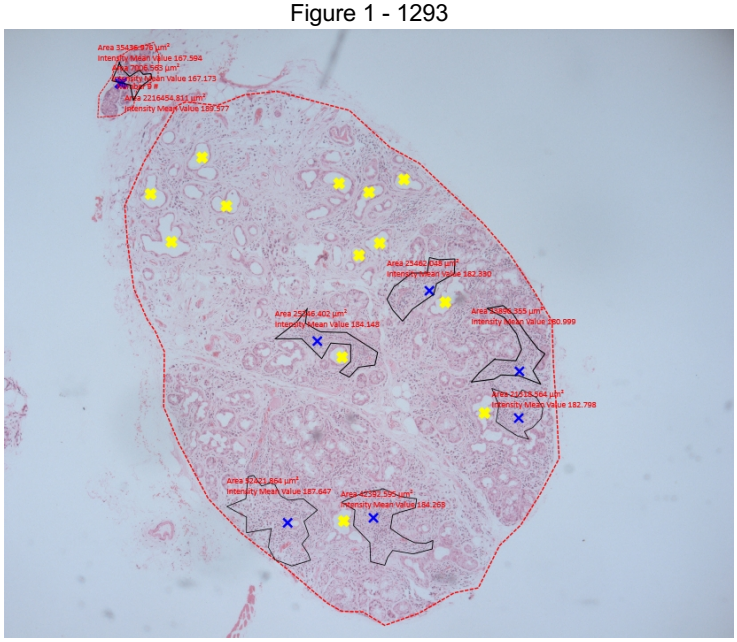

Conclusions: Morphometry can be considered as an important tool for interpretation of labial biopsies in pSS to improve histopathological evaluation and to minimize inter-observer variability. Additional histological variables may be included in development of minor diagnostic criteria after consensus guidelines between working groups.

1294 Sebaceous Neoplasms of the Near-East: Rate of HR-HPV Infection and Relation to Immunohistochemical Surrogate Markers

Maelle Saliba[1], Rana El Hajj[2], Fatmeh Abbas[1], Muhammad Shaheen[1], Shaarif Bashir[3], Umer Nisar Sheikh[4], Asif Loya[3], Rami Mahfouz[5], Ibrahim Khalifeh[1]

[1]American University of Beirut Medical Center, Beirut, Lebanon, [2]American University of Beirut, Beirut, Lebanon, [3]Shaukat Khanum Memorial Cancer Hospital, Lahore, Punjab, Pakistan, [4]Shaukat Khanum Memorial Cancer Hospital, Lahore, Lahore, Pakistan, [5]American University of Beirut Medical Center, Beirut, Lebanon

Disclosures: Maelle Saliba: None; Rana El Hajj: None; Fatmeh Abbas: None; Muhammad Shaheen: None; Shaarif Bashir: None; Umer Nisar Sheikh: None; Asif Loya: None; Ibrahim Khalifeh: None

Background: Sebaceous neoplasms (SNs) and carcinomas (SCs) represent rare skin adnexal tumors that exhibit a predilection to the ocular region. The carcinogenic role of environmental factors such as high-risk HPV (HR-HPV) infection and the significance of surrogate markers (p16 and p53) have yet to be fully understood.

Design: A total of 113 resected SNs (5 sebaceous adenomas, 10 sebaceomas and 98 sebaceous carcinomas) from the Near-East were reviewed. Clinical information (age, gender, size and anatomic location of lesions), microscopic variables, as well as the expression profiles of several immunohistochemical markers (EMA, CK5/6, p63, p40, AR, p16 and p53) were documented. All cases were evaluated by fluorescently labeled polymerase chain reaction analysis for the detection of HR-HPV, followed by a DNA microarray hybridization for subtype detection.

Results: HR-HPV was identified in 8.0% of cases (8 SCs and 1 sebaceoma) with a predominantly ocular location (7/9 cases, 77.8%). There was no preference to age and gender. HPV-16 accounted for 4/9 cases (44.4%) and HPV-66 for 2/9 (22.2 %). HPV-18, HPV-43 and HPV-52 were detected in the remaining cases. As compared to HR-HPV negative SCs, HR-HPV positive SCs were more likely to exhibit an infiltrative pattern of invasion (50% vs 24.4%), were less frequently cystic (11.1% vs 4.4%) and showed less sebaceous differentiation. They also displayed more brisk inflammatory infiltrates (33.3% vs 23.1%) and necrosis (44.4% vs 13.5%). Cases did not differ in terms of background solar elastosis. Of note, koilocytic surface changes were noted in 21.2% of all cases and associated verrucae vulgaris in 3 cases. P16 immunohistochemical expression was a sensitive but non-specific marker of infection (block-like p16 positivity in 88.9% of HR-HPV positive SNs vs 60.0% of HR-HPV negative SNs). While diffuse AR positivity was less frequently noted in HR-HPV positive lesions (55.6% vs 74.3%), high p53 labeling index expression was noted in roughly half of cases with no distinction to HPV status. Markers EMA, CK5/6, p63 and p40 showed no differential staining between the subgroups.

Conclusions: HR-HPV infection is attributed a role in the development of both benign and malignant SNs and can be histologically suspected based on subtle morphologic and immunohistochemical clues, especially in the setting of ocular lesions. P16, a surrogate marker of HPV infection in other settings, would be more useful as a diagnostic marker than a specific indicator of HPV infection in SNs.

1295 Predictors of PD-L1 Expression in Sebaceous Neoplasia: A Study of 215 Near-Eastern Cases

Maelle Saliba[1], Muhammad Shaheen[1], Rana El Hajj[2], Fatmeh Abbas[1], Umer Nisar Sheikh[3], Shaarif Bashir[4], Asif Loya[4], Ibrahim Khalifeh[1]
[1]American University of Beirut Medical Center, Beirut, Lebanon, [2]American University of Beirut, Beirut, Lebanon, [3]Shaukat Khanum Memorial Cancer Hospital, Lahore, Lahore, Pakistan, [4]Shaukat Khanum Memorial Cancer Hospital, Lahore, Punjab, Pakistan

Disclosures: Maelle Saliba: None; Muhammad Shaheen: None; Rana El Hajj: None; Fatmeh Abbas: None; Umer Nisar Sheikh: None; Shaarif Bashir: None; Asif Loya: None; Ibrahim Khalifeh: None

Background: The diagnosis of sebaceous carcinoma (SC) is followed by a grim disease course often entailing orbital exenteration, chemotherapy and/or radiation therapy. Characterization of the tumoral immune microenvironment in sebaceous neoplasms (SNs) is crucial for assessing the efficacy of immune checkpoint inhibitors in the treatment of SC.

Design: A total of 215 resected sebaceous neoplasms (17 sebaceous adenomas, 15 sebaceomas and 183 SCs) from the Near-East were reviewed. Clinical information including age, gender, size and anatomic location of lesions was collected. Microscopic examination documented several histopathologic variables as well as the immunohistochemical expression profile of markers CK5/6, P63, AR, EMA, p16, p53, PD-L1 and CD8. The percentage of PD-L1 staining cells was assessed in both tumor cells and inflammatory tumor infiltrates. Each case was accordingly attributed a Combined Positive Score (CPS) following recommendations for Head and Neck squamous cell carcinoma.

Results: A CPS ≥1 was seen with slight preference in Female (50.9%) vs Male patients (41.8%), and in extraocular (57.9%) vs ocular locations (42.1%). PD-L1 expression by tumoral inflammatory infiltrates was higher in malignant (M=16 for SC) than in benign lesions (M=1 in sebaceous adenoma, M=6 in sebaceoma). Such a pattern of PD-L1 expression was not noted in tumor cells. A higher CPS reflected a higher density of CD8 + T-lymphocytes along with a higher degree of malignancy; 93.3% of sebaceous adenomas had a null CPS while high CPSs (≥20) were seen in 13.3% of sebaceomas and 17.3% of SCs, each (see table). Microscopically, infiltrative and comedocarcinoma-like SCs were more likely to show a CPS ≥1 than nodular SCs (67.6%, 62.5% and 42.6%, respectively). The same applied to cases with a brisk rather than non-brisk inflammatory infiltrate (CPS ≥1 in 76.9% vs 39.6%), cases with or without necrosis (63.3% vs 44.2%) and cases with or without brisk apoptosis (51.1% vs 20.8%). Along with the degree of sebaceous differentiation, the expression of various markers of differentiation (CK5/6, p40, p63, AR, p16 and EMA) varied inversely to the CPS score [figure 2]. Within cases with a CPS ≥1, 60.6% of cases exhibited p53 overexpression.

	CPS ***Mean (Range)***	**CPS category**			**% of PD-L1 + tumor cells** ***Mean (Range)***	**% of PD-L1 + inflammatory cells** ***Mean (Range)***	**% of CD8+ TL** ***Mean***
		Nul	**Low (1-20)**	**High (≥20)**			
Sebaceous adenoma	0 (0-5)	93.3%	6.7%	0.0%	0	1 (0-30)	25
Sebaceoma	3 (0-20)	66.7%	20.0%	13.3%	4 (0-60)	9 (0-90)	33
Sebaceous carcinoma	7 (0-90)	48.6%	34.1%	17.3%	2 (0-70)	16 (0-80)	55

Figure 1 - 1295

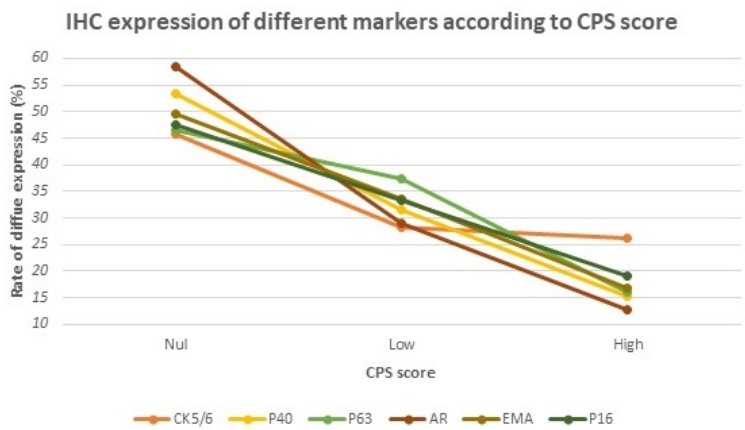

Conclusions: A significant number of SCs express PD-L1 at therapeutic levels. This supports the interest of evaluating anti-PD-L1 immunotherapy in SC, especially in cases with aggressive morphology and brisk inflammatory infiltrates.

1296 The Genomic Landscape of Young Patients with Oral Squamous Cell Carcinoma (OSCC)

Laveniya Satgunaseelan[1], Dario Strbenac[2], Kitty Lo[3], Maggie Lee[1], Cali Willet[4], Tracy Chew[4], Rosemarie Sadsad[5], Carsten Palme[6], Jean Yang[2], Jonathan Clark[7], Ruta Gupta[8]
[1]Royal Prince Alfred Hospital, Camperdown, NSW, Australia, [2]School of Mathematics and Statistics, The University of Sydney, Sydney, NSW, Australia, [3]University of Sydney, Sydney, NSW, Australia, [4]University of Sydney, Chippendale, NSW, Australia, [5]University of Sydney, Camperdown, NSW, Australia, [6]Missenden Road, NSW, Australia, [7]Chris O'Brien Lifehouse, Camperdown, NSW, Australia, [8]Royal Prince Alfred Hospital, Sydney, NSW, Australia

Disclosures: Laveniya Satgunaseelan: None; Dario Strbenac: None; Kitty Lo: None; Maggie Lee: None; Cali Willet: None; Tracy Chew: None; Rosemarie Sadsad: None; Carsten Palme: None; Jean Yang: None; Jonathan Clark: None; Ruta Gupta: None

Background: Oral cavity squamous cell carcinoma has traditionally affected older individuals with a history of tobacco and alcohol abuse. However, a recent alarming increase in the incidence of OSCC has been seen in young patients without tobacco or alcohol use, or HPV integration. The genomic landscape of OSCC in this young cohort has not been characterised.

Design: DNA was extracted from fresh frozen tissue from 16 non-HPV OSCC patients under the age of 50. Clinicopathological data, including pattern of invasion (POI), smoking history, alcohol consumption, adjuvant therapy and follow-up data were collected. Whole genome sequencing was performed (Illumina NovaSeq 6000). Data was analysed following alignment to hg38. Copy number amplifications were considered at a ploidy of 4 or greater and deletions at a ploidy of 1.5 or less.

Results: There were 9 males and 7 females, with a median age of 45 years. 4 patients were smokers. 7 patients had a pushing POI and 9 had infiltrative POIs. 3 patients showed recurrence and 2 patients are deceased. The median tumour mutation burden was 11729 (range 4902 to 20944). Whilst the median tumour mutation burden was higher in those with perineural invasion (11903 vs 10752), lymph node metastases (12083 vs 11514) and extranodal extension (12820 vs 11514), the difference did not reach statistical significance. All patients showed mutational signature 1. 2 patients showed mutational signatures 2 and 13 (AID/APOBEC). No mutation signature 4 was seen in smokers. 10 patients showed whole genome duplication and were more likely to have a worse POI. All patients with recurrence showed whole genome duplication. Chromosome 3q amplification was seen in all patients. Chromosome 3p, which harbours the *VHL* tumour suppressor gene, was deleted in 7 of 16 patients. *EGFR* and *MYC* amplification was seen in 9 of 16 patients.

Conclusions: Patients with adverse prognostic factors showed higher tumor mutation burden. Whole genome duplication was associated with an infiltrative POI and clinical recurrence. In contrast to 16% *EGFR* alteration in all HPV-negative head and neck SCC (HNSCC) (TCGA 2015), *EGFR* amplification occurred in 56% of this young OSCC cohort. Single nucleotide variant analysis is being performed. In conclusion, on preliminary analysis, OSCC in <50 years of age shows a higher incidence of mutation signature 1, whole genome duplication, 3p deletion, 3q amplification, and *EGFR* amplification as compared with conventional HNSCC.

1297 Molecular Profiling of EWSR1-rearranged Clear Cell Myoepithelial Carcinoma of Salivary Glands Identifies Prevalent PLAG1 Oncogene Fusions

Alena Skalova[1], Simon Andreasen[2], Nikola Ptakova[3], Petr Steiner[4], Jan Laco[5], Hanna Majewska[6], Martina Baneckova[7], Roderick Simpson[8], Katalin Kiss[9], Tomas Vanecek[10], Michal Michal[10]
[1]Charles University, Faculty of Medicine in Plzen, Plzen, Czech Republic, [2]Rigshospitalet, Copenhagen, Denmark, [3]Molecular and Genetic Laboratory, Biopticka Lab, Ltd, Plzen, Czech Republic, [4]Biopticka laborator s.r.o., Pilsen, Czech Republic, [5]The Fingerland Department of Pathology, Charles University, Faculty of Medicine and University Hospital, Hradec Kralove, Czech Republic, [6]Warmia and Mazury University, Olsztyn, Warmia and Mazury, Poland, [7]Charles University, Faculty of Medicine in Plzen, Pilsen, Czech Republic, [8]University of Calgary, Calgary, AB, [9]Diagnostic Centre Rigshospitalet, Copenhagen University Hospital, Copenhagen, Denmark, [10]Biopticka laborator s.r.o., Plzen, Czech Republic

Disclosures: Alena Skalova: None; Simon Andreasen: None; Nikola Ptakova: None; Petr Steiner: None; Jan Laco: None; Hanna Majewska: None; Martina Baneckova: None; Roderick Simpson: None; Katalin Kiss: None; Tomas Vanecek: None; Michal Michal: None

Background: Myoepithelial carcinoma (MC) of salivary glands is underrecognized challenging entity with broad morphological spectrum, and includes a *EWSR1*-rearranged clear cell variant. MC is generally an aggressive salivary gland cancer with largely unknown genetic features.

Design: A retrospective review of Salivary Gland Tumor Registry of the authors files (AS and MM) was conducted by searching the key words “clear cell myoepithelial carcinoma” , “hyalinizing clear cell”, and “clear cell malignant myoepithelioma”. The search yielded 94 clear cell myoepithelial carcinomas (CCMC) with available tissue for molecular analysis of *EWSR1* rearrangement using FISH. The tumors positive for *EWSR1* gene break were tested by next generation sequencing (NGS) using fusion-detecting panels. NGS results were confirmed by reverse transcription polymerase chain reaction (RT-PCR) and/or fluorescence in situ hybridization (FISH).

Results: Seventeen cases originally diagnosed as CCMC (17/94) revealed split signals for *EWSR1* by FISH. Ten cases were analyzable with NGS, but in 5 cases the tissue was not analyzable, and in two cases no additional tissue material was available. Fusion transcripts *LIFR-PLAG1* and *CTNNB1-PLAG1* were found, both in two cases. Dual *CHCHD7-PLAG1* and *FUS-GIPR* fusion was identified in one case. In addition, seven cases including those with PLAG1 fusion were positive for *PLAG1* rearrangement by FISH. All fusions were confirmed by RT-PCR or FISH. In two cases fusion of *EWSR1* namely *EWSR1-CREB3L1* and *EWSR1-ATF* were found by NGS.

Conclusions: Novel findings in our NGS study suggest that *EWSR1*-rearranged CCMC is a fusion-driven disease with prevalent *PLAG1*-oncogenic fusions, including *CTNNB1-PLAG1* and *LIFR-PLAG1* in most cases. *EWSR1*-rearranged cases with productive *EWSR1* gene fusions represent a minority of cases, and in the rest of them, the *EWSR1* break probably represents a passenger mutation with no biological impact.

1298 Novel Rearrangements in Salivary Gland Tumors Detected by Next Generation Sequencing Assay: Series of 104 Fusion Positive Cases

Alena Skalova[1], Tomas Vanecek[2], Petr Martinek[2], Nikola Ptakova[3], Abbas Agaimy[4], Jan Laco[5], Luka Brcic[6], Martina Baneckova[7], Olena Koshyk[8], Michal Michal[2]

[1]Charles University, Faculty of Medicine in Plzen, Plzen, Czech Republic, [2]Biopticka laborator s.r.o., Plzen, Czech Republic, [3]Molecular and Genetic Laboratory, Biopticka Lab, Ltd, Plzen, Czech Republic, [4]Universitätsklinikum Erlangen, Germany, Erlangen, Germany, [5]The Fingerland Department of Pathology, Charles University, Faculty of Medicine and University Hospital, Hradec Kralove, Czech Republic, [6]Medical University of Graz, Graz, Austria, [7]Charles University, Faculty of Medicine in Plzen, Pilsen, Czech Republic, [8]CSD Health Care Pathology lab, Kyiv, Kyivska, Ukraine

Disclosures: Alena Skalova: None; Tomas Vanecek: None; Petr Martinek: None; Nikola Ptakova: None; Abbas Agaimy: None; Jan Laco: None; Luka Brcic: None; Martina Baneckova: None; Olena Koshyk: None; Michal Michal: None

Background: Salivary gland tumors (SGT) are diagnostically challenging neoplasms characterized by extensive morphological variability. In recent years, considerable progress in salivary gland taxonomy has been reached by the discovery of tumor type-specific fusion oncogenes generated by chromosome translocations. These genetic aberrations do not only serve as robust diagnostic tools in classification, but they also represent potential targets of therapy.

Design: A total cohort of 216 SGTs of various morphologies were tested for fusion transcripts within the years 2017-2019. Most of the cases were sent to our institution for second opinion and molecular profiling. RNA from formalin fixed paraffin embedded samples was isolated and targeted next generation sequencing (NGS) was used to detect both known and novel fusion transcripts. The panels included *NTRK1, NTRK2, NTRK3, RET* and multiple other genes commonly rearranged in solid tumors.

Results: Gene fusions were detected in 104 SGT cases (104/216) (48%). Among the fusion positive SGTs, 62 (60%) occurred in the parotid gland, 4 (4%) in the submandibular gland, 22 (21%) in minor salivary glands of the oral cavity, 13 (13%) in sinonasal mucosa, and one case each (2%) in the thyroid, sublingual gland, and liver metastasis from submandibular gland primary. Regarding tumor type distribution and molecular profiling, most commonly tested were secretory carcinoma (SC, n=36) with the fusion *ETV6-NTRK3* (n=33), *ETV6-RET* (n=2) and novel *VIM-RET* (n=1); intraductal carcinoma (IC, n=15) with *NCOA4-RET* (n=12), *TRIM27-RET* (n=2), *KIAA1217-RET* (n=1); adenoid cystic carcinoma (AdCC, n=15) with *MYB-NFIB* (n=15); mucoepidermoid carcinoma (MEC, n=8) with *CRTC1-MAML2* (n=6), and *CRTC3-MAML2* (n=2). Myoepithelial carcinoma (MyoCC, n=9) and epithelial-myoepithelial carcinoma (Epi_MyoCC, n=2) revealed spectrum of *PLAG1* rearrangements, including *LIFR-PLAG1* (n=4), *CTNNB1-PLAG1* (n=2), *CHCHD7-PLAG1* (n=1), *GEM-PLAG1* (n=1), and novel fusions *HMGA2-FLI41278* (n=1), and *FUS-GIPR* (n=1). Most notable findings were novel fusions in 4 SGTs, including these tumor types: *VIM-RET* in SC, *FUS-GIPR* in low-grade MEC, *HMGA2-FLI41278* in apocrine variant of Epi_MyoCC, and *NTF3-PLAG1* in benign oncocytic myoepithelioma (Table 1).

Table 1. Novel gene fusions in salivary gland tumors detected by NGS

No.	Age/sex	Diagnosis	Site	Gene fusion by NGS	Confirmed by FISH or RT-PCR
1	67/F	MyoCC	Parotid gland	*FUS-GIPR*	FISH
2	56/F	SC	Parotid gland	*VIM-RET*	RT-PCR
3	57/F	Oncocytic ME	Parotid gland	*NTF3-PLAG1*	RT-PCR
4	57/F	Epi_MyoCC	Parotid gland	*HMGA2-FLI41278*	FISH

Abbreviations: MyoCC=Myoepithelial carcinoma; SC=Secretory carcinoma; ME=myopithelioma; IC=Intraductal carcinoma; Epi_MyoCC=epithelial myoepithelial carcinoma with apocrine features;

Conclusions: A novel finding in our study has been a discovery of four SGTs with unknown fusions including *VIM-RET* in SC, *FUS-GIPR* and *HMGA2-FLI41278* in MyoCC and Epi_MyoCC, respectively. A case of benign oncocytic myoepithelioma revealed novel

fusion *NTF3-PLAG1*. In addition to novel findings, molecular testing identified total of 52 SGTs (50%) with potentially targetable fusions, NTRK3 (n=33), NTRK1 (n=1), and RET (n=18).

1299 Molecular Profiling of Salivary Oncocytic Mucoepidermoid Carcinomas Helps to Resolve Diagnostic Dilemma with Low-Grade Oncocytic Lesions

Olga Stanowska[1], Abbas Agaimy[2], Laura Ardighieri[3], Petr Steiner[4], Piero Nicolai[5], Monika Durzyńska[6], Hanna Majewska[7], Monika Prochorec-Sobieszek[8], Elwira Bakula-Zalewska[9], Martina Baneckova[10], Michal Michal[11], Alena Skalova[12]
[1]Department of Pathology, Maria Sklodowska-Curie Cancer Center - Institute of Oncology, Warsaw, Poland, [2]Universitätsklinikum Erlangen, Germany, Erlangen, Germany, [3]Covo, BG, Italy, [4]Biopticka laboratory s.r.o., Pilsen, Czech Republic, [5]University of Brescia, Brescia, Italy, [6]Maria Sklodowska-Curie Institute - Oncology Center, Warsaw, Poland, [7]Warmia and Mazury University, Olsztyn, Warmia and Mazury, Poland, [8]Maria Skladowska Curie Institute - Oncology Center, Warsaw, Poland, [9]Warsaw, Poland, [10]Charles University, Faculty of Medicine in Plzen, Pilsen, Czech Republic, [11]Biopticka laboratory s.r.o., Plzen, Czech Republic, [12]Charles University, Faculty of Medicine in Plzen, Plzen, Czech Republic

Disclosures: Olga Stanowska: None; Abbas Agaimy: None; Laura Ardighieri: None; Petr Steiner: None; Piero Nicolai: None; Monika Durzyska: None; Hanna Majewska: None; Monika Prochorec-Sobieszek: None; Elwira Bakula-Zalewska: None; Martina Baneckova: None; Michal Michal: None; Alena Skalova: None

Background: Oncocytic mucoepidermoid carcinoma (OMEC) is a rare but diagnostically challenging variant of mucoepidermoid carcinoma (MEC). OMEC is notable for differential diagnostic considerations that are raised as a result of overlap with other benign and low-grade oncocytic salivary gland tumors. Diffuse and strong immunoreactivity of p63 protein may be useful in distinguishing OMEC from its mimics. However, focal p63 staining can be present in benign oncytomas. Moreover, mucocytes may be very few and hardly discernable in OMEC, and therefore molecular testing for *MAML2* rearrangement can be a useful supportive ancillary test for exact diagnosis. Recently two index cases of low-grade oncocytic neoplasms without any mucous cells, received as consults (AA and AS), were reclassified as OMEC, based on molecular profiling.

Design: A retrospective review of Salivary Gland Tumor Registry of the authors files (AS, MM, and MPS) was conducted searching for “low grade/uncertain oncocytic tumor”, “oncocytoma” and “oncocytic carcinoma” in the period 1996 to 2019. The search yielded 125 salivary gland neoplasms; including 19 cases fulfilling the following criteria: predominant oncocytic features (>75% tumor cells), solid and cystic growth pattern (>50% solid), at least focal invasive growth, and features suspicious of malignancy, such as cellular atypia, necrosis and/or enhanced mitotic and proliferative activity. All these cases were stained with mucicarmine and PAS (Periodic Acid Shiff), and investigated immunohistochemically (IHC) for S100 protein and p63/p40. The tumors with IHC positivity for p63 and/or p40, and S100 negativity, irrespectively of mucicarmine staining, were tested by next generation sequencing (NGS) using fusion-detecting panels in order to detect *MAML2* gene rearrangements. NGS results were confirmed by reverse transcription polymerase chain reaction (RT-PCR) and/or fluorescence in situ hybridization (FISH)

Results: Two index cases from consult practice (AS and AA) of purely oncocytic low grade neoplasms without discernable mucinous cells, revealing a *CRTC1-MAML2* using NGS were reclassified as OMEC. In addition, in 6 (6/19) additional oncocytic tumors, retrieved from the files, the *MAML2* gene rearrangement was detected (Table 1). Presence of mucocytes, pattern of p63 immunopositivity and mucicarmine staining were inconsistent findings.

Table 1. Oncocytic neoplasms reclassified as OMEC by molecular detection of *MAML2* gene rearrangement

No.	Age/sex	Original dg.	Site	Gene fusion by NGS	Confirmed by FISH or RT-PCR
1	48/F	Oncocytic neoplasm of uncertain malignant potential	Parotid gl.	*CRTC1-MAML2*	-
2	53/M	Oncocytic neoplasm	Parotid gl.	ND	FISH - *MAML2*
3	45/F	Recurrent oncocytoma	Sublingual gl.	*CRTC1-MAML2*	-
4	74/M	Oncocytic neoplasm, possibly OMEC	Parotid gl.	*CRTC1-MAML2*	FISH - *MAML2*
5	83/F	PA with oncocytic metaplasia	Parotid gl.	*CRTC1-MAML2*	RT-PCR- *CRTC1-MAML2*
6	41/F	Oncocytic neoplasm of uncertain malignant potential	Parotid gl.	ND	FISH - *MAML2*
7	46/M	Benign mucinous oncocytoma	Parotid gl.	NA	FISH - *MAML2*
8	71/F	Multifocal oncocytoma	Parotid gl.	Neg.	FISH - *MAML2*

Abbreviations: ND=not done; gl=gland;NA=not analyzable;neg.=no fusions found;PA=pleomorphic adenoma;OMEC=oncocytic mucoepidermoid carcinoma;

Conclusions: Distinguishing OMEC with exclusive oncocytes from oncocytoma and oncocytic carcinoma can be very challenging, and is critical for proper clinical management. D

1300 Low-Grade Tubulo-Acinar Sinonasal Adenocarcinoma: A Specific Entity with Recurrent Beta-Catenin Mutations

Edward Stelow[1], Stacey Mills[1]
[1]*University of Virginia Health System, Charlottesville, VA*

Disclosures: Edward Stelow: None; Stacey Mills: None

Background: Sinonasal adenocarcinomas (SNACs) are diverse in histology. After salivary-gland type tumors and intestinal-type adenocarcinomas are excluded, SNACs are usually only classified as high grade or low grade based on cytologic features, mitotic activity and necrosis. While this is useful for predicting behavior, it does not necessarily lead to the distinction of truly specific tumors. Recently, occasional low-grade SNACs have been shown to have recurrent translocations and rare tumors have been shown to have beta-catenin mutations. Here we describe a histologically and immunophenotypically distinct low-grade SNAC characterized by recurrent beta-catenin abnormalities.

Design: All low-grade SNACs that have been seen at our institution were reviewed. Tumors were further classified as predominately tubulo-acinar, mucinous and papillary or other. Clinicopathologic features and immunohistochemical results including beta-catenin immunostaining were recorded.

Results: 29 low-grade SNACs were reviewed. Six had a predominately tubulo-acinar pattern of growth, 14 had a predominately papillary pattern of growth with mucinous cells and 9 showed other histology. Of the six tumors with a predominately tubulo-acinar pattern of growth, 5 involved the nasal cavity alone. These tumors were equally distributed between the sexes. Five of these tumors arose in patients younger than 20-years old. All had markedly similar histology (Figure 1). Tumors were polypoid, bulging masses measuring up to 2 cm and covered by an intact, normal appearing Schneiderian epithelium. The subepithelial tissue was packed with back to back, frequently fused, tubulo-acinar proliferations. These were lined by a single layer of cuboidal to columnar epithelial cells with delicate faint to eosinophilic cytoplasm and bland round nuclei. Squamous metaplasia or morule formation was frequently seen. Mitotic figures were rare and necrosis was not seen. All 6 tumors expressed strong, aberrent nuclear beta-catenin. Tumors uniformly expressed S100 and sox10 and did not express DOG1, p63 and SMA. Mammaglobin was expressed focally only in a single case.

Figure 1 - 1300

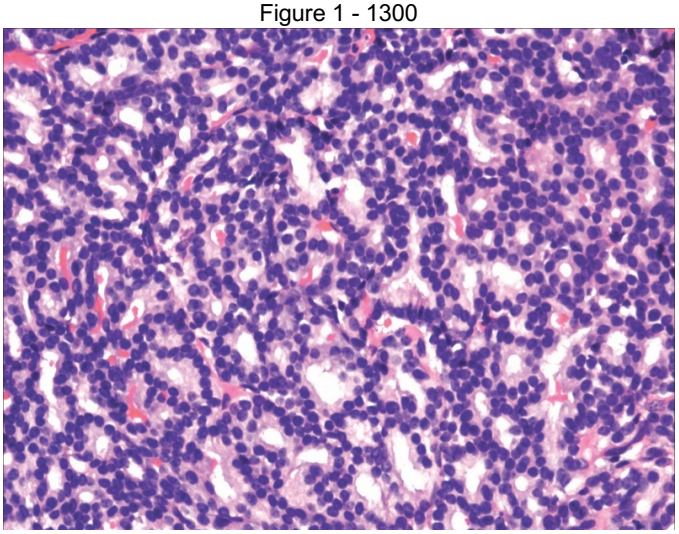

Conclusions: Low-grade tubulo-acinar SNAC is a distinct tumor that appears to arise most frequently in young people. Tumors have consistent histological and immunohistochemical findings and are characterized by beta-catenin mutations.

1301 Immunohistochemical Evaluation of Nuclear Protein in Testis (NUT) Expression on Tumors and Normal Tissues from Various Organs

Nabil Tabish[1], Haiyan Liu[1], Jianhui Shi[1], Fan Lin[1]
[1]*Geisinger Medical Center, Danville, PA*

Disclosures: Nabil Tabish: None; Haiyan Liu: None; Jianhui Shi: None; Fan Lin: None

Background: Nuclear protein in testis (NUT)-positive carcinomas are rare and aggressive tumors and are frequently underdiagnosed as poorly differentiated carcinoma. Immunohistochemical (IHC) detection of NUT expression is believed to be nearly 100% specific for diagnosis. Data on the NUT expression in other tumors were limited. This study investigated the expression of NUT in a large series of poorly differentiated carcinomas and other tumors from various organs.

Design: IHC analysis of NUT (C52B1 rabbit monoclonal antibody, Cell Signaling Technology) was performed on 1236 cases of tumor and normal tissues on tissue microarray (TMA) sections, including 3 cases of confirmed NUT midline carcinoma, mesothelioma (N=18), lung neuroendocrine carcinoma (CA) (N=24), lung adenocarcinoma (ADC) (N=88), lung squamous cell CA (N=66), papillary thyroid CA (N=47), ENT squamous cell CA (N=28), breast fibroadenoma (N=20), pancreatic neuroendocrine tumor (N=33), pancreatic ADC (N=43), adrenal pheochromocytoma (N=14), endometrial CA (N=59), ovary papillary serous CA (N=41), clear cell CA of uterus and ovary (N=22), melanoma (N=32), skin neuroendocrine CA (N=27), invasive urothelial CA (N=43), bladder small cell CA (N=24), prostatic ADC (N=38), germ cell tumors (N=60), colonic ADC (N=164), angiosarcoma (N=12), papillary renal cell carcinoma (RCC) (N=33), clear cell RCC, low grade (N=79), clear cell RCC, high grade (N=51), hepatocellular CA (N=47), liver metastatic neuroendocrine CA (N=18), glioblastoma multiforme (N=23), mantle cell lymphoma (N=13) and hairy cell leukemia (N=1). Samples from normal tissue included pancreas (N=13), rectum/appendix/colon (N=39) and ilium/duodenum/stomach (N=13). Nuclear expression for NUT was interpreted as negative (no tumor cells stained), 1+ (<25%), 2+ (26-50%), 3+ (51-75%), and 4+ (>75%). Normal testicular tissue and the 3 confirmed NUT-positive cases were used as positive controls.

Results: Diffuse nuclear positivity was seen in 3 confirmed NUT-positive cases. Focal expression was observed in 1 of 60 (2%) germ cell tumors, 5 of 164 (3%) colonic ADCs, and 4 of 47 HCCs (9%), respectively. All other tumors and normal tissues were negative for NUT. Representative cases are shown in Figure 1.

Figure 1 - 1301

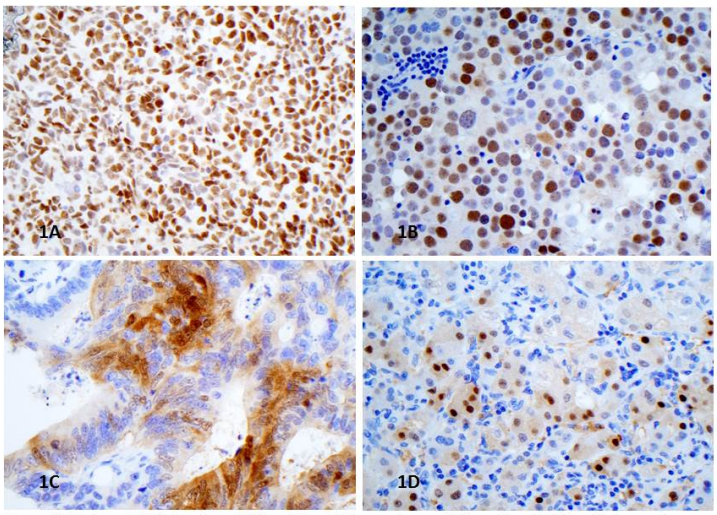

Figure 1 (1A through 1D) showing a NUT-positive midline carcinoma (1A), and focal NUT positivity rarely seen in other tumors including seminoma (1B), colonic adenocarcinoma (1C), and hepatocellular carcinoma (1D).

Conclusions: Our data demonstrated the IHC detection of NUT is highly specific for diagnosing a NUT midline carcinoma since nearly all tumors tested were negative. Caution should be taken because focal NUT positivity can be rarely seen in in germ cell tumors, hepatocellular CA, and colonic ADC.

1302 Why and How to Diagnose Synovial Sarcoma in Head and Neck Region. A Detailed Clinicopathologic Study Emphasizing Diagnostic Utility of Immunohistochemical Markers and Poor Prognosis

Muhammad Tariq[1], Nasir Ud Din[2], Alka Rani[1], Abbas Agaimy[3]
[1]Aga Khan University Hospital, Karachi, Sindh, Pakistan, [2]The Aga Khan University Hospital, Karachi, Sindh, Pakistan, [3]Universitätsklinikum Erlangen, Germany, Erlangen, Germany

Disclosures: Muhammad Tariq: None; Nasir Ud Din: None; Alka Rani: None; Abbas Agaimy: None

Background: Synovial Sarcoma (SS) is a distinct malignant neoplasm which commonly involves extremities in young and middle-aged individuals. Head and neck region is a rare site for synovial sarcoma. The most common malignant neoplasm of this region is carcinoma which, in its poorly differentiated (sarcomatoid) form, can acquire spindle morphology and lose expression for epithelial markers such as Cytokeratins and Epithelial Membrane Antigen (EMA).

SS is usually not considered as a differential diagnosis. In addition, due to positive expression of Cytokeratins and EMA, it can be misdiagnosed as poorly differentiated/spindle cell carcinoma.

Our study was aimed at describing the clinicopathological, histological and immunohistochemical (IHC) features of SS in head and neck region which would help in its diagnosis. Moreover, we also attempted to understand disease behavior by assessing follow up information.

Design: We conducted a descriptive cross section study on cases diagnosed as SS of head and neck region between January 2010 and August 2019. We identified 33 cases. Clinicopathologic features such as age, gender, size and location were available from pathology reports. H&E and IHC stained slides of these cases were reviewed by two pathologists for histological features and IHC profile. Follow up information was either available from patient's medical records or obtained from patients (or their relatives) via telephone conversation.

Results: Patients' age ranged widely from 10 to 60 years (median=18 years). Male: Female ratio was 2:1. The most common tumor location was soft tissue of the neck. Majority of the cases (N=29) were monophasic or poorly differentiated. Necrosis was observed in 9 (27.2%) cases. All 6 cases tested for SYT FISH analysis were positive. Clinicopathological and IHC features are summarized in the table.

Follow up was available for 16 patients (10 to 100 months; median=21 months). All 16 patients underwent surgical excision, 6 (37.5%) patients received adjuvant chemotherapy and 5 (31.2%) received chemotherapy. More than half of the patients died of disease.

Table: Summary of clinicopathologic and IHC features

Clinicopathological features	**Expression/Frequency (%)**
Age (Years)	10-60
Range	32.3
Mean	18
Median	
Tumor Size (cm)	1-12
Range	5.4
Mean±SD	4.5
Median	
Tumor Location	
Neck	16(48.5%)
Head	6(18.2%)
Oral Cavity	3(9.1%)
Nasal Cavity	3(9.1%)
Larynx	3(9.1%)
Orbit	2(6.1%)
Histologic type	19(57.6%)
Monophasic	4 (12.1%)
Biphasic	10(30.3%)
Poorly differentiated	
Mitotic count/10HPF	2-80
Range	20.4
Mean	13
Median	
Immunohistochemical stains	23/24 (95.8%)
TLE1	26/33 (78.8%)
EMA	11/26 (42.3%)
CytokeratinAE1/AE3	3/6 (50%)
Cytokeratin CAM5.2	6/11 (54.5%)
Cytokeratin 7	13/19 (68.4%)
Cytokeratin 19	1/4 (25%)
Cytokeratin 5/6	2/6 (33.3%)
p63	0/34
CD34	1/24 (4.2%)
ASMA	0/24
Desmin	5/24 (20.8%)
S100	0/5
HMB45	2/2 (100%)
CyclinD1	

Follow up (n=16)	9(56.2%)
Died of disease	3(18.8%)
Recurrence	4(25%)
Metastasis	

Conclusions: SS should always be considered as a differential diagnosis in all head and neck tumors with spindle morphology. Combination of TLE1 and epithelial markers' expression is the most helpful clue. Aberrant expression of S100, ASMA, Cytokeratin 5/6 and p63 might pose diagnostic challenge. These tumors behave aggressively with high death, recurrence and metastasis rates.

1303 MDM2 is a Useful Diagnostic Marker for the Diagnosis of Nasopharyngeal Carcinoma

Cecilia Taverna[1], Abbas Agaimy[2], Marco Santucci[3], Alessandro Franchi[4]
[1]University of Florence, Florence, Italy, [2]Universitätsklinikum Erlangen, Germany, Erlangen, Germany, [3]University of Florence, Firenze, FI, Italy, [4]University di Pisa, Pisa, Italy

Disclosures: Cecilia Taverna: None; Abbas Agaimy: None; Marco Santucci: None; Alessandro Franchi: None

Background: The *MDM2* gene appears to be involved in the development of nasopharyngeal carcinoma. The aim of this study was to examine MDM2 expression in a series of nasopharyngeal carcinoma biopsies to explore its potential diagnostic significance.

Design: The study cohort consisted of 26 nasopharyngeal carcinomas, including 22 EBV positive non-keratinizing squamous cell carcinomas (NKSCC), 1 EBV negative NKSCC and 3 EBV negative keratinizing SCC. For comparison, we selected 48 oropharyngeal carcinomas, including 17 HPV positive NKSCC (14 non-keratinizing and 3 keratinizing) and 31 HPV negative SCCs (28 keratinizing and 3 non-keratinizing). In addition, we examined MDM2 expression in a group of 26 cervical lymph node metastases, including 5 with primitive EBV positive nasopharyngeal NKSCC and 21 from oropharyngeal carcinoma (18 non keratinizing HPV positive, 1 keratinizing HPV positive, 1 keratinizing HPV negative and 1 non-keratinizing HPV negative). Finally, 2 bone metastases from EBV positive nasopharyngeal NKSCC were also included. A tissue microarray was constructed from formalin-fixed paraffin embedded tumor tissue specimens. Sections were immunostained for MDM2 using the IF2 monoclonal antibody (Invitrogen, Milan, Italy). In situ hybridization for EBER and CISH analysis for the MDM2 gene were also conducted in all cases.

Results: Overall, MDM2 positivity was detected in 28 of 102 SCCs (27.2%). MDM2 positivity was significantly more frequent in EBV positive NKSCC (80%) than in oropharyngeal HPV positive NKSCC (6.1%) and keratinizing SCCs (9.4%)($p<0.001$, Pearson chi square). Considering only the primary tumors, 86.4% of the nasopharyngeal carcinomas were positive, versus 13.5% of the oropharyngeal carcinomas ($p<0.001$, Pearson chi square). Considering the lymph node metastases, 3 of 5 of the EBV positive carcinomas with nasopharyngeal primary were positive, whereas only one of the HPV positive carcinomas was positive. Finally, both the bone metastases from EBV positive nasopharyngeal carcinoma were positive for MDM2. No amplification of the MDM2 gene was identified by CISH analysis.

Conclusions: Our data indicate that MDM2 could be a valuable diagnostic marker to support the diagnosis of nasopharyngeal EBV positive NKSCC.

1304 Orbit Solitary Fibrous Tumor: Report of 12 Cases

Lester Thompson[1], Sofia Liou[2], Kenneth Feldman[3]
[1]Southern California Permanente Medical Group, Woodland Hills, CA, [2]University of California Los Angeles, Los Angeles, CA, [3]Southern California Permanente Medical Group, Harbor City, CA

Disclosures: Lester Thompson: None; Sofia Liou: None; Kenneth Feldman: None

Background: Solitary fibrous tumors (SFTs) of the orbit are rare. In order to further characterize the clinical and pathologic features of solitary fibrous tumor arising at this anatomic site, 12 cases of orbital solitary fibrous tumor were analyzed in conjunction with a review of cases reported from the English literature.

Design: Retrospective

Results: SFTs of the orbit are equally distributed between males (n=5) and females (n=7) with a mean patient age of 46.8 years (median 44.5 years; range 18-76 years) at initial diagnosis. The patients typically presented with swelling or mass around the orbit, exophthalmos (n=7), proptosis (n=10), ptosis (n=5) and visual changes (n=6), while pain, tearing, and headaches were less common. Tumors were orbital (n=10) or upper eyelid (n=2); orbital tumors were 5 each intraconal and extraconal, respectively. Tumors were an average of 2.5 cm (median 2.6 cm; range 0.6-3.7 cm), with male patients having slightly larger tumors than females (2.8 vs. 2.2 cm). Microscopically, the tumors were characterized by cytologically bland spindle cells with patternless growth, hypocellular and hypercellular areas, variable

amounts of collagen, and ectatic, branching blood vessels. One tumor was considered to be histologically malignant based on profound pleomorphism and increased mitotic activity. By immunohistochemistry, all cases had a strong nuclear STAT6 expression, with 11 of 12 cases CD34-reactive. Curiously, patients managed with pre-surgical embolization showed reduced or absent STAT6 reactivity around embolic material. All patients were managed with excision without radiation. Three patients showed persistent or recurrent disease (mean 33.6 months), with one patient developing a distant femur metastasis (86.9 months). Overall follow-up was 65.8 months (mean): 9 patients alive or dead ***without*** disease (mean 71.3 months), three patients ***with*** disease (mean 49.4 months).

Figure 1 - 1304

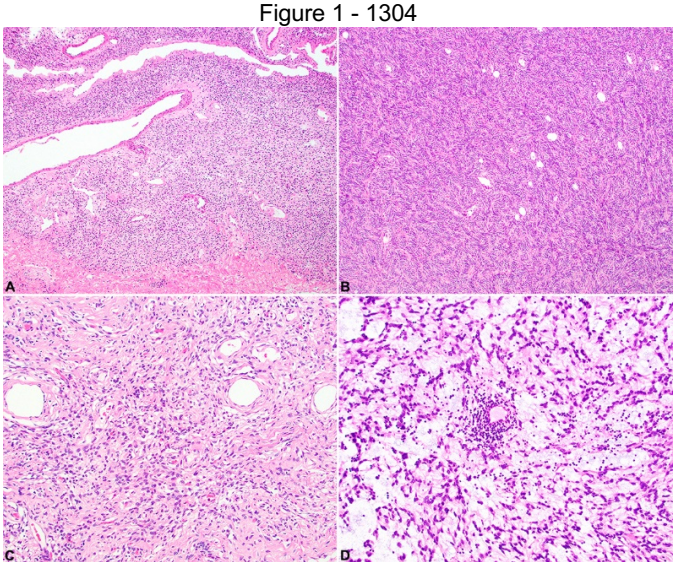

Figure 2 - 1304

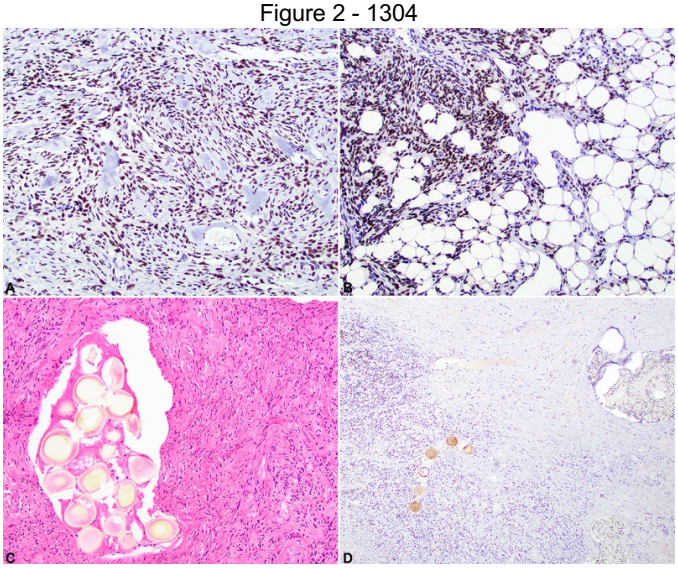

Conclusions: Orbital SFTs are very rare, but can be reliably diagnosed based on the presence of characteristic morphologic features as well as immunohistochemical expression of STAT6 and CD34. The majority of orbital solitary fibrous tumors show a benign clinical course; however, local recurrence and metastasis may be seen, requiring close clinical follow-up.

1305 Salivary Gland Lymphoepithelial Carcinoma EBER-association in Endemic vs. Non-Endemic Patients: A Report of 16 Cases

Lester Thompson[1], Roman Carlos[2], Justin Bishop[3], Lisa Rooper[4]
[1]Southern California Permanente Medical Group, Woodland Hills, CA, [2]Centro Clinico de Cabeza y Cuello, Guatemala City, Guatemala, [3]University of Texas Southwestern Medical Center, Dallas, TX, [4]The Johns Hopkins University School of Medicine, Baltimore, MD

Disclosures: Lester Thompson: None; Justin Bishop: None; Lisa Rooper: None

Background: Lymphoepithelial carcinoma in salivary glands (LECSG) are rare neoplasms, reported in endemic populations (southeastern Chinese) with a strong Epstein-Barr virus (EBV) association. A series comparing endemic with non-endemic patients has not been reported.

Design: Retrospective

Results: LECSG are equally distributed between males (n=8) and females (n=8) with a median (median 54 years; range 18-85years) at initial diagnosis. Ten patients were white, 4 Asian, and 2 black. The patients typically presented with swelling or mass for an average of 11.6 months. Tumors affected only major salivary glands: parotid (n=13); submandibular (n=3). Tumors were an average of 2.9 cm (range 1.5-5.8 cm). Eight of 16 (50%) patients had cervical lymph node metastases at presentation. No patients had nasopharyngeal or oropharyngeal tumors. One patient each had atopic dermatitis and dermatomyositis. Microscopically, the tumors were widely infiltrative, characterized by large polygonal to spindled cells arranged in a syncytial, lattice-like network in a background of lymphoplasmacytic cells. The neoplastic cells showed an open-vesicular nuclear chromatin to a more basaloid-morphology, with hyperchromatic nuclei and less cytoplasm, with nearly all of the cases associated with lymphoepithelial lesions/sialadenitis. By immunohistochemistry, 8 of 16 cases has a strong, diffuse EBER expression (4 of 4 Asians; 4 of 12 non-Asians), with all cases CK-pan reactive, CK5/6 and p63 reactive. All patients were managed with wide, radical excision, 4 with concurrent chemoradiation, and 5 with radiation alone; there was no difference between patients managed with chemo/radiation than those without: follow-up mean 3.2 vs 4.5 years, respectively. Distant metastasis (lung and bone) developed in 2 patients. Overall follow-up (mean 3.8 years) revealed 13 patients alive or dead without evidence of disease (mean 4.2 years); 2 alive with disease (mean 1.0 year), and one who died of disease at 4.2 years. The patients with disease at last follow-up all had

Group IV disease (2 whites; 1 Asian). High stage (IV) had a shorter mean survival than lower stage patients: 3.0 versus 4.3 years, respectively.

Figure 1 - 1305

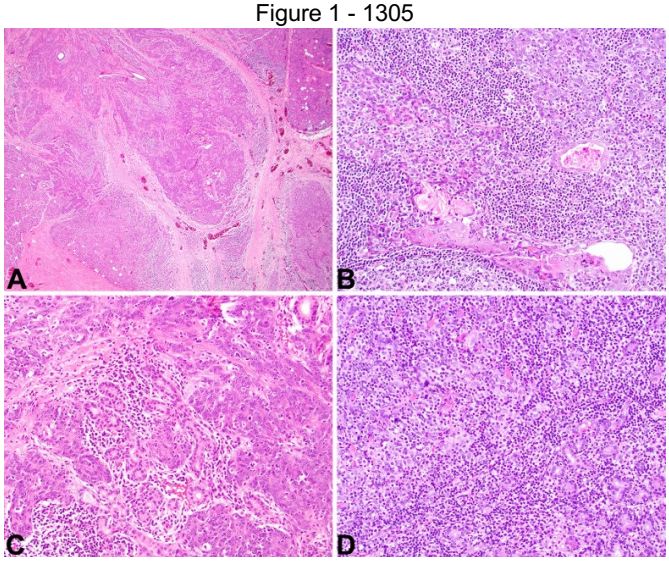

Figure 2 - 1305

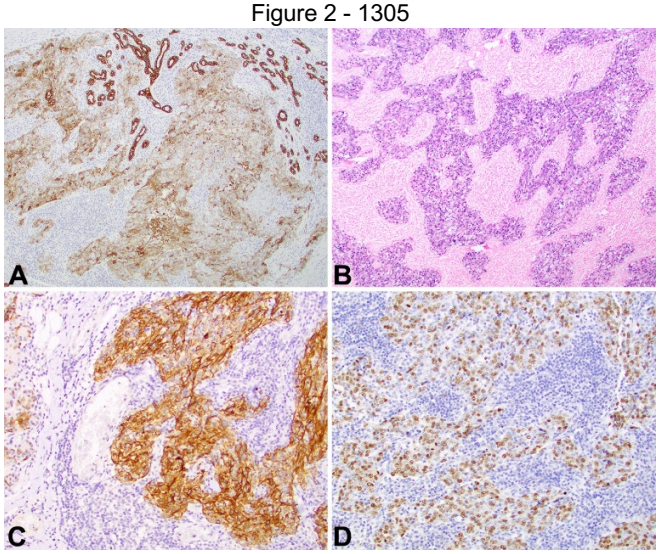

Conclusions: LECSG are uncommon primary neoplasms. Concurrent lymphoepithelial lesions may help suggest a primary tumor. The tumors, irrespective of race or ethnicity, may express EBER. There is an overall good survival even without combination chemoradiation therapy, although stage dependent.

1306 SATB2 Expression Profile of Odontogenic Tumors

Kevin Trowell[1], Paul Zhang[2]
[1]Hospital of the University of Pennsylvania, Philadelphia, PA, [2]Hospital of the University of Pennsylvania, Media, PA

Disclosures: Kevin Trowell: None; Paul Zhang: None

Background: Special AT-rich sequence binding protein (SATB2) is a transcription factor involved in osteoblast differentiation and craniofacial development. SATB2 expression has been shown to be selectively expressed in human tissue, including bone tumors and sarcomas with osteoblastic differentiation. Recently, SATB2 expression has been investigated in murine and human tooth development by immunohistochemistry, however expression studies including neoplastic odontogenic processes have not been performed. In this study, we assess expression of SATB2 by immunohistochemistry in two tumors of odontogenic origin: odontogenic keratocyst and ameloblastoma.

Design: We searched our institutional database for cases of ameloblastoma and odontogenic keratocyst, obtained from 2015 to 2018. SATB2 immunohistochemistry was performed on representative paraffin-embedded tissue blocks. SATB2 staining was qualitatively graded in the epithelial and stromal components, and scored on the following scale: 0 (no expression), 1+ (weak expression), 2+ (strong expression).

Results: We examined 25 cases of ameloblastoma and 30 cases of odontogenic keratocysts. SATB2 staining results are shown in the provided table. Ameloblastomas showed positive epithelial staining (1+) in 6 and stromal staining in 20 (80%) of the 25 cases. Odontogenic keratocysts showed negative epithelial staining in all 30 cases but stromal staining in 27 (90%) of the 30 cases.

Ameloblastoma (n=25)			
	Epithelium staining	n=	%
	0	19	76%
	1+	6	24%
	2+	0	0%
	Stromal staining		
	0	5	20%
	1+	8	32%
	2+	12	48%
Odontogenic Keratocyst (n=30)			
	Epithelium staining	n=	%
	0	30	100%
	1+	0	0%
	2+	0	0%
	Stromal staining		
	0	3	10%
	1+	6	20%
	2+	21	70%

Figure 1 - 1306

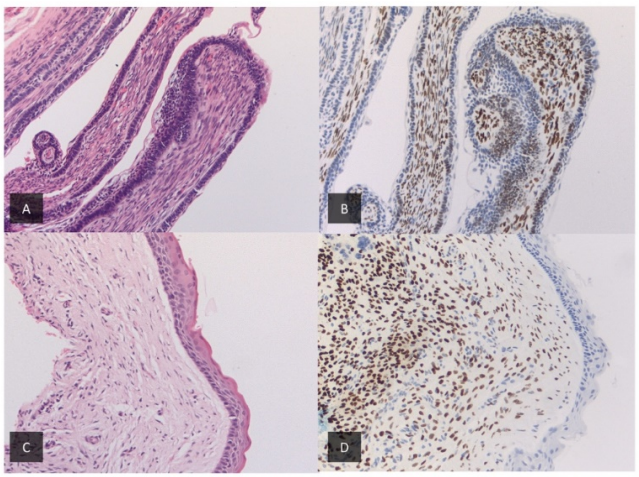

Figure 1: Ameloblastoma (A, H&E) Ameloblastoma with SATB2 staining epithelium and stroma (B); Odontogenic keratocyst (C, H&E), with SATB2 staining stroma only

Conclusions: SATB2 is positive in the epithelial component of ameloblastoma in 6/25 (24%) of cases, while it is negative in all cases of odontogenic keratocyst. This might reflect the difference in terminal differentiation of these two epithelia. However, stromal cells in both odontogenic tumors are frequently express SATB2. This finding supports that both neoplastic epithelia are intimately associated with odontogenic mesenchyme.

1307 Incidentally Discovered Papillary Thyroid Cancer in Lateral Neck Dissections: To Treat or Not to Treat?

William Twaddell[1], Jamie Hittman[2]
[1]Baltimore, MD, [2]University of Maryland, Baltimore, MD

Disclosures: William Twaddell: None

Background: Papillary thyroid carcinoma (PTC) is the most common type of thyroid cancer, and frequently goes undetected in asymptomatic patients. Though PTC has an overall excellent prognosis, it still has metastatic potential. The most common nodal metastatic sites are central neck (level VI) or lateral cervical (I-IV). Occasionally, metastatic PTC with occult primary cancer is discovered incidentally

during lateral neck dissections for other cancers of the head and neck. There is debate on whether treatment, surgery, or observation is indicated for PTC without metastasis; the clinical significance of incidental PTC metastases has not been fully characterized.

Design: We searched our pathology database at the University of Maryland for cases of neck dissections between 1/1/2015 and 6/29/2019 and found 11 patients out of 535 (2%) who had incidental PTC metastases to lateral cervical nodes. All dissections were performed for squamous cell carcinoma (SCC) of the head and neck. Cases were reviewed for clinical and histopathologic features of metastatic PTC. Additionally, immunohistochemical stains for cyclin D1 were performed on PTC-positive nodes, as cyclin D1 overexpression is a known predictor of aggressive behavior in PTC.

Results: Age range was from 49 to 77 years old, with 6 female and 5 male. Of the 11 patients, 1 was lost to follow-up, 2 died of complications of SCC and the rest survive today. Of the 5 patients who had thyroidectomy, 3 were treated with radioactive iodine (RAI). All tumors in resected thyroid specimens were smaller than 0.6 cm. 1 patient had known multinodular thyroid. 6/9 (66%) of metastatic tumors had Cyclin D1 overexpression. No patients with incidentally discovered PTC metastases had any evidence of recurrent disease.

Table 1.

Sex	Age	# of Positive Nodes	Cyclin D1	Size of Primary	Treatment of PTC	Outcome
F	49	3	Overexpressed	0.2 cm	Thyroidectomy	Alive
F	77	1	Overexpressed	Unknown	None	Died
M	59	1	Overexpressed	0.1 cm	Thyroidectomy, RAI	Alive
M	60	1	Case missing, not performed	0.6 cm	Thyroidectomy	Alive
F	79	1	Normal	Unknown	Monitored	Died
F	57	1	Overexpressed	0.05 cm	Thyroidectomy, RAI	Alive
M	65	1	Overexpressed	0.25 cm	Thyroidectomy, RAI	Alive
M	65	3	Overexpressed	Unknown	None	Unknown
F	59	1	Normal	Unknown	Monitored	Alive
M	61	1	Psamomma body only, not performed	Unknown	None	Alive
F	75	1	Normal	Unknown	Monitored	Alive

Conclusions: In this case series, incidentally discovered PTC metastases had minimal effect on clinical outcome. Additionally, we found no evidence that patients treated with radioactive iodine or surgery for their primary tumors had better outcomes than those treated with close observation. However, cyclin D1 overexpression as seen in the majority of cases here has been associated with more aggressive behavior. While a larger study is indicated, it seems possible that conservative therapy should be considered for such patients.

1308 Clinical and Histopathologic Features of Oral Bluntly Invasive Squamous Cell Carcinoma

Diana Wang[1], Tiffany Chen[2], Reshma Menon[3], Leela Breitman[4], Sook-Bin Woo[5]
[1]Harvard School of Dental Medicine, Boston, MA, [2]Brookline, MA, [3]Harvard School of Dental Medicine, Malden, MA, [4]Harvard School of Dental Medicine, Brookline, MA, [5]Brigham and Women's Hospital, Harvard Medical School, Lexington, MA

Disclosures: Diana Wang: None; Tiffany Chen: None; Reshma Menon: None; Leela Breitman: None; Sook-Bin Woo: *Grant or Research Support*, Bristol Myers Squibb

Background: Bluntly invasive squamous cell carcinoma (BISCCa) is a form of squamous cell carcinoma (SCCa) that invades with a broad pushing front, similar to verrucous carcinoma. These lesions are typically bulky (at least three times that of adjacent normal mucosa), predominantly endophytic, with bulbous rete ridges, mild-to moderate cytologic atypia, and presence of intraepithelial eosinophils, often associated with microabscesses. The aim of this study is to further characterize histopathologic features and report on staging, lymph node metastasis, and recurrence rate.

Design: Resected cases from 2010 to 2019 that were diagnosed as “atypical endophytic squamous proliferation suspicious for at least bluntly BISCCa” or “BISCCa” (cohort 1) were evaluated for specific histopathologic criteria as noted above. Clinical data were abstracted from the electronic medical record. We evaluated a second cohort of mostly incisional biopsy cases for similar morphologic features of BISCCa (cohort 2).

Results: In cohort 1, there were 19 patients (20 cases) (12 female, 7 male) with a median age of 74 years and 68.4% has a smoking history (average 30 pack year history). Nine cases (45.0%) occurred on the gingiva, hard palatal mucosa and retromolar trigone area, 8 (40.0%) on the tongue, and 3 (15.0%) on the buccal/lip mucosa. All presented with clinical Stage I or II disease and none (including two cases with lymph node dissection) exhibited lymph node involvement. All cases underwent surgical excision with no additional therapy required. Six of 19 cases (31.5%) had local recurrence. These cases exhibited a bulky epithelial proliferation with an endophytic growth

pattern. An exophytic or papillary surface was seen in 19 cases (95.0%). All 20 cases (100.0%) showed thick parakeratosis and 19 cases (95.0%) exhibited bulbous rete ridges with an average epithelial thickness 5.1 times that of the adjacent normal epithelium. The epithelium showed mild to severe epithelial atypia in all cases. Microabscesses and intraepithelial eosinophils were seen in 10 cases (50.0%). All cases showed no evidence of perineural or lymphovascular invasion. These results were similar to those seen in cohort 2 of 38 cases.

Conclusions: Although associated with high rates of local recurrence, BISCCa generally present as low-stage tumors with low risk of metastases, typically requiring only local surgical treatment.

1309 The AJCC8 Staging System for Head and Neck Cutaneous Squamous Cell Carcinoma (HNcSCC) – A Survey of Head and Neck Cancer Clinicians

Francesca Watts[1], Carsten Palme[2], Sandro Porceddu[3], Puma Sundaresan[4], Jonathan Clark[5], Ruta Gupta[6]
[1]Department of Tissue Pathology and Diagnostic Oncology, Royal Prince Alfred Hospital, Sydney, NSW, Australia, [2]Missenden Road, NSW, Australia, [3]University of Queensland, Brisbane, QLD, Australia, [4]University of Sydney, Sydney, NSW, Australia, [5]Chris O'Brien Lifehouse, Camperdown, NSW, Australia, [6]Royal Prince Alfred Hospital, Sydney, NSW, Australia

Disclosures: Francesca Watts: None; Carsten Palme: None; Sandro Porceddu: None; Puma Sundaresan: None; Jonathan Clark: None; Ruta Gupta: None

Background: The 8th edition of the American Joint Committee on Cancer Staging Manual (AJCC8) includes the staging system for cSCC within the head and neck chapter for the first time. The new HNcSCC staging system lacks homogeneity and distinctiveness, particularly with regards to the pN categories and stage III and stage IV disease. In addition, the pN categories for HNcSCC is similar to that of mucosal SCC, despite the vastly different biological behaviour of these diseases.

Design: A literature review was undertaken to determine the prognostic utility of the current staging system and identify avenues for its improvement.
A survey of 19 questions was developed to elicit the views of clinicians on the utility and appropriateness of the current staging system, and how it could be improved.
The survey was created and the data collected electronically using REDCap software accessed through the University of Sydney; it was distributed internationally via email to clinicians from a range of disciplines via specialist societies (Table 1). Results were analyzed in Microsoft Excel.

Results: Literature review (using search terms terms “head and neck”, “cutaneous SCC”, “prognosis” and “AJCC”) yielded 17 relevant manuscripts; of these, 9 described primary research into the prognostic performance of the staging system, and identified the use of ENE, relevance of the pN3a category, and the prognostic capacity of the nodal category as areas for refinement.

105 survey responses (Table 1) were received. 74/105 (71%) felt that mucosal and HNcSCC require different nodal staging categories. 66/105 (63%) respondents thought that immunosuppression should be included in the staging system. 73/105 (70%) of respondents thought that soft tissue metastases portend a worse prognosis compared to ENE. Respondents rarely saw pN3a tumours – 38/105 (38%) see these tumours never/ almost never and 42/105 (40%) felt that the current N stage is a poor predictor of survival.

Table 1. Respondent demographics	
Specialist societies distributing the survey	
International Federation of Head and Neck Cancer Societies	International
Australian and New Zealand Head and Neck Cancer Society	Australian
International Academy of Pathology	International
Head and Neck Cancer International Group	International
Countries	
Australia	27
Japan	29
The Netherlands	10
Germany	6
New Zealand	6
USA and Canada	6
Ireland	4
Mexico	3
South Africa	2
Other	12
Disciplines	
Pathologists	47
Surgeons	43
Radiation Oncologists	12
Medical Oncologists	2
Radiologists	1
Type of practice	

Tertiary centre, teaching hospital or cancer centre	88
Community Practice	8
Private practice	7
Other	2

Conclusions: The views of specialists experienced in the diagnosis and treatment of HNcSCC, from a variety of countries and disciplines, align with evidence regarding the limitations of the AJCC8 HNcSCC nodal staging categories. There was high rate of agreement that HNcSCC merits a nodal staging system distinct from mucosal SCC, that factors such as immunosuppression and the presence of soft tissue metastases should be considered for inclusion, and that the use of ENE should be modified.

1310 NR4A3 Immunohistochemistry Reliably Discriminates Acinic Cell Carcinoma from its Mimics

Kristine Wong[1], Vickie Jo[2], Jason Hornick[2]
[1]Brigham and Women's Hospital, Boston, MA, [2]Brigham and Women's Hospital, Harvard Medical School, Boston, MA

Disclosures: Kristine Wong: None; Vickie Jo: *Employee*, Merck and Co; Jason Hornick: *Consultant*, Eli Lilly; *Consultant*, Epizyme

Background: Acinic cell carcinoma (AciCC) has recently been shown to harbor the recurrent t(4;9)(q13;q31) translocation, which leads to upregulation of Nuclear Receptor Subfamily 4 Group A Member 3 (NR4A3). Thus far, only a single study has evaluated the utility of NR4A3 immunohistochemistry (IHC) in the diagnosis of AciCC, using a tissue microarray to assess most non-AciCC tumor types. The goal of this study was to validate the performance of NR4A3 IHC in AciCC and a large cohort of other salivary gland tumors.

Design: Whole tissue sections were obtained from 144 tumors, including 36 AciCC, 28 secretory carcinomas (SC), 20 mucoepidermoid carcinomas (MEC), 20 polymorphous adenocarcinomas (PAC), 20 pleomorphic adenomas (PA), and 20 salivary duct carcinomas (SDC). IHC for NR4A3 (clone H-7) was performed; nuclear staining was semi-quantitatively scored by intensity (weak, moderate, strong) and extent (0: 0%, 1+: <5%, 2+: 5-50%, and 3+: >50%). At least 2+ staining in tumor cells was considered a positive result.

Results: Of the 36 cases of AciCC, 29 (81%) were primary tumors and 7 (19%) were recurrent/metastatic disease. The primary site was parotid gland in 31 (86%) cases and minor salivary gland in 5 (14%) cases. 32 (89%) were histologically low grade, while 4 (11%) demonstrated high grade transformation. By IHC, NR4A3 was positive in 33 (92%) AciCC overall, with strong 3+ staining in 29 (81%) cases, strong 2+ staining in 3 (8%) cases, and moderate 3+ staining in 1 (3%) case. All cases of recurrent/metastatic AciCC and tumors with high grade transformation were positive. All cases of SC were negative for NR4A3 by IHC, with 26 (93%) cases demonstrating no staining and 2 (7%) cases with weak 1+ staining. Similarly, all cases of MEC (0/20) and SDC (0/20) were negative for NR4A3 by IHC. Of the PAC and PA, 3/20 (15%) and 1/20 (5%) cases demonstrated weak 2+ staining.

Conclusions: NR4A3 IHC is sensitive and specific for AciCC. Although rare cases of other salivary tumors may show weak focal or multifocal staining, moderate-strong and/or diffuse staining is a consistent and diagnostic feature of AciCC.

1311 Quantitative Analysis of the Head and Neck Squamous Cell Carcinoma Tumor Microenvironment and Correlation with PD-L1 Immunohistochemistry Using a Novel Multiplexed Immunofluorescence Assay

Kristine Wong[1], Vickie Jo[2], Jonathan Nowak[1], Scott Rodig[1], Neal Lindeman[3], Lynette Sholl[1], Kristen Felt[4], Glenn Hanna[5], James Lindsay[5], Priti Kumari[5]
[1]Brigham and Women's Hospital, Boston, MA, [2]Brigham and Women's Hospital, Harvard Medical School, Boston, MA, [3]Harvard Medical School, Brigham and Women's Hospital, Boston, MA, [4]Dana-Farber Cancer Institute, Boston, MA, [5]Dana Farber Cancer Institute, Boston, MA

Disclosures: Kristine Wong: None; Vickie Jo: *Employee*, Merck and Co; Jonathan Nowak: None; Scott Rodig: None; Neal Lindeman: None; Lynette Sholl: *Consultant*, LOXO Oncology; Kristen Felt: None; Glenn Hanna: *Grant or Research Support*, Bristol Myers Squibb; *Advisory Board Member*, Merck; James Lindsay: None; Priti Kumari: None

Background: Pembrolizumab has been recently approved as a first-line therapy for recurrent/metastatic head and neck squamous cell carcinoma (HNSCC) expressing PD-L1. Immunohistochemistry (IHC) is currently the standard method for PD-L1 evaluation, but accurate assessment can be challenging. To overcome limitations of IHC and to more fully interrogate the immune landscape of HNSCC, we employed a novel multiplex immunofluorescence (mIF) assay that is run in our CLIA-certified laboratory in near-realtime on active patient specimens.

Design: Whole tissue sections of HNSCC were evaluated using mIF with the following markers: cytokeratin, PD-1, PD-L1, CD8, FOXP3 and DAPI. The PD-L1 tumor proportion score (TPS) and combined positive score (CPS), as well as densities of CD8, FOXP3, and PD-1 positive cells, were determined using pathologist-supervised machine learning and a customized analysis pipeline. Data were analyzed for

association with HPV status, T stage, site (primary vs. metastatic), and prior therapy. PD-L1 IHC (E1L3N) was performed for correlation with mIF.

Results: Our cohort consisted of 45 HNSCC from 42 patients, including 16 (38%) with HPV-related disease; 38 (84%) were primary tumors and 7 (16%) were metastases. Primary tumor sites were: 22 (52%) oral cavity, 1 (2%) hypopharynx, 1 (2%) larynx, 18 (43%) oropharynx. By mIF, TPS and CPS were >1% in 80% and 98% of cases, respectively. Both TPS and CPS from mIF correlated well with PD-L1 IHC (Pearson r=0.85 and 0.78, respectively). Using CPS cutoffs of 1 and 20, mIF was 98% and 91% accurate compared to IHC for classifying tumors as PD-L1 positive or negative, respectively. Significantly higher densities of $CD8^+$, $PD\text{-}1^+$, and $FOXP3^+$ cells were detected at the tumor-stroma interface compared to intratumoral regions (p<0.01). Finally, HPV-related tumors had significantly higher densities of $CD8^+PD\text{-}1^+$ cells compared to HPV-negative tumors (p<0.0001), but did not exhibit significant differences in PD-L1 expression.

Conclusions: Multiplexed immunofluorescence can assess the HNSCC tumor immune microenvironment and correlates well with PD-L1 IHC. Moreover, mIF can simultaneously provide quantitative and geographic data regarding immune cell densities and identify differences in the tumor microenvironment that correlate with clinicopathologic features not captured by PD-L1 IHC alone, such as HPV status. These data verify mIF as a clinically viable method to quantify critical and novel biomarkers within the tumor microenvironment to guide immunotherapies.

1312 Head and Neck (H&N) Malignant Mesenchymal Neoplasms with GLI1 Gene Alterations: A Pathologic Entity with Distinct Histologic Features and Potential for Distant Metastasis

Bin Xu[1], Koping Chang[2], Andrew Folpe[3], Yu-Chien Kao[4], Shiuan-Li Wey[5], Hsuan-Ying Huang[6], Lisa Rooper[7], Justin Bishop[8], Brendan Dickson[9], Jen-Chieh Lee[10], Cristina Antonescu[1]
[1]Memorial Sloan Kettering Cancer Center, New York, NY, [2]National Taiwan University Hospital, Taipei City, Taiwan, [3]Mayo Clinic, Rochester, MN, [4]New Taipei City, Taiwan, [5]Hsinchu Mackay Memorial Hospital, Hsinchu City, Taiwan, [6]Chang Gung Memorial Hospital, Kaohsiung City, TWN, Taiwan, [7]The Johns Hopkins University School of Medicine, Baltimore, MD, [8]University of Texas Southwestern Medical Center, Dallas, TX, [9]Mount Sinai Health System, Toronto, ON, [10]Taipei City, Taiwan

Disclosures: Bin Xu: None; Koping Chang: None; Andrew Folpe: None; Yu-Chien Kao: None; Shiuan-Li Wey: None; Hsuan-Ying Huang: None; Lisa Rooper: None; Justin Bishop: None; Brendan Dickson: None; Jen-Chieh Lee: None; Cristina Antonescu: None

Background: Soft tissue tumors with *GLI1*-related fusions or amplifications have been recently described as a unique pathologic entity with established risk of malignancy. In this study, we investigate a cohort of 10 H&N lesions, including 7 from the tongue, harboring GLI1 fusions or amplifications, for their clinicopathologic features.

Design: The pathologic files of the authors were searched for H&N tumors with *GLI1* alterations. The diagnosis was confirmed by FISH (n=9) or targeted RNA sequencing (n=2). The histologic features, immunophenotype and clinical outcome were reviewed.

Results: The tumors commonly affected males in their 30s (M:F ratio 4:1; range 1-65). The primary site was tongue (n=7), neck (n=2), and submandibular gland (n=1). All 10 tumors showed a multinodular growth pattern, nested architecture separated by a delicate, arborizing vascular network, monotonous round to ovoid nuclei, and clear cytoplasm. Tumor nest protrusion into vascular spaces was observed in all except 3 cases. Seven tumors harbored *GLI1* fusions with the following partners: *ACTB* (n=4), *PTCH1* (n=2), or *MALAT1* (n=1). The remaining 3 cases showed co-amplifications of *GLI1* with *CDK4* and *MDM2* genes. The clinicopathologic parameters did not differ significantly between the two molecular groups. Tumors were positive for S100 protein in 5/9, CD56 3/3, SMA 3/9, CK 2/7, and EMA 1/4 cases respectively. Desmin, SOX10, CD34, and ERG were negative. STAT6, CDK4 and MDM2 were positive in *GLI1*-amplified tumors. Of 5 patients with follow up, 2 (1 each with *GLI1*-amplification and *GLI1-PTCH1* fusion) developed distant metastases, at 6 and 83 months, respectively. Both tumors showed high MI (6-7/10 HPFs) and tumor necrosis. The remaining 3 were disease-free.

Conclusions: H&N region, particularly tongue, is a common location for *GLI1*-related mesenchymal tumors. They typically present as a highly vascular, nested epithelioid neoplasm with clear cytoplasm and often S100 protein positivity. Although a morphologic overlap was noted with the previously reported 'pericytoma with t(7,12) translocation', often occurring in the tongue, our findings expand the original findings, to include a more variable immunophenotype, propensity for late distant metastases, and alternative mechanisms of GLI1 oncogenic activation, such as various *GLI1* fusion partners or *GLI1* co-amplifications with *MDM2* and *CDK4* genes.

*BX and KC are co-first authors, equal contributions

1313 The p16 Overexpression and Rb Loss Correlate with Transcriptionally Active High-Risk HPV Infection in Oropharyngeal Squamous Cell Carcinoma

Hidetaka Yamamoto[1], Rina Jiromaru[1], Yui Nozaki[1], Takahiro Hongo[1], Yoshinao Oda[1]
[1]Kyushu University, Fukuoka, Japan

Disclosures: Hidetaka Yamamoto: None; Rina Jiromaru: None; Yui Nozaki: None; Yoshinao Oda: None

Background: Overexpression of p16 is a highly sensitive but not a perfect surrogate marker for transcriptionally active high-risk human papillomavirus (HR HPV) infection in oropharyngeal squamous cell carcinoma (OPSCC). Beside HPV specific testing, more cost-effective marker is required

Design: In this study, we examined expression status of p16 and Rb by immunohistochemistry and transcriptionally active HR HPV infection by mRNA in situ hybridization in 177 cases of OPSCC.

Results: HR HPV and p16 was positive in 105 (59.3%) and 113 (63.8%) cases, respectively, and thus, 8/113 cases (7.1%) of p16-positive tumors were HPV negative. Rb status was divided into preserved expression (>90%, n=69), partial loss (10-90%, n=97) and complete loss (<10%, n=11). Among HPV-positive cases (n=105), Rb pattern was typically partial loss (97 cases, 92.4%) and rarely complete loss (8 cases, 7.6%) but not preserved expression (0%). In contrast, among HPV-negative cases (n=72), Rb pattern was typically preserved expression (69 cases, 95.8%) and rarely complete loss (3 cases, 4.2%) but not partial loss (0%). Collectively, among p16-positive cases (n=113), tumors with Rb preserved expression were exclusively HPV negative (n=6), those with Rb partial loss were exclusively HPV positive (n=97), and those with Rb complete loss were either HPV positive (n=8) or negative (n=2). As compared with p16 alone, the combination of p16 overexpression and Rb partial/complete loss showed equally excellent sensitivity (each 100%) and improved specificity (97.2% vs 88.9%) and positive predictive value (98.1% vs 92.9%).

Conclusions: The results suggest that combined use of p16 and Rb immunohistochemistry could be a reliable and cost-effective method to predict HR HPV infection in OPSCC.

1314 Pan-Trk Immunoreactivity, ETV6-NTRK3 Fusion Variants and RET Rearrangement in Salivary Secretory Carcinoma

Hidetaka Yamamoto[1], Yui Nozaki[1], Yoshinao Oda[1]
[1]Kyushu University, Fukuoka, Japan

Disclosures: Hidetaka Yamamoto: None; Yui Nozaki: None; Yoshinao Oda: None

Background: Salivary secretory carcinoma (SASC) is associated with gene rearrangements involving most often *ETV6-NTRK3* and rarely *ETV6-RET, ETV6-MET* or *VIM-RET*. We aimed to elucidate the potential diagnostic utility of immunohistochemistry with pan-Trk antibody and its relationship with fusion gene subtype in SASC.

Design: We examined 33 cases of SASC and 16 cases of morphological mimics (10 acinic cell carcinomas, 3 intraductal carcinomas, 2 cystadenocarciomas and 1 cystadenoma) for pan-Trk immunoreactivity and gene rearrangement of *ETV6, NTRK3* and *RET* gene using fluorescence in situ hybridization (FISH) and reverse transcription-polymerase chain reaction (RT-PCR).

Results: All 33 SASCs were positive for S-100 and mammaglobin. Thirty cases (90.9%) harbored *ETV6-NTRK3* fusion gene transcripts by RT-PCR and/or both *ETV6* and *NTRK3* gene rearrangements by FISH, and 3 cases (9.1%) had *RET* gene rearrangement by FISH. Most *NTRK3*-rearranged SASCs (25/33 cases; 75.8%) had conventional type of fusion between *ETV6* exon 5 and *NTRK3* exon 15, whereas 2 cases (6.1%) had both conventional fusion and variant fusion between *ETV6* exon 4-*NTRK3* exon 15. In the remaining 3 cases (9.1%), RT-PCR failed to detect any of *ETV6* exon 4/5-*NTRK3* exon 14/15 fusions despite the presence of both *ETV6* and *NTRK3* rearrangements by FISH, suggesting an *ETV6-NTRK3* fusion with as-yet-undetermined break point. Nevertheless, all the 33 SASCs with *ETV6-NTRK3* fusion and/or *NTRK3* rearrangement showed nuclear and cytoplasmic immunoreactivity for pan-Trk. In contrast, 3 cases of *RET*-rearranged SASCs showed negative or only weak cytoplasmic staining for pan-Trk. All 16 non-SASC tumors were negative for pan-Trk.

Conclusions: Nuclear and cytoplasmic immunoreactivity for pan-TRK well correlates with the presence of *ETV6-NTRK3* gene fusion variants in SASC, and may be helpful to distinguish *ETV6-NTRK3* fusion-negative salivary tumors, including *RET*-rearranged SASC and non-SASC tumors.

1315 Oral Squamous Cell Carcinoma in Patients Less than 45 years of Age: Clinicopathologic Features and Comparison with Carcinomas in Older Patients

Lin Zhang[1], Joe Rodriguez[1], Jianmin Ding[1], Songlin Zhang[1], Zhenjian Cai[1], Karan Saluja[2], Hui Zhu[1]
[1]The University of Texas Health Science Center at Houston, Houston, TX, [2]UT Health Science Center at Houston, Houston, TX

Disclosures: Lin Zhang: None; Zhenjian Cai: None; Karan Saluja: None; Hui Zhu: None

Background: Oral squamous cell carcinoma (OSCC) is a common cancer in patients more than 50 years of age and is strongly associated with smoking and alcohol consumption. OSCC in young patients, however, is not uncommon, and increasing incidence has been reported in recent years. The etiology and pathogenesis are puzzling in these patients with controversial data exists in the literature. In this study, we compared the clinicopathologic features of OSCC in young versus older patients.

Design: We identified 63 patients with OSCC diagnosed before the age 45 and 47 consecutive patients older than 60 years as a control group. The electronic medical records were reviewed. Tissue microarrays were built in duplicates from surgical specimens. Immunohistochemical stains for p16, p53, Cyclin D1, PD-L1 (Agilent Dako), MLH1, MSH2, PMS2, and MSH6 were performed. For p16 and p53, strong diffuse staining in >75% of cells is scored as positive; for Cyclin D1, positive staining in >50% of cells is scored as positive. PD-L1 expression level was calculated according to the Interpretation Manual for Head and Neck Squamous Cell Carcinoma (Agilent Dako).

Results: Compared with the older patient population, OSCC in the younger patients is less frequently associated with smoking and alcohol consumption and affects more female patients. P16 expression is more common in OSCC from young patients (25% vs. 4.3%, P-value 0.003). There is no significant difference in Cyclin D1 and p53 expression between these two groups. In both groups, tumor proportion score (TPS) > 1 for PD-L1 staining is seen in a significant number of patients (32% and 42% respectively). None of the studied cases shows loss of MMR expression in both groups (Table 1).

	Smoking and/or alcohol	Male/ Female	Stage III and IV	P16	Cyclin D1	P53	PD-L1 TPS >1	MSI Panel MLH1 MSH2 PSM2 MSH6
<45	39/63 (62%)	42/21 (2:1)	40/56 (71%)	16/63 (25%)	22/63 (35%)	13/63 (21%)	20/63 (32%)	Retained nuclear stain 63/63 (100%)
>60	38/47 (81%)	37/10 (3.7:1)	32/47 (68%)	2/47 (4.3%)	13/47 (28%)	8/47 (17%)	20/47 (42%)	Retained nuclear stain 47/47 (100%)
P Value	0.03	N/A	0.7	0.003	0.4	0.7	0.2	1

Conclusions: OSCC in young patients has different clinicopathologic features compared with oral SCC in older patients. Expression of p16 is more commonly seen in the young patient population. Considering that previous studies demonstrated a low frequency of human papilloma virus (HPV) in OSCC in young patients, our data suggest that a non-viral dysregulation of the retinoblastoma (Rb)/p16 pathway might play a role in the pathogenesis of OSCC. All 110 cases in this study show retained nuclear expression of mismatch repair proteins, suggesting that deficient mismatch repair is rare in oral SCC. PD-L1 expression is common in oral SCC, supporting targeted therapy with PD-1/PD-L1 inhibitors in high stage tumors.